

Essays on Asset Allocation and Derivatives

Inaugural-Dissertation
zur Erlangung des Doktorgrades
des Fachbereichs Wirtschaftswissenschaften
der Johann Wolfgang Goethe-Universität
Frankfurt am Main



vorgelegt von
Dipl.-Vw. Eva Schneider aus Lich

Frankfurt am Main 2007

Danksagung

Die vorliegende Arbeit entstand während meiner Tätigkeit als wissenschaftliche Mitarbeiterin am Fachbereich Wirtschaftswissenschaften der Goethe-Universität Frankfurt. Sie wurde im Februar 2008 als Dissertationsschrift angenommen.

Zunächst möchte ich Herrn Prof. Dr. Schlag, dem Erstgutachter meiner Dissertation und Leiter des Lehrstuhls für Derivate und Financial Engineering, danken. Sowohl persönlich als auch fachlich habe ich sehr von meiner Zeit am Lehrstuhl profitiert. Dies ist vor allem Herrn Schlag zu verdanken, der durch seine freundschaftliche und motivierende Führung des Lehrstuhls viel zur angenehmen und produktiven Arbeitsatmosphäre beigetragen hat. Auch als Dozent und Koautor konnte ich von seinem Wissen und Erfahrungsschatz profitieren. Hierfür bin ich ihm sehr dankbar.

Ich danke auch den weiteren Mitgliedern meiner Prüfungskommission, Herrn Prof. Dr. Raimond Maurer, Herrn Jun.-Prof. Dr. Holger Kraft, Herrn Prof. Dr. Uwe Hassler und Herr Prof. Dr. Dietrich Ohse für die Begutachtung und das Interesse an meiner Arbeit.

Besonderer Dank gilt Prof. Dr. Nicole Branger, die mich sowohl während meines Studiums als auch während der Anfangszeit am Lehrstuhl motiviert und angeleitet hat und stets bereit war, inhaltliche Fragen zu diskutieren und hierbei ihr Wissen weiterzugeben.

Des Weiteren möchte ich David Horn und Norman Seeger danken, die mich als Kollegen und Koautoren auf meinem Weg zur Promotion begleitet haben. Auch Raisa Beygelman, Dr. Burkart Mönch und Grigory Vilkov danke ich herzlich für die schöne gemeinsame Zeit am Lehrstuhl. Die freundschaftliche Atmosphäre hat sicherlich sehr zum Gelingen dieser Arbeit beigetragen.

Ebenfalls danke ich unserer Sekretärin Frau Peschel, die immer ein offenes Ohr für Probleme und Sorgen der Mitarbeiter hatte und uns mit guten Ratschlägen und Ermunterungen zur Seite stand. Großer Dank gilt auch den studentischen Hilfskräften des Lehrstuhls für ihre exzellente Arbeit und die gute und angenehme Atmosphäre, durch die sie den Lehrstuhl bereichert haben. Die schönen Weihnachts- und Geburtstagsfeiern am Lehrstuhl wären ohne ihr Engagement nicht möglich gewesen.

Auch meinen Freunden und Kollegen aus dem Graduiertenkolleg danke ich für die nette gemeinsame Zeit an der Uni. Nicht nur in fachlicher, sondern auch in persönlicher Hinsicht habe ich die Zusammenarbeit sehr genossen.

Nicht zuletzt gilt mein Dank meiner Familie, Heike und Jana Schneider, Dr. Ulrike und Dr. Hans-Jobst Krautheim und meinem Verlobten Sebastian Krautheim. Sie haben mich durch alle Höhen und Tiefen meiner Promotionszeit begleitet und damit einen nicht zu unterschätzenden Beitrag zu der Entstehung dieser Arbeit geleistet.

Frankfurt, April 2008

Eva Schneider

Inhaltsverzeichnis

Part I Zusammenfassung

Zusammenfassung

Eva Schneider 3

Part II Research Papers

Optimal Portfolios When Volatility can Jump

Nicole Branger, Christian Schlag, Eva Schneider 15

Derivatives Trading in a General Equilibrium Model With Stochastic Volatility and Jumps

Nicole Branger, Christian Schlag, Eva Schneider 39

Continuous-time Volatility Component Models: Option Pricing and Asset Allocation

Eva Schneider 65

Hedging in the Presence of Microstructural Noise

David Horn, Eva Schneider, Grigory Vilkov 99

Part III Appendix

Curriculum Vitae 131

Ehrenwörtliche Erklärung 135

Abbildungsverzeichnis

Optimal Portfolios When Volatility can Jump

Fig. 1	<i>Optimal Risk Exposures and Asset Positions for Varying Investment Horizons</i>	34
Fig. 2	<i>Portfolio Improvement from Including Derivatives [%]</i>	35
Fig. 3	<i>Realized Exposures for Varying Investment Horizons</i>	36
Fig. 4	<i>Cumulative Distribution Functions of Terminal Wealth in the Presence of Model Risk</i>	37
Fig. 5	<i>Cumulative Distribution Functions of Terminal Wealth in the Presence of Parameter Risk</i>	38

Derivatives Trading in a General Equilibrium Model with Stochastic Volatility and Jumps

Fig. 1	<i>Demand for Risk Factors ($\gamma^{(1)} = 2.0, \gamma^{(1)} = 4.0$)</i>	61
Fig. 2	<i>Demand for Risk Factors ($\gamma^{(1)} = 0.8, \gamma^{(1)} = 2.0$)</i>	62
Fig. 3	<i>Demand for Risk Factors ($\gamma^{(1)} = 0.5, \gamma^{(1)} = 0.8$)</i>	63
Fig. 4	<i>Trading Volume in Derivatives</i>	64

Continuous-time Volatility Component Models:

Option Pricing and Asset Allocation

Fig. 1	<i>Smile Dynamics in the SLRM-Model</i>	93
Fig. 2	<i>Smile Dynamics in the Model of Bates (2000)</i>	94
Fig. 3	<i>Optimal Stock Position in the Model of Bates (2000)</i>	95
Fig. 4	<i>Comparison of Stock Positions</i>	96
Fig. 5	<i>Utility Loss from Model Mis-Specification</i>	97

Hedging in the Presence of Microstructural Noise

Fig. 1	<i>Sensitivity of Call Price</i>	120
Fig. 2	<i>Sensitivity of IV-Smile</i>	121
Fig. 3	<i>Sensitivity of Option Delta</i>	122
Fig. 4	<i>Sensitivity of Option Vega</i>	123
Fig. 5	<i>Objective Function and Standard Deviation of Hedging Errors for σ_v and κ</i>	124
Fig. 6	<i>Objective Function and Standard Deviation of Hedging Errors for σ_v and θ</i>	125
Fig. 7	<i>Objective Function and Standard Deviation of Hedging Errors for V_0 and σ_v</i>	126
Fig. 8	<i>Objective Function and Standard Deviation of Hedging Errors for θ and κ</i>	127
Fig. 9	<i>Bid-Ask Spread vs. Standard Deviation of Hedging Error</i>	128

Tabellenverzeichnis

Optimal Portfolios When Volatility can Jump

Tab. 1	<i>Jump Size Distribution</i>	33
Tab. 2	<i>Calibrated Parameters</i>	33
Tab. 3	<i>Parameter Intervals</i>	33

Derivatives Trading in a General Equilibrium Model with Stochastic Volatility and Jumps

Tab. 1	<i>Jump Size Distribution</i>	60
Tab. 2	<i>Parameter Values for Numerical Computations</i>	60

Continuous-time Volatility Component Models: Option Pricing and Asset Allocation

Tab. 1	<i>Calibrated \mathbb{Q}-Parameters</i>	92
--------	------------------------------------------------------	----

Hedging in the Presence of Microstructural Noise

Tab. 1	<i>Bid-Ask Spreads on S&P100 Individual Stock Put Options</i>	118
Tab. 2	<i>Data Description</i>	118
Tab. 3	<i>Standard Deviations of Hedging Errors</i>	119

Zusammenfassung

Zusammenfassung

Eva Schneider

1 Thematische Einordnung

Die Arbeit befasst sich mit den Eigenschaften neuester zeitstetiger Aktienkursmodelle in Bezug auf optimale Portfolioplanung, Derivatebewertung und -hedging. Hierbei wird auch insbesondere auf die Auswirkungen einer Modellfehlspezifikation eingegangen.

Das bekannteste Bewertungsmodell für Optionspreise ist sicherlich das Modell von Black und Scholes (1973). Schon allein die Existenz des impliziten Volatilitätssmiles verdeutlicht aber, dass die Modellannahmen zu strikt sind, um das Verhalten von empirisch beobachteten Aktienkursen und Optionspreisen zu erklären. Um die Erklärungskraft von Optionspreismodellen zu erhöhen, werden daher zusätzliche Aspekte von Aktienkursen in die Modellierung aufgenommen. So wurde bereits in Merton (1976) das Sprung-Diffusions-Modell eingeführt, welches nicht nur stetige Bewegungen, sondern auch diskrete Sprünge im Aktienkurs zulässt. Eine andere Erweiterung betrifft die Modellierung einer stochastischen Volatilität des Aktienkurses. Zu den bekanntesten Modellen dieser Klasse zählt das Modell von Heston (1993).

In neueren Modellen werden diese Komponenten kombiniert. So gibt es in dem Modell von Bakshi, Cao und Chen (1997) neben stochastische Zinsen sowohl stochastische Volatilität als auch Sprünge im Aktienkurs. Das Modell von Bates (2000) erlaubt die Modellierung von Sprüngen im Aktienkurs und hat als weitere Besonderheit, dass die stochastische Volatilität aus zwei Komponenten besteht. Duffie, Pan und Singleton (2000) verallgemeinern diese Modellansätze unter der Klasse der affinen Sprung-Diffusions-Modelle, welche beispielsweise auch Modelle mit Sprüngen in der Volatilität beinhalten.

Neuere empirische Studien wie Eraker, Johannes und Polson (2003) oder Broadie, Chernov und Johannes (2007) kommen zu dem Ergebnis, dass sowohl stochastische Vola-

tilität als auch Sprünge im Aktienkurs und in der Volatilität nötig sind, um Optionspreise und Aktienkurse in ausreichendem Maße zu erklären. Auch Modelle mit mehreren Volatilitätskomponenten haben viele wünschenswerte Eigenschaften wie Christoffersen, Heston und Jacobs (2007) zeigen.

Trotz ihres Erfolgs bei der Optionsbewertung gibt es nur wenige Autoren, die sich mit der Fundierung dieser Modelle im allgemeinen Gleichgewicht beschäftigen. Ältere Studien wie Bick (1986) im Fall homogener Agenten und Dumas (1989) für den Fall heterogener Agenten arbeiten zumeist auf Basis einer Black und Scholes (1973)-Dynamik. Nur wenige neuere Studien wie Dieckmann und Gallmeyer (2005) beziehen auch Sprünge mit ein. Auch die optimale Portfolioplanung in diesen Modellen wird in der Literatur noch unzureichend betrachtet. Eine Ausnahme hiervon stellen Liu, Longstaff und Pan (2003) und Liu und Pan (2003) dar.

Liu und Pan (2003) leiten die optimalen Portfoliopositionen eines Investors mit konstanter relativer Risikoaversion in einem Sprung-Diffusions-Modell mit stochastischer Volatilität her. Im Rahmen ihrer Analyse führen sie eine Methodik ein, die unter Annahme eines vollständigen Marktes zunächst die optimalen Positionen in den Risikofaktoren herleitet, welche anschließend in Wertpapierpositionen umgerechnet werden können. Der Vorteil dieser Herangehensweise liegt darin, dass die Ergebnisse einfach ökonomisch zu interpretieren sind und die Risikopositionen flexibel auf die jeweils gehandelten Wertpapiere umgerechnet werden können. Außerdem ermöglicht der Vergleich ihrer Ergebnisse mit denen auf einem unvollständigen Markt, den ökonomischen Wert von (marktvervollständigenden) Derivaten zu berechnen.

Im Gegensatz hierzu arbeiten Liu, Longstaff und Pan (2003) in einem unvollständigen Kapitalmarkt. Sie untersuchen den Einfluss von Sprüngen im Aktienkurs und in der Volatilität auf die optimale Aktienposition eines Investors. Insbesondere betrachten sie hierbei auch den Nutzenverlust, den ein Investor erleidet, der Sprünge im Aktienkurs bei seiner Portfolioplanung ignoriert.

Je komplizierter die Optionsbewertungsmodelle, um so wichtiger wird es aus theoretischer und praktischer Sicht auch zu analysieren, welche Konsequenzen eine Fehlspezifikation des angenommenen Modells hat. Dass eine eindeutige Identifizierung des Modells schwierig sein kann, zeigen beispielsweise Dennis und Mayhew (2004). Sie verdeutlichen in ihrer Arbeit, dass allein wegen der Existenz von mikrostrukturellen Störungen, wie des Bid-Ask-Spreads, unter bestimmten Umständen ein Sprung-Diffusions-Modell anhand der

resultierenden Optionspreise nicht von einem Modell ohne Sprünge unterschieden werden kann.

Diese Fehlspezifikation kann zwei Ausprägungen haben: Modellrisiko, welches die Fehlspezifikation der Modellklasse bezeichnet und Parameterrisiko, bei dem zwar das grundsätzliche Modell identifiziert ist, nicht aber die konkrete Parametrisierung. Liu, Longstaff und Pan (2003) betrachten die Konsequenzen von Modellrisiko im Rahmen der optimalen Portfolioplanung, andere Autoren analysieren die Konsequenzen, die eine Fehlspezifikation auf die Bewertung von Optionen oder deren Hedging hat.

Figlewski (2004) beispielsweise analysiert den Fehler, der bei einer Value-at-Risk-Schätzung unter Annahme des Black und Scholes (1973)-Modells entsteht, wenn der wahre Aktienkursprozess einer Dynamik mit stochastischer Volatilität und Sprüngen folgt. Schoutens, Simons und Tistaert (2003) zeigen den Einfluss von Modellrisiko auf die Bewertung exotischer Derivate, An und Suo (2003) auf ihr Hedging. He, Kennedy, Coleman, Forsyth, Li und Vetzal (2006) zeigen die Konsequenzen von Parameterrisiko, indem sie für ein Sprung-Diffusions-Modell mit lokaler Volatilitätsfunktion verschiedene, ähnlich gute Kalibrierungen aufstellen und jeweils die Performance eines auf ihnen basierten Hedgeportfolios analysieren.

2 Struktur und Inhalt der Arbeit

Die vorliegende Dissertation besteht aus vier Forschungspapieren:

- *Optimal Portfolios When Volatility can Jump* von Nicole Branger, Christian Schlag und Eva Schneider
- *Derivatives Trading in a General Equilibrium Model with Stochastic Volatility and Jumps* von Nicole Branger, Christian Schlag und Eva Schneider
- *Continuous-time Volatility Component Models: Option Pricing and Asset Allocation* von Eva Schneider
- *Hedging in the Presence of Microstructural Noise* von David Horn, Eva Schneider und Grigory Vilkov

In dem Forschungspapier *Optimal Portfolios When Volatility can Jump* beschäftigen wir uns mit der optimalen Portfolioplanung in einem zeitstetigen stochastischen Volatilitätsmodell, welches als Besonderheit im Vergleich zu vorherigen Arbeiten Sprünge in der

Volatilität zulässt. Diese Sprungkomponente ist in unserem Forschungspapier besonders flexibel modelliert. So sind grundsätzlich Sprünge stochastischer Höhe ausschließlich im Aktienkurs, ausschließlich in der Volatilität, aber auch gemeinsame Sprünge beliebiger Korrelation möglich.

In diesem Modellrahmen leiten wir die optimale Portfolioallokation eines Investors mit konstanter relativer Risikoaversion auf einem vollständigen Kapitalmarkt her. Hierbei orientieren wir uns an der Methodik von Liu und Pan (2003). Die Besonderheit ihres Ansatzes liegt darin, dass nicht optimale Positionen in den gehandelten Wertpapieren hergeleitet werden, sondern dass zunächst optimale Positionen in den einzelnen Risikofaktoren ermittelt werden. Durch die Annahme eines vollständigen Kapitalmarkts ist es möglich, diese Risikopositionen anschließend in Wertpapierpositionen zu übersetzen.

In unserem Modellrahmen mit korrelierten gemeinsamen Sprüngen in Aktienkurs und Volatilität erhält man bezüglich der optimalen Risikoposition ein interessantes Ergebnis. Im Gegensatz zu vorherigen Arbeiten besteht die optimale Nachfrage nach Sprungrisiko nicht mehr nur aus einer myopischen Komponente, sondern auch aus einer Hedging-Komponente. Insbesondere bedeutet dies, dass ein Investor im Optimum selbst dann noch eine Position im Sprungrisikofaktor einnimmt, wenn die Prämie für diesen Faktor gleich Null ist. Seine optimale Position würde in einem solchen Fall allein durch die Möglichkeit des Hedgings der stochastischen Investitionsmöglichkeiten getrieben werden. Eine durch einen Volatilitätssprung induzierte Veränderung in den Risikoprämien (je Risikoeinheit), und damit eine Veränderung der Investitionsmöglichkeiten, könnte nämlich durch eine entsprechende Position im Sprungrisiko kompensiert werden.

Weiterhin erlaubt uns ein Vergleich mit den Ergebnissen von Liu, Longstaff und Pan (2003), den ökonomischen Wert von Derivaten zu berechnen. Hierzu vergleichen wir den Nutzen eines Investors, der durch ein Investment in Derivate eine optimale Position in den Risikofaktoren erreichen kann, mit dem Nutzen eines Investors, der ausschließlich in die Aktie und das Geldmarktkonto investieren kann. Dieser Nutzengewinn kann je nach Parameterkonstellation erheblich sein und ist für einen Investor mit 10-jährigem Anlagehorizont in etwa vergleichbar mit einer zusätzlichen sicheren Rendite von 5% per annum.

Der letzte Abschnitt des Forschungspapiers beschäftigt sich mit dem Einfluss von Modell- und Parameterrisiko auf die erwartete Vermögensverteilung zu Ende des Anlagehorizonts. Im Rahmen des Modellrisikos analysieren wir, welche Auswirkungen eine

Vernachlässigung bzw. ein fälschliches Hinzunehmen von Sprüngen in der Volatilität hat. Auch Parameterrisiko betrifft vor allem die Sprungparameter, da diese sich auf seltene Ereignisse beziehen und somit empirisch schwer zu schätzen sind. In beiden Fällen zeigt sich, dass vor allem die optimale Position im Sprungrisiko für den Investor eine Gefahr in sich birgt. Wird diese aufgrund von Modell- oder Parameterrisiko überschätzt, so kann der Investor bei Auftreten dieses diskreten Ereignisses mit einem Mal sein vollständiges Vermögen verlieren und somit theoretisch einen unendlich großen Nutzenverlust erleiden.

Während die Analyse im ersten Forschungspapier im partiellen Gleichgewicht durchgeführt wird, handelt es sich in dem Forschungspapier *Derivatives Trading in a General Equilibrium Model with Stochastic Volatility and Jumps* um ein allgemeines Gleichgewichtsmodell. Insbesondere wird hier die Dynamik der Preisprozesse gehandelter Wertpapiere nicht exogen vorgegeben, sondern zunächst selbst innerhalb eines Lucas (1978)-Tree-Modells bestimmt. Hierzu wird der schon im vorherigen Forschungspapier vorgestellte Sprung-Diffusions-Prozess mit stochastischer Volatilität und Sprüngen in der Volatilität als Dynamik für die Dividendenzahlung zugrunde gelegt. Zusätzlich wird angenommen, dass die Ökonomie aus zwei (Gruppen von) Investoren besteht, die sich nur in der Höhe ihrer Risikoaversion unterscheiden. Dies impliziert für den repräsentativen Investor (RI) die im Folgenden wichtige Eigenschaft, dass er trotz der konstanten relativen Risikoaversion der Einzelinvestoren eine sinkende relative Risikoaversion besitzt.

Zur Herleitung des kurzfristigen Zinssatzes und der Risikoprämien wird nun ausgenutzt, dass der RI wegen der Nichtsättigungseigenschaft immer die gesamte Dividende konsumieren und daher 100% des Aktienkurses halten wird. Ebenso kann im Aggregat kein Vermögen im Geldmarktkonto gehalten werden. Die auf dem Kapitalmarkt gezahlten Prämien entsprechen daher gerade den vom RI geforderten Prämien und der Zinssatz ist derjenige, bei dem der RI indifferent zwischen Geldanlage und Aufnahme eines Kredits ist. Nach Aufstellung des stochastischen Diskontierungsfaktors ist es uns im Folgenden möglich, den Aktienkurs mit Hilfe numerischer Verfahren zu berechnen.

Weiterhin entspricht die optimale Nachfrage des RI nach Risikofaktoren gerade der Risikoposition des Gesamtvermögens der Ökonomie und damit der Dynamik des Aktienkurses. Im Falle einer homogenen Ökonomie ist die myopische Komponente der Risikoposition gerade gleich eins. Bei heterogenen Investoren hängt ihre Größe davon ab, inwiefern die erwartete zukünftige Risikoaversion des RI von der aktuellen abweicht. Im Gegensatz zu den Ergebnissen einer partiellen Gleichgewichtsanalyse ist die durch Hedging motivier-

te Position in den einzelnen Risikofaktoren nicht monoton in der Risikoaversion des RI. Jede Abweichung der Risikoposition im Aktienkurs von eins stellt einen Unterschied im Vergleich zur Dividendendynamik dar und wird in der Literatur als 'Excess Volatility' bezeichnet. Somit kann unser Modell dieses empirische beobachtete Phänomen sehr gut erklären.

Wiederum über Verwendung der numerischen Lösung von Differentialgleichungen und Fourierinversion können auch die optimalen Portfoliopositionen der Einzelinvestoren hergeleitet werden und ein Vergleich zwischen ihnen erlaubt Rückschlüsse auf den Handel von Risikofaktoren. Es wird deutlich, dass der Wunsch zu handeln in erster Linie durch Unterschiede in der myopischen Komponente getrieben wird, die Hedging-Komponente spielt in absoluten Werten nur eine untergeordnete Rolle. Vor allem im Fall des Volatilitätsrisikofaktors ist die Handelsrichtung zwischen den beiden Investoren abhängig von den konkreten Zahlenwerten der Risikoaversionskoeffizienten. Es kann nicht im Vorhinein gesagt werden, ob der mehr oder der weniger risikoaverse Investor die Position kauft oder verkauft. Es zeigt sich, dass sich das Handelsvolumen von Risikofaktoren selbst bei moderaten Niveaus der Risikoaversion auf bis zu 20% der Marktkapitalisierung belaufen kann.

Im Gegensatz zu den ersten beiden basiert das Forschungspapier *Continuous-time Volatility Component Models: Option Pricing and Asset Allocation* nicht auf Sprung-Diffusions-Modellen, sondern es werden Modelle mit unterschiedlicher Spezifikation der stochastischen Volatilitätskomponente betrachtet. Hierbei werden deren Eigenschaften in Bezug auf Optionsbewertung und optimale Portfolioplanung mit dem Modell von Heston (1993), welches nur eine Volatilitätskomponente enthält, verglichen. Insbesondere wird auf das Modell von Bates (2000) und das von Duffie, Pan und Singleton (2000) vorgestellte Modell mit stochastischen langfristigen Mittelwert (SLRM) eingegangen.

Es zeigt sich, dass das Modell von Bates (2000) einige sehr interessante Eigenschaften aufweist, die es im Vergleich zum Modell von Heston (1993) und zum SLRM-Modell deutlich hervorheben. Was die Optionsbewertung angeht, schafft es das Modell von Bates (2000) auf relativ einfache Art und Weise nicht nur den empirisch beobachteten Smile zu einem Zeitpunkt zu reproduzieren, sondern es hat auch die besondere Eigenschaft, dass sich die grundsätzliche Form des Smiles innerhalb einer Parametrisierung im Zeitverlauf verändern kann. Im Modell von Bates (2000) können durch eine Verschiebung in den Gewichtsanteilen der beiden Volatilitätskomponenten verschiedene, empirisch beobachte-

te Phänomene daher konsistent erklärt werden. Trotz konstant bleibender Gesamtvarianz generiert das Modell von Bates (2000) unterschiedliche Levels des Smiles, und seine Krümmung und Steigung können sich ändern.

Auch in Bezug auf die optimale Portfolioplanung verhält sich das Modell von Bates (2000) nicht wie andere affine Modelle. Die optimale Aufteilung des Vermögens eines Investors mit konstanter relativer Risikoaversion auf Aktie und Geldmarktkonto ist nicht in geschlossener Form lösbar. Stattdessen muss auf das numerische Lösen einer Differentialgleichung, hier mittels finiter Differenzen-Methode, zurückgegriffen werden. Weiterhin ist die optimale Aktienposition im Gegensatz zu anderen affinen Modellen zustandsabhängig. Es ist also nicht allein der Planungshorizont und der Risikoaversionskoeffizient, der über die optimale Aufteilung zwischen Aktie und Geldmarktkonto entscheidet, sondern zusätzlich muss der Zustand der Ökonomie, das heißt die Höhe der Volatilitätskomponenten, bekannt sein.

Im letzten Abschnitt wird auch in diesem Forschungspapier auf die Auswirkungen von Modellfehlspezifikation eingegangen. Hierzu wird zunächst eine allgemeine Vorgehensweise zur Berechnung des Nutzenverlustes mit Hilfe der finiten Differenzen-Methode vorgestellt. Mittels dieser Methodik, die grundsätzlich auf unterschiedliche Arten von Modellfehlspezifikation angewendet werden kann, wird der Nutzenverlust eines Investors, der die Existenz von Volatilitätskomponenten ignoriert, berechnet. Es stellt sich heraus, dass der resultierende Nutzenverlust weitaus geringer ist als im Fall der Vernachlässigung von Sprungkomponenten.

In dem Forschungspapier *Hedging in the Presence of Microstructural Noise* betrachten wir eine andere Art von Fehlspezifikation, nämlich nicht die Modell- sondern die Parameterfehlspezifikation. Insbesondere untersuchen wir im Rahmen des Heston (1993)-Modells, welche Auswirkungen eine Fehlschätzung der Parameter auf die Hedgingperformance hat. Grundsätzlich ist es nicht nur die Seltenheit von Ereignissen, die eine korrekte Parameterschätzung erschwert, sondern auch die Existenz von mikrostrukturellen Störungen. Wie Dennis und Mayhew (2004) zeigen, ist beispielsweise die eindeutige Identifizierung einer Modellklasse anhand von Optionspreisen wegen ihres Bid-Ask-Spreads nicht möglich. Ebenso sind theoretisch alle Parameterkonstellationen, die Preise innerhalb des Bid-Ask-Spreads liefern, für ein gegebenes Modell nicht zu unterscheiden. Ein auf diesen verschiedenen Parametrisierungen basierter Hedge kann aber trotzdem unterschiedlich gut sein.

Genau dieser Einfluss auf die Hedgingperformance soll in unserem Forschungspapier untersucht werden.

Zunächst zeigen wir auf, welche Parameter des Heston (1993)-Modells besonders anfällig für dieses Parameterrisiko sind. Dies sind solche Parameter, die anhand von Optionspreisen schwer identifizierbar sind, deren Größe aber einen bedeutenden Einfluss auf den Aufbau des Hedgeportfolios hat. In einer einfachen Sensitivitätsanalyse scheinen vor allem die Parameter Rückholgeschwindigkeit κ , Volatilität der Varianz σ_v , sowie die Korrelation zwischen Aktienkurs- und Varianzprozess ρ diese Eigenschaft zu haben.

Um diese ersten Ergebnisse zu bestätigen, führen wir im Folgenden eine Monte-Carlo-Simulation durch. Hierzu gehen wir von einem konservativen Ansatz aus, indem wir annehmen, dass der Investor bei der Kalibrierung alle Parameter des Heston (1993)-Modells, bis auf zwei, richtig schätzt. Anschließend ermitteln wir die Menge der Parametrisierungen, die Optionspreise liefern, die innerhalb des Bid-Ask-Spreads nicht von den als wahr angenommenen Preisen unterscheidbar sind. Der Vergleich zwischen Kalibrationsgüte einerseits und aus Parametrisierung resultierender Hedgingperformance andererseits ergibt Folgendes. Zwar lässt sich in der Regel von der Kalibrationsgüte auf die Hedgingperformance schließen, es gibt aber auch Ausnahmen. Im Fall des Parameters σ_v kann es sein, dass sich die Kalibrationsgüte bei einer Fehlschätzung nur geringfügig verschlechtert, während die resultierende Hedgingperformance rapide abnimmt. Weiterhin gibt es Parameter, die sich gegenseitig stark beeinflussen. So ist das langfristige Mittel der Varianz θ für kleine Werte von κ nahezu nicht zu identifizieren, während es für große Werte von κ sehr leicht zu kalibrieren ist.

Ein weiteres interessantes Ergebnis, welches sich schon in der einleitenden Analyse andeutet, ist folgendes. Sind unter den zur Kalibrierung verwendeten Optionen nur wenige weit aus dem Geld liegende (OTM-Optionen), so verschlechtert sich die Hedgingperformance massiv. Bei einem mittleren Bid-Ask-Spread von 10% sind viele der Parameter, aber insbesondere der Parameter ρ , nur noch sehr schwer zu identifizieren. Den Zusammenhang zwischen Bid-Ask-Spread und aus Parameterfehlspezifikation resultierender Verschlechterung der Hedgingperformance haben wir im Folgenden genauer quantifiziert. So kann man je nach Parameterkonstellation folgende Beobachtungen anstellen. Bei einem mittleren Bid-Ask-Spread von 5% muss der Investor mit einer zusätzlichen Standardabweichung des Hedgefehlers von bis zu 2% rechnen, stehen ihm bei der Kalibrierung außerdem keine OTM-Optionen zur Verfügung, mit bis zu 11%. Stehen dem Investor nur Optionen kurz-

er Restlaufzeit zu Verfügung, so ist die Verschlechterung im Vergleich zu dem Fall eines breiten Laufzeit-Spektrums nur marginal. Zur Parameteridentifizierung ist also ein breites Strike-Spektrum enorm wichtig, während die Laufzeiten eine untergeordnete Rolle spielen. Man erhält beispielsweise nach einer Kalibrierung ohne OTM-Optionen bei einem mittleren Bid-Ask-Spread von 5% eine ähnliche Hedgingperformance wie nach einer Kalibrierung zu einem breiten Strike-Spektrum mit einem Bid-Ask-Spread von 20%.

Im letzten Abschnitt verdeutlichen wir mit Hilfe einer empirischen Studie die Relevanz unserer Analyse. Es zeigt sich, dass scheinbar geringfügige Unterschiede in der Kalibrierung deutliche Auswirkungen auf die Hedgingperformance haben können. Insbesondere beim Hedging von OTM-Optionen treten Unterschiede von bis zu 20 Prozentpunkten in der Standardabweichung des relativen Hedgefehlers auf, je nachdem, ob die Kalibrierung zum Bid-, Ask- oder Midpreis erfolgt ist.

Literaturverzeichnis

- An, Y. und W. Suo, 2003, The Performance of Option Pricing Models on Hedging Exotic Options, Working Paper.
- Bakshi, G., C. Cao und Z. Chen, 1997, Empirical Performance of Alternative Option Pricing Models, *Journal of Finance* 52, 2003–2049.
- Bates, D.S., 2000, Post-'87 Crash Fears in the S&P Futures Option Market, *Journal of Econometrics* 94, 181–238.
- Bick, A., 1986, On Viable Diffusion Processes, *Journal of Finance* 45, 673–689.
- Black, F. und M. Scholes, 1973, The Pricing of Options and Corporate Liabilities, *Journal of Political Economy* 81, 637–654.
- Broadie, M., M. Chernov und M. Johannes, 2007, Model Specification and Risk Premia: Evidence From Futures Options, *Journal of Finance* 62, 1453–1490.
- Christoffersen, P., S. Heston und K. Jacobs, 2007, The Shape and the Term Structure of the Index Smirk: Why Multifactor Stochastic Volatility Models Work So Well, Working Paper.
- Dennis, P. und S. Mayhew, 2004, Microstructural Biases in Empirical Tests of Option Pricing Models, EFA 2004 Maastricht Meetings Paper No. 4875.

- Dieckmann, S. und M. Gallmeyer, 2005, The Equilibrium Allocation of Diffusive and Jump Risks with Heterogeneous Agents, *Journal of Economic Dynamics and Control* 29, 1547–1576.
- Duffie, D., J. Pan und K. Singleton, 2000, Transform Analysis and Asset Pricing for Affine Jump Diffusions, *Econometrica* 68, 1343–1376.
- Dumas, B., 1989, Two-Person Dynamic Equilibrium in the Capital Market, *Review of Financial Studies* 2, 157–188.
- Eraker, B., M. Johannes und N. Polson, 2003, The Impact of Jumps in Volatility and Returns, *Journal of Finance* 58, 1269–1300.
- Figlewski, S., 2004, Estimation Error in the Assessment of Financial Risk Exposure, Working Paper.
- He, C., J.S. Kennedy, T. Coleman, P.A. Forsyth, Y. Li und K. Vetzal, 2006, Calibration and Hedging under Jump Diffusion, *Review of Derivatives Research* 9, 1–35.
- Heston, S.L., 1993, A Closed-Form Solution for Options with Stochastic Volatility with Applications to Bond and Currency Options, *Review of Financial Studies* 6, 327–343.
- Liu, J., F.A. Longstaff und J. Pan, 2003, Dynamic Asset Allocation with Event Risk, *Journal of Finance* 58, 231–259.
- Liu, J. und J. Pan, 2003, Dynamic Derivatives Strategies, *Journal of Financial Economics* 69, 401–430.
- Lucas, R.E., 1978, Asset Prices in an Exchange Economy, *Econometrica* 46, 1429–1445.
- Merton, R.C., 1976, Option Pricing When Underlying Stock Returns are Discontinuous, *Journal of Financial Economics* 3, 125–144.
- Schoutens, W., E. Simons und J. Tistaert, 2003, A Perfect Calibration! Now What?, Working Paper.

Research Papers

Optimal Portfolios When Volatility can Jump

Nicole Branger, Christian Schlag, Eva Schneider

The paper has been accepted for publication in the *Journal of Banking and Finance*. It was presented at

- Swiss Society for Financial Market Research, Zurich (07.04.2006)
- Gesellschaft für Klassifikation, Berlin (08.03.2006 - 10.03.2006)
- Paris International Meeting on Finance, Paris (19.12.2005 - 20.12.2005)
- Deutsche Gesellschaft für Finanzwirtschaft, Augsburg (07.10.2005 - 08.10.2005)
- European Summer Symposium in Financial Markets, Gerzensee (23.07.2005-29.07.2005)
- Brown Bag Seminar, Goethe University, Frankfurt am Main (01.06.2005)

Summary. We consider an asset allocation problem in a continuous-time model with stochastic volatility and (possibly correlated) jumps in both the asset price and its volatility. First, we derive the optimal portfolio for an investor with constant relative risk aversion. The demand for jump risk includes a hedging component, which is not present in models without volatility jumps. We further show that the introduction of derivative contracts can have a substantial economic value. We also analyze the distribution of terminal wealth for an investor who uses the wrong model when making portfolio choices, either by ignoring volatility jumps or by falsely including such jumps although they are not present in the true model. Finally, we also investigate the impact of estimation risk. The terminal wealth distribution exhibits fatter tails than under the correct model, and in some cases there is also significant default risk.

1 Introduction and Motivation

The key risk factors considered in option pricing models, besides the diffusive price risk of the underlying asset, are stochastic volatility and jumps, both in the asset price and its volatility. Models that include some or all of these factors were developed by Merton (1976), Heston (1993), Bates (1996), Bakshi, Cao and Chen (1997), and Duffie, Pan and Singleton (2000). The importance of jumps in volatility has become apparent in

recent studies, which try to explain the time series properties of both stock and option prices, like Eraker, Johannes and Polson (2003), or Broadie, Chernov and Johannes (2007). In an asset allocation context, the main papers analyzing the impact of jumps are Liu, Longstaff and Pan (2003), Liu and Pan (2003) and Dieckmann and Gallmeyer (2005). Whereas Dieckmann and Gallmeyer (2005) consider the equilibrium allocation of diffusive and jump risks between heterogeneous agents in an exchange economy, Liu, Longstaff and Pan (2003) and Liu and Pan (2003) study a pure asset allocation problem.

In this paper, we first investigate the impact of jumps in volatility on the investor's optimal portfolio. Second, we assess the utility gain generated by the availability of derivatives. Third, we analyze the distribution of terminal wealth and the induced utility loss for an investor who uses a mis-specified model, which may be either one that does not contain volatility jumps although the true model does, or one containing such jumps although they are not part of the true model. Fourth, we show that parameter risk, which is another source of potential problems in an asset allocation process, can have consequences which are similar to those of model mis-specification.

Our analysis ties up some loose ends in the literature. We consider the portfolio planning problem in a very general setup with stochastic volatility, jumps in the stock price, and, in particular, jumps in volatility. Thereby, we extend the comparison of diffusion risk and jump risk in Liu, Longstaff and Pan (2003) to the more realistic case when derivatives are actually available to the investor. By considering a model that includes jumps in volatility, we also extend the framework in Liu and Pan (2003) who study the benefits from trading derivatives in a model without jumps in volatility.

The framework suggested here represents a significant generalization of both of these papers. We solve the model for the general case of correlated jumps in the stock price and in volatility. For the numerical analysis, we restrict the model to the simpler case where jump sizes are deterministic and where both the stock price and its volatility jump simultaneously. This allows us to focus on the key aspects of our model and it also allows for an easy comparison with the results of Liu, Longstaff and Pan (2003) and Liu and Pan (2003).

When we derive the optimal portfolio of a CRRA investor, we assume a complete market to concentrate on the impact of jumps. In the spirit of Merton (1971) we separate the overall demand for a risk factor into a myopic and a hedging component. With jumps in volatility, the optimal demand for jump risk now also contains a hedging component

not present in the Liu and Pan (2003) economy. The reason is that part of the volatility hedging can now be achieved by trading jump risk, while otherwise, all the hedging is done by trading diffusion risk.

Via derivatives the investor can achieve her optimal exposures to the fundamental risk factors. The introduction of derivatives thus always increases the investor's utility, when prices and risk premia are given exogenously. We show that this utility gain is economically significant.

Model mis-specification and parameter risk are important issues in the context of asset allocation. Given that the true model is not known, we assume that the investor either wrongly uses a model without jumps in volatility, or that she falsely includes volatility jumps in the asset allocation although they are not present in the true data generating process. With a wrong model, the investor calculates the optimal exposure to the risk factors incorrectly. Furthermore, she relies on the wrong sensitivities of the derivatives to compute the associated asset positions. Note that this second mistake can only happen when derivatives are traded, but not in a setup like in Liu, Longstaff and Pan (2003). In both situations with model mis-specification, we show that the distribution of terminal wealth exhibits more mass in both the left and the right tail. In particular, the risk of bankruptcy increases significantly. Our results imply there is nothing like a simple robust hedge against mis-specification. When measuring the impact of parameter mis-estimation, we find it to be comparable to model mis-specification in terms of its consequences for the investor's utility losses. For example, adding just one standard error to the estimated jump size in the stock price makes this parameter so close to zero that the investor basically builds her decisions on a model without price jumps.

In Section 2 we present the model. Section 3 contains the solution to the portfolio planning problem and its economic interpretation. Section 4 provides a numerical example for the impact of volatility jumps. The economic value of derivatives in the context of our model is discussed in Section 5, and model mis-specification and estimation risk are analyzed in Section 6. Section 4 concludes.

2 Model Setup

The dynamics of the stock price S and the instantaneous variance V under the true measure P are given by the following stochastic differential equations:

$$dS_t = \mu_t S_t dt + \sqrt{V_t} S_t dB_t^{(1)} + S_{t-} \left(\sum_{j,k} x^{(j)} dN_t^{(j,k)} - E^P[X] \lambda^P V_t dt \right) \quad (1)$$

$$dV_t = \kappa^P (\bar{v}^P - V_t) dt + \sigma_V \sqrt{V_t} \left(\rho dB_t^{(1)} + \sqrt{1 - \rho^2} dB_t^{(2)} \right) + \left(\sum_{j,k} y^{(k)} dN_t^{(j,k)} - E^P[Y] \lambda^P V_t dt \right). \quad (2)$$

The stock price and the variance are driven by the independent Brownian motions $B^{(1)}$ and $B^{(2)}$ and by $M \equiv J \cdot K$ independent Poisson processes $N^{(j,k)}$, each with (stochastic) intensity $\lambda^P V_t p_{jk}$ ($j = 1, \dots, J; k = 1, \dots, K$). The P -probability that a jump of any type occurs over the next time interval is equal to $\lambda^P V_t dt$, and given that a jump has occurred, the random jump sizes (X, Y) for the stock price and the variance are modeled as discrete random variables with realizations $(x^{(j)}, y^{(k)})$ and respective probabilities p_{jk} . The variance jumps have to be restricted to $y^{(k)} \geq 0$ in order to avoid negative variances, and stock price jumps have to be larger than minus one to avoid negative stock prices. The mean jump sizes are $E^P[X]$ and $E^P[Y]$.

This setup allows us to model jumps in the stock price only, jumps in the variance only, and simultaneous jumps in both. Table 1 summarizes the structure. Pure price jumps can be described by pairs $(x^{(j)}, y^{(1)}) = (x^{(j)}, 0)$ for $j \geq 2$. Analogously, pure variance jumps are represented by pairs $(x^{(1)}, y^{(k)}) = (0, y^{(k)})$ for $k \geq 2$. The correlation structure of price and variance jumps can be generated by an appropriate specification of the joint probabilities $p_{j,k}$ for $j, k \geq 2$. The event $(x^{(1)}, y^{(1)}) = (0, 0)$ is assigned zero probability in the jump size distribution, since it represents the case of no jump at all.

The interest rate r is constant and the market prices of risk are given exogenously. Following Liu and Pan (2003), we specify the pricing kernel ξ via

$$d\xi_t = -\xi_t \left(r dt + \eta^{B1} \sqrt{V_t} dB_t^{(1)} + \eta^{B2} \sqrt{V_t} dB_t^{(2)} \right) + \xi_{t-} \left\{ \sum_{j,k} \left(\frac{\lambda^Q q_{jk}}{\lambda^P p_{jk}} - 1 \right) dN_t^{(j,k)} - \left(\frac{\lambda^Q}{\lambda^P} - 1 \right) \lambda^P V_t dt \right\}.$$

The market prices of risk $\eta^{Bi} V_t$ represent the compensation per unit of $\sqrt{V_t} dB_t^{(i)}$ ($i = 1, 2$). The premium for an exposure of $+\alpha$ to a jump of size $(x^{(j)}, y^{(k)})$ (i.e. for an increase of $\alpha \cdot 100\%$ in wealth if such a jump occurs) is $\alpha \cdot (p_{jk} \lambda^P - q_{jk} \lambda^Q) V_t$. The expected excess return on equity $\mu_t - r$ is then given by $(\eta^{B1} + E^P[X] \lambda^P - E^Q[X] \lambda^Q) V_t$.

Liu and Pan (2003) have shown that in a complete market the investor can choose optimal risk factor exposures instead of optimal asset positions. To achieve market completeness with a *finite* number of traded assets in our model economy, we have to assume a discrete jump size distribution with a finite number of realizations. Nevertheless, our setup is rich enough to analyze differences between the three types of jumps discussed above. To complete the market, we need $M = J \cdot K$ derivative instruments. This assumption may not be realistic for all underlying assets, but we consider it to be justified for the major stock market indices with a large number of actively traded options.

3 Portfolio Planning Problem

3.1 Optimal Portfolio

Let ϕ_t and $\psi_t^{(i)}$, $i = 1, 2, \dots, M$, represent the fractions of wealth invested in the stock and in the M derivative assets, respectively. The stochastic differential equation for wealth is then given by

$$dW_t = W_{t-} \left\{ \left(1 - \phi_t - \sum_{i=1}^M \psi_t^{(i)} \right) r dt + \phi_t \frac{dS_t}{S_{t-}} + \sum_{i=1}^M \psi_t^{(i)} \frac{dO_t^{(i)}}{O_{t-}^{(i)}} \right\},$$

where $O_t^{(i)}$ denotes the price of the i -th derivative asset. For the following analysis, it is more useful to work with exposures to the fundamental risk factors $B^{(1)}$, $B^{(2)}$, and to the $M - 1$ different jump events. Following Liu and Pan (2003), we rewrite the dynamics of wealth in terms of these exposures:

$$\begin{aligned} dW_t = & rW_t dt + \theta_t^{B^1} W_t \left(\eta^{B^1} V_t dt + \sqrt{V_t} dB_t^{(1)} \right) + \theta_t^{B^2} W_t \left(\eta^{B^2} V_t dt + \sqrt{V_t} dB_t^{(2)} \right) \\ & + W_{t-} \left(\sum_{j,k} \theta_t^{N^{(j,k)}} dN_t^{(j,k)} - \sum_{j,k} q_{jk} \theta_t^{N^{(j,k)}} \lambda^Q V_t dt \right). \end{aligned} \quad (3)$$

On a complete market any exposure $(\theta_t^{B^1}, \theta_t^{B^2}, \theta_t^{N^{(j,k)}})$ can be obtained by suitable positions in the stock, the money market account, and the contingent claims. $\theta_t^{N^{(j,k)}}$ stands for the fraction of wealth invested in the risk factor $dN^{(j,k)}$, and thus gives the relative jump in wealth when there is a jump of size $x^{(j)}$ in the stock price and of size $y^{(k)}$ in volatility. For example, $\theta_t^{N^{(j,k)}} < 0$ means that the investor's wealth will decrease by $\theta_t^{N^{(j,k)}} \cdot 100$ percent when a jump of type (j, k) occurs.

Lemma 0.1 (Optimal exposures to fundamental risk factors). *The optimal exposures to the fundamental risk factors are given by*

$$\theta_t^{*B1} = \frac{\eta^{B1}}{\gamma} + \rho\sigma_V H(\tau) \quad (4)$$

$$\theta_t^{*B2} = \frac{\eta^{B2}}{\gamma} + \sqrt{1 - \rho^2}\sigma_V H(\tau) \quad (5)$$

$$\theta_t^{*N(j,k)} = \left[\left(\frac{p_{jk}\lambda^P}{q_{jk}\lambda^Q} \right)^{1/\gamma} - 1 \right] + \left(\frac{p_{jk}\lambda^P}{q_{jk}\lambda^Q} \right)^{1/\gamma} \left[e^{H(\tau)y^{(k)}} - 1 \right] \quad (6)$$

where $\tau = T - t$, and h and H solve the system

$$h'(\tau) = \kappa^P \bar{v}^P H(\tau) + \frac{1 - \gamma}{\gamma} r \quad (7)$$

$$H'(\tau) = a + b H(\tau) + c H^2(\tau) + \lambda^Q \sum_{j,k} q_{jk} \left[\left(\frac{p_{jk}\lambda^P}{q_{jk}\lambda^Q} \right)^{1/\gamma} \exp\{y^{(k)} H(\tau)\} \right] \quad (8)$$

with the boundary conditions $h(0) = H(0) = 0$ and

$$\begin{aligned} a &= \frac{1 - \gamma}{2\gamma^2} [(\eta^{B1})^2 + (\eta^{B2})^2] + \frac{1 - \gamma}{\gamma} \lambda^Q - \frac{1}{\gamma} \lambda^P \\ b &= -(\kappa^P + E^P[Y]\lambda^P) + \frac{1 - \gamma}{\gamma} \sigma_V \left(\rho\eta^{B1} + \sqrt{1 - \rho^2}\eta^{B2} \right) \\ c &= \frac{1}{2} \sigma_V^2. \end{aligned}$$

The indirect utility $J(t, w, v)$ is given by

$$J(t, w, v) = \frac{w^{1-\gamma}}{1-\gamma} \exp\{\gamma h(\tau) + \gamma H(\tau)v\}. \quad (9)$$

In Liu and Pan (2003), the volatility jump size Y is identically equal to zero, and Equation (8) reduces to a Riccati equation with a closed-form solution. In our model, the system (7)–(8) has to be solved numerically. Like in Liu and Pan (2003), our function H has the properties $H(\tau) \geq 0$ for $\gamma < 1$, $H(\tau) \leq 0$ for $\gamma > 1$, and $H(\tau) = 0$ for the log-investor with $\gamma = 1$ (see Appendix A), so that J is increasing in V for $\gamma \neq 1$.

3.2 Structure of Optimal Demand

The optimal demand in (4), (5), and (6) has two components first identified by Merton (1971). The investor wants to earn the risk premia (myopic demand), but also has the desire to hedge against unfavorable changes in the investment opportunity set, i.e. in our framework against changes in V (hedging demand).

In the general case where $H(\tau) \neq 0$, the investor cares about potentially adverse changes in the investment opportunity set, which generates a hedging demand in volatility. This demand is met by a position in all risk factors which have an impact on volatility, no matter whether these factors carry a premium or not. In our model with jumps in volatility, there will thus be a hedging demand for diffusion risk and also for jump risk. This latter is not present in the model analyzed by Liu and Pan (2003).

The sign of the hedging demand for volatility risk depends on the relative risk aversion γ . As discussed in Liu (2001) and Bhamra and Uppal (2006) and shown above in the discussion of the properties of the function H , the investor takes a long position in volatility for $\gamma < 1$, a short position for $\gamma > 1$, and she does not hedge for $\gamma = 1$.

The function $H(\tau)$ determines not only the direction, but also the size of the hedging demand. For $\gamma > 1$, an inspection of (8) shows that the hedging demand is increasing in the horizon and converges to an upper bound.¹ For an increasing planning horizon, the investor cares more and more about changes in the investment opportunity set, so that her hedging position will converge to a risk-minimizing hedge. Obviously, there is no use in increasing it beyond this level, since this would again increase risk.

By a similar argument, we can see that the larger the investor's risk aversion, the lower her myopic demand. This decreases the exposure to the stochastic investment opportunity set, and thus will ultimately also decrease the hedging demand, even if the desire to hedge increases. Indeed, it can be shown that the hedging demand per unit of myopic exposure converges to some limiting value when risk aversion goes to infinity.

We now analyze the demand for jump risk. Jump events are characterized by the jump sizes for the stock and the variance. However, one can see from Equation (6), that it is only the size of variance jumps $y^{(k)}$ that matters for jump demand. The myopic demand for jumps only depends on the respective risk premium, while the hedging demand is driven by the impact of the jump event on volatility, and thus depends on $y^{(k)}$ only. For two jump sizes $0 < y^{(a)} < y^{(b)}$, the hedging demand is larger in absolute terms for the larger jump $y^{(b)}$.

¹ For very small values of $\gamma < 1$ where the investor is nearly risk-neutral, we refer the reader to Kim and Omberg (1996). Kraft (2003) and Korn and Kraft (2004) also analyze the technical aspects of asset allocation in continuous time in detail.

Finally, it is interesting to see how the investor hedges against a volatility jump of size $y^{(k)}$. If there are several jump events with this same volatility jump size but different stock jump sizes, she can split her hedging demand between these jump risk events. Consider e.g. two pairs of jump size realizations $(x^{(a)}, y^{(k)})$ and $(x^{(b)}, y^{(k)})$ where $x^{(b)} < x^{(a)} < 0$ and assume that the more severe stock price jump earns the larger risk premium, i.e.

$$1 < \frac{\lambda^Q q_{ak}}{\lambda^P p_{ak}} < \frac{\lambda^Q q_{bk}}{\lambda^P p_{bk}}.$$

As can be seen from Equation (6), the hedging demand is then largest for the moderate jump event $(x^{(a)}, y^{(k)})$ with the lower risk premium. These are the jump events for which the myopic demand is smallest. Thus, the investor mainly uses those jump events in which she has a small myopic position for hedging, but does not increase an already large myopic position.

4 Numerical Example: Deterministic Jumps

One of the main topics of our paper is the impact of variance jumps on the structure of the optimal demand functions. As we have seen in Section 3, with jumps in volatility the jump demand exhibits a hedging component in addition to the speculative part. We now investigate the impact of variance jumps and their size on optimal exposures to risk factors and optimal portfolio decisions.

For this numerical example, we focus on the framework used for the examples in Liu, Longstaff and Pan (2003) with deterministic jump sizes for the asset price and the variance, i.e. we set $X \equiv \mu_X$ and $Y \equiv \mu_Y$. The pricing of jump risk then only depends on the difference between λ^P and λ^Q , and the market is complete with two non-redundant derivatives only.² Assuming the empirically well-supported case $\mu_X < 0$ and $\mu_Y > 0$, a jump decreases prices and simultaneously increases volatility, which can be regarded as an increase in uncertainty after a market crash. The numerical example is based on the benchmark parametrization in Liu, Longstaff and Pan (2003). Table 2 summarizes these values as Parametrization I, which will serve as the benchmark for later comparisons across models.

² See Liu and Pan (2003) for the necessary restriction on the local sensitivity matrix and the transformation from risk exposures to asset positions.

To assess the impact of variance jumps, we compare the optimal portfolio for Parametrization I to one where $\mu_Y = 0$. The other parameters are adjusted such that the overall characteristics of the investment opportunity set are as similar as possible across the two values of μ_Y . In general, the parameters plugged in the model chosen by the investor must yield correct values for expected stock returns, option prices, and risk premia (see Appendix B). This parametrization for $\mu_Y = 0$ is shown as Parametrization II in Table 2.

We assume that the derivatives used by the investor to form her portfolio are the two 3-month call options also used for the calibration. Note that this choice is arbitrary, since in our complete markets setting any two linearly independent derivative contracts could be used. So the optimal exposures represent the basic result, whereas the optimal asset positions are 'derived'.

The left panel of Figure 1 shows the optimal exposures to the fundamental risk factors for varying time horizons and the two values of μ_Y . For very short horizons the optimal exposures almost exclusively reflect myopic demand, so all differences between the parametrizations can be attributed to different risk premia.³ When $\mu_Y = 0$ we are in the Liu and Pan (2003) case and all the variance risk is attributed to the two diffusion risk factors, which increases the hedging component of the demand, while for jump risk, there is only myopic demand, which does not depend on the planning horizon. For positive μ_Y , jump risk becomes relevant for the hedging of volatility risk. Consequently, the planning horizon now has an impact on the optimal exposure to jump risk, while it has less impact on the optimal diffusion exposure.

For the asset positions, shown in the right panel of Figure 1, the differences between the two models are much more pronounced. This is true even for $\tau = 0$, despite very similar optimal exposures. The main reason are differences in the sensitivities of the derivatives across the two models. The value of μ_Y thus has a significant impact on the optimal portfolio. For example, for $\mu_Y = 0$ the optimal position in the stock is negative for longer planning horizons, while it is positive for $\mu_Y > 0$. Finally, we observe that for longer planning horizons the optimal positions tend towards an 'asymptotic' value depending on μ_Y .

³ Note that in our example, the risk premia differ only for $\sqrt{V}dB^{(2)}$.

5 Economic Value of Derivatives

In contrast to the economy discussed in Liu, Longstaff and Pan (2003), the market is assumed to be complete in our model. A comparison to their setup allows us to assess the economic value of trading derivatives, thus also extending the analysis of Liu and Pan (2003) to the case with jumps in volatility. Clearly, this represents a first step, since the prices of assets already traded are assumed to remain unchanged when derivatives are introduced. Compared to a situation with an incomplete market, the investor's utility will thus increase.

To measure this increase, we use the portfolio improvement $\mathcal{R}^{\mathcal{W}}$ as proposed by, among others, Liu and Pan (2003). It is defined as the annualized percentage difference in certainty equivalent wealth $\mathcal{R}^{\mathcal{W}} = T^{-1} \ln \left(\mathcal{W} / \widehat{\mathcal{W}} \right)$, where \mathcal{W} and $\widehat{\mathcal{W}}$ are the certainty equivalent wealth levels for the case with and without derivatives, respectively.⁴ The certainty equivalent wealth $\widehat{\mathcal{W}}$ can be computed in closed form following Liu, Longstaff and Pan (2003), while the computation of \mathcal{W} can only be done numerically.

The analysis is based on Parametrization I from Table 2. Figure 2 illustrates $\mathcal{R}^{\mathcal{W}}$ as a function of the planning horizon τ , the speed of mean reversion κ^P , the jump risk premium λ^Q / λ^P , and the variance jump size μ_Y . Note that we do not recalibrate the model, but only vary one parameter at a time.

The dependence of $\mathcal{R}^{\mathcal{W}}$ on τ can be interpreted as follows. For $\tau = 0$, there is only myopic demand, and the portfolio improvement of 3% arises from the investor's ability to achieve this optimal speculative demand. For increasing τ , there is an additional gain from a better hedge position, and the improvement stabilizes at roughly 5.5% for horizons beyond two years.

For κ^P between 1 and 2, the investor's optimal demand in an economy with derivatives is most different from the risk package offered by the stock and the money market account only, and $\mathcal{R}^{\mathcal{W}}$ is maximal. When κ^P increases, shocks in variance have a smaller impact, and the variance of variance decreases. Consequently, the hedging demand tends to zero, and the portfolio improvement is only due to the possibility to achieve the optimal myopic exposure.

⁴ \mathcal{W} and $\widehat{\mathcal{W}}$ are defined implicitly via $J(0, W_0, V_0) = (1 - \gamma)^{-1} \mathcal{W}^{1-\gamma}$ and $\widehat{J}(0, W_0, V_0) = (1 - \gamma)^{-1} \widehat{\mathcal{W}}^{1-\gamma}$ with J (\widehat{J}) representing the indirect utility function with (without) derivatives. Since the investor has constant relative risk aversion, $\mathcal{R}^{\mathcal{W}}$ does not depend on W_0 .

The impact of λ^Q is shown in the lower left graph. The higher λ^Q relative to the (fixed) λ^P , the larger the compensation for jump risk, and the more valuable it becomes to have derivatives available to put together an optimal portfolio. Furthermore, a change in λ^Q changes the optimal myopic exposure to jump risk and the hedging exposure to all three risk factors. The portfolio improvement again increases in the difference between the resulting optimal exposure and the one achievable through the stock only.

Finally, the lower right graph shows the portfolio improvement for a varying variance jump size μ_Y . The larger μ_Y , the larger the variance of variance, and the larger the investor's hedging demand. Trading in derivatives thus becomes more valuable, and the portfolio improvement increases in μ_Y .

6 Model Mis-Specification and Parameter Sensitivities

6.1 Model Mis-Specification

In the context of volatility jumps, model mis-specification can go two ways. The investor either uses a model that is 'too small', e.g. by ignoring volatility jumps, or one that is 'too large', e.g. by including such jumps although they are not part of the true model. When different models are used, the analysis in Section 4 has shown that asset positions and optimal exposures to risk factors usually change noticeably. However, the ultimate measure for the impact of model mis-specification is the loss in utility the investor has to suffer when using incorrect dynamics for the stock price or for volatility.

When derivatives are traded, the investor makes two mistakes in case of model mis-specification. First, she calculates the (seemingly) optimal exposure to the risk factors, where she uses the improper model. Second, she transforms these exposures into asset demands, using the sensitivities of the derivatives from the incorrect model. This second mistake is not made in the setup of Liu, Longstaff and Pan (2003), who only consider trading in the stock and the money market account, i.e. in linear claims with model-independent sensitivities.

We first consider the situation where the true model is given by Parametrization I from Table 2, while the investor ignores volatility jumps, i.e. uses Parametrization II from Table 2. The left panel of Figure 3 shows the realized exposures as a function of the planning horizon. A comparison of these graphs with the (seemingly) optimal exposures

from the left panel of Figure 1 shows that the use of incorrect sensitivities can have a significant impact. In particular, in the correct model with $\mu_Y = 0.22578$, the optimal exposure to jump risk is increasing in the planning horizon (in absolute terms), while in the improper model with $\mu_Y = 0$, the investor considers a constant exposure to be optimal, and she ends up with an exposure to jump risk that is actually decreasing in the planning horizon (in absolute terms).

The right panel of Figure 3 shows the results for the opposite case of model misspecification. The realized exposures to the risk factors are higher in absolute value compared to the optimal case, so that the investor holds positions with a higher level of risk. Whereas the optimal exposure to jump risk in the true model is now constant for all investment horizons, the realized exposure increases with the investment horizon in absolute value.

Knowledge of realized exposures under a mis-specified model is the necessary prerequisite to determine the utility loss suffered by an investor who bases her decision on an incorrect specification. Since the sensitivities of the derivatives depend on the current level of volatility, the difference between optimal and realized risk exposures will in general depend on V , too. Thus, the indirect utility for the mis-specified model cannot be computed in closed-form as in Liu, Longstaff and Pan (2003), but we have to resort to Monte Carlo simulation.

Furthermore, the lower bound on the jump risk exposure, $\theta^N \geq -1$ which is supposed to prevent default naturally holds for the (seemingly) optimal exposure, but not for the realized exposure. Thus, default becomes possible in a mis-specified model, and in the realistic case of $\gamma \geq 1$, the utility of terminal wealth will go to minus infinity. The indirect utility may thus take on large negative values, and the portfolio improvement as calculated in Section 5 has no real meaning anymore. We therefore focus on the comparison of the distributions of terminal wealth for the true and the mis-specified model.

In our simulation exercise we use 500,000 runs with two time steps per day. The assets available to the investor are the stock, the money market account, and two call options with a constant maturity of three months and strike prices equal to 90 and 100 percent of the current stock price. This implies that the investor always trades in a new set of options. We simulate the dynamics of the investor's wealth using the realized exposures to the risk factors.

The results are shown in Figure 4. The upper (lower) graphs show the cumulative distribution functions of terminal wealth for an investment horizon of 1 year (5 years). In the two graphs in the left column the true model contains jumps in volatility, whereas in the right column, $\mu_Y = 0$ in the true model.

In general the use of a wrong model generates a higher probability of large positive levels of terminal wealth, but also a higher risk of ending up with a wealth close to zero. Surprisingly, in the case where the true model does not contain volatility jumps and where the investor thus uses a model that is too sophisticated, the difference between the two distributions is even more pronounced. Additionally, we observe a shortfall probability of roughly 5% for an investment horizon of 5 years. The right panel of Figure 3 can help to explain this seemingly strange result. It shows that when a model with jumps in volatility is used, the realized exposures to the risk factors are much higher than optimal. Especially for jump risk, the realized exposure is much too high, so that if a jump occurs, wealth may easily become negative.

Our results thus emphasize the importance of identifying the correct model, since there is no simple hedge against model mis-specification. Neither the use of a (perhaps) too simple nor the use of a (perhaps) too sophisticated model offers a reliable protection against significant utility losses.

6.2 Parameter Sensitivities

A second problem besides model mis-specification is parameter risk. In this case, the investor uses the correct type of model, but with incorrect parameters. Given that the parameters have to be estimated, this mistake is quite likely to happen due to sampling error. To assess its impact, we apply the same methodology as above, with the only difference that now the true and the assumed model are of the same type, but with different parametrizations.

The true model is given by Parametrization I from Table 2. We then consider a one standard error deviation from the point estimate for each parameter individually. The exact numerical values for the point estimates as well as for the upper and lower bounds are given in Table 3. The standard errors are taken from the empirical studies of Pan (2002) and Eraker, Johannes and Polson (2003). Since jump events are rare, estimation risk is certainly an issue for the jump intensity and the jump sizes of stock

and volatility. Furthermore, we consider a mis-estimation of the speed of mean reversion κ^P . Different from the above analysis, we do not recalibrate the model since we want to focus on a situation where only one parameter is varied. It is clear that the initial prices for the derivatives in our asset allocation problem will then change. However, this seems preferable to the case where the model is recalibrated, since then all the parameters would change simultaneously, which would make it basically impossible to measure the impact of estimation error in only one parameter.

Figure 5 compares the distributions of optimal terminal wealth with and without parameter risk. The larger the differences, the larger the utility loss. A first look at the graphs shows that estimation risk for κ^P , μ_Y , and λ^P has very similar consequences, while μ_X seems to play a special role. The reason for this is that the upper bound of the interval for μ_X in Table 3 is very close to zero, so that estimation risk almost turns into model mis-specification by assuming a model without price jumps. The realized jump exposure will often violate the bound $\theta^N \geq -1$, so that one jump leads to immediate default.

Furthermore, it is obvious that estimation risk can be just as significant as the risk of model mis-specification. For example, the area between the distributions for a variation of λ^P between its upper and lower bound is absolutely comparable to the left graph in the lower panel of Figure 4, which compares the distributions for the case when the investor incorrectly omits volatility jumps from her model.

7 Conclusion

Jumps in volatility are a phenomenon recently discussed in the literature dealing with the properties of stock prices or with option pricing. One of the main questions is in which situations and for which problems the inclusion of this additional risk factor has a significant economic impact.

We discuss a continuous-time asset allocation problem under very general dynamics for the stock price and its variance. The jump size distribution can capture both simultaneous jumps in the two processes as well as individual jumps in the stock price or the variance. Nevertheless, we retain market completeness by introducing a sufficient number of additional traded assets.

The main result of our theoretical analysis is that, compared to the case without jumps in volatility, the demand for jump risk now also exhibits a hedging component.

The hedging demand against unfavorable changes in volatility is now split up between the two diffusions and the jump factor.

Besides this theoretical innovation, we also assess the economic benefits generated by the availability of derivatives. In our framework derivatives actually complete the market, so that an investor who has access to derivatives can achieve any desired exposure to the fundamental risk factors. Our results show that the gains from trading derivatives are indeed economically significant.

Since complicated option pricing models are sometimes hard to calibrate to market data we investigate the cases in which an investor either uses a simplified model ignoring volatility jumps, or a too sophisticated model which wrongly includes volatility jumps. We find that both ways of model mis-specification have a significant impact on optimal exposures and portfolios.

Furthermore, the risk that parameters are estimated with error represents a source of significant utility losses for the investor. These losses can even reach the same magnitude as those observed for model mis-specification. Taken together our results emphasize the importance of identifying the correct model and show that the issue of jumps in volatility should not be ignored.

The analysis in this paper is performed with exogenously specified market prices of risk. Further research could therefore focus on general equilibrium issues and on a comparison of the impact of stochastic volatility with that of investor heterogeneity. This would also allow us to see which investors take long and short positions, and to study the trading volume in derivatives.

References

- Bakshi, G., C. Cao and Z. Chen, 1997, Empirical Performance of Alternative Option Pricing Models, *Journal of Finance* 52, 2003–2049.
- Bates, D.S., 1996, Jumps and Stochastic Volatility: Exchange Rate Processes Implicit in Deutsche Mark Options, *Review of Financial Studies* 9, 69–107.
- Bhamra, H.S. and R. Uppal, 2006, The role of risk aversion and intertemporal substitution in dynamic consumption-portfolio choice with recursive utility, *Journal of Economic Dynamics and Control* 30, 967–991.

- Broadie, M., M. Chernov and M. Johannes, 2007, Model Specification and Risk Premia: Evidence From Futures Options, *Journal of Finance* 62, 1453–1490.
- Dieckmann, S. and M. Gallmeyer, 2005, The Equilibrium Allocation of Diffusive and Jump Risks with Heterogeneous Agents, *Journal of Economic Dynamics and Control* 29, 1547–1576.
- Duffie, D., J. Pan and K. Singleton, 2000, Transform Analysis and Asset Pricing for Affine Jump Diffusions, *Econometrica* 68, 1343–1376.
- Eraker, B., M. Johannes and N. Polson, 2003, The Impact of Jumps in Volatility and Returns, *Journal of Finance* 58, 1269–1300.
- Heston, S.L., 1993, A Closed-Form Solution for Options with Stochastic Volatility with Applications to Bond and Currency Options, *Review of Financial Studies* 6, 327–343.
- Kim, T.S. and E. Omberg, 1996, Dynamic Nonmyopic Portfolio Behavior, *Review of Financial Studies* 9, 141–161.
- Korn, R. and H. Kraft, 2004, On the Stability of Continuous-Time Portfolio Problems with Stochastic Opportunity Set, *Mathematical Finance* 14, 403–414.
- Kraft, H., 2003, Optimal Portfolios and Heston’s Stochastic Volatility Model, Working Paper.
- Liu, J., 2001, Dynamic Portfolio Choice and Risk Aversion, Working Paper.
- Liu, J., F.A. Longstaff and J. Pan, 2003, Dynamic Asset Allocation with Event Risk, *Journal of Finance* 58, 231–259.
- Liu, J. and J. Pan, 2003, Dynamic Derivatives Strategies, *Journal of Financial Economics* 69, 401–430.
- Merton, R.C., 1971, Optimum Consumption and Portfolio Rules in a Continuous Time Model, *Journal of Economic Theory* 3, 373–413.
- Merton, R.C., 1976, Option Pricing When Underlying Stock Returns are Discontinuous, *Journal of Financial Economics* 3, 125–144.
- Pan, J., 2002, The Jump-Risk Premia Implicit in Options: Evidence from an Integrated Time-Series Study, *Journal of Financial Economics* 63, 3–50.

A Properties of the Function $H(\tau)$

Since $H(0) = 0$, it follows from the differential equation (8) that

$$H'(0) = \frac{1-\gamma}{2\gamma^2} [(\eta^{B1})^2 + (\eta^{B2})^2] + \frac{1-\gamma}{\gamma} \lambda^Q - \frac{1}{\gamma} \lambda^P + \lambda^Q \sum_{j,k} q_{jk} \left[\left(\frac{p_{jk} \lambda^P}{q_{jk} \lambda^Q} \right)^{1/\gamma} \right].$$

The first term on the right hand side obviously shares the sign of $1 - \gamma$. With $\lambda^P = \alpha \lambda^Q$ and $\alpha > 0$ rewrite the remaining terms as

$$\lambda^Q f(\alpha) = \lambda^Q \left[\frac{1-\gamma}{\gamma} - \frac{1}{\gamma} \alpha + \sum_{j,k} q_{jk} \left[\left(\frac{p_{jk}}{q_{jk}} \right)^{1/\gamma} \right] \alpha^{1/\gamma} \right].$$

With λ^Q positive, this expression will be positive if and only if $f(\alpha)$ is positive. The function $f(\alpha)$ has a local extremum at

$$\alpha^* = \left(\sum_{j,k} q_{jk} \left[\left(\frac{p_{jk}}{q_{jk}} \right)^{1/\gamma} \right] \right)^{-\gamma/(1-\gamma)}$$

with

$$f(\alpha^*) = \left(\frac{1}{\gamma} - 1 \right) (1 - \alpha^*).$$

The second derivative with respect to α is positive (negative) for $\gamma < 1$ ($\gamma > 1$), so that there is a global minimum (maximum) at α^* . With Jensen's inequality and $\sum_{j,k} q_{jk} \left[\frac{p_{jk}}{q_{jk}} \right] = 1$, it follows that $\alpha^* \leq 1$ for all values of γ . The associated function values $f(\alpha^*)$ are then negative in the case $\gamma > 1$ and positive for $\gamma < 1$, so that $f(\alpha)$ is non-negative for $\gamma < 1$ and non-positive for $\gamma > 1$.

Assume now $\gamma > 1$. Then, $H'(0) < 0$, and the function $H(\tau)$ moves into negative territory over the first infinitesimal step in τ direction. Since the derivative of H is negative when H is equal to zero, and H is continuous in γ , the function can never cross the zero line. An analogous argument can be made in the case when $\gamma < 1$.

B Calibration

For the calibration, the following parameters were restricted to be identical across models: the instantaneous expected excess return on the stock (given by $(\eta^{B1} + \mu_X(\lambda^P - \lambda^Q))\bar{v}^P$), the instantaneous variance of stock returns (given by $\bar{v}^P + \mu_X^2 \lambda^P \bar{v}^P$), the instantaneous variance of variance (given by $\sigma_V^2 \bar{v}^P + \mu_Y^2 \lambda^P \bar{v}^P$ in the model with volatility jumps and

by $\sigma_V^2 \bar{v}^P$ in the one without), the average time between two jumps (given by $(\lambda^P \bar{v}^P)^{-1}$), and the relative jump size in the stock price (given by μ_X). To ultimately calibrate the model we use two European call options with a time to maturity of three months and strike prices equal to 90% and 100% of the initial stock price and a European call with one month to maturity and a strike price equal to 90% of the initial stock price.

Table 1. Jump Size Distribution

	$Y = y^{(1)} \equiv 0$	$Y = y^{(2)}$	\dots	$Y = y^{(K)}$
$X = x^{(1)} \equiv 0$	$p_{11} = 0$	p_{12}	\dots	p_{1K}
$X = x^{(2)}$	p_{21}	p_{22}	\dots	p_{2K}
\vdots	\vdots	\vdots	\ddots	\vdots
$X = x^{(J)}$	p_{J1}	p_{J2}	\dots	p_{JK}

The table shows the jump size distribution in our model. X is the random jump size in the stock price, Y is the size of the variance jump, where we assume $Y \geq 0$. The event $X = 0, Y = 0$ is assigned a zero probability in the joint distribution of X and Y , since it represents the event that no jump has occurred.

Table 2. Calibrated Parameters

	μ_Y	κ^P	κ^Q	\bar{v}^Q	σ_V	ρ	η^{B1}	η^{B2}
I	0.226	5.300	2.403	0.048	0.225	-0.570	2.45	-2.000
II	0.000	1.450	0.500	0.063	0.380	-0.321	2.45	-1.808

Parametrization I corresponds to the benchmark case of Liu, Longstaff and Pan (2003). Parametrization II is the case without jumps in volatility which corresponds to the model setup of Liu and Pan (2003). For both parameterizations, $\mu_X = -0.25$, $\lambda^P = 1.84$, and $\lambda^Q = 11.65$.

Table 3. Parameter Intervals

	κ^P	μ_Y	λ^P	μ_X
Upper Bound	3.40	0.150	1.04	-0.05
Point Estimate	5.30	0.226	1.84	-0.25
Lower Bound	7.20	0.300	2.64	-0.45

The parameter point estimates as well as the upper and lower bounds (computed as the point estimate plus and minus one standard deviation, respectively) are adapted from the empirical estimates of Pan (2002) in the case of κ^P , λ^P and μ_X and Eraker, Johannes and Polson (2003) for μ_Y .

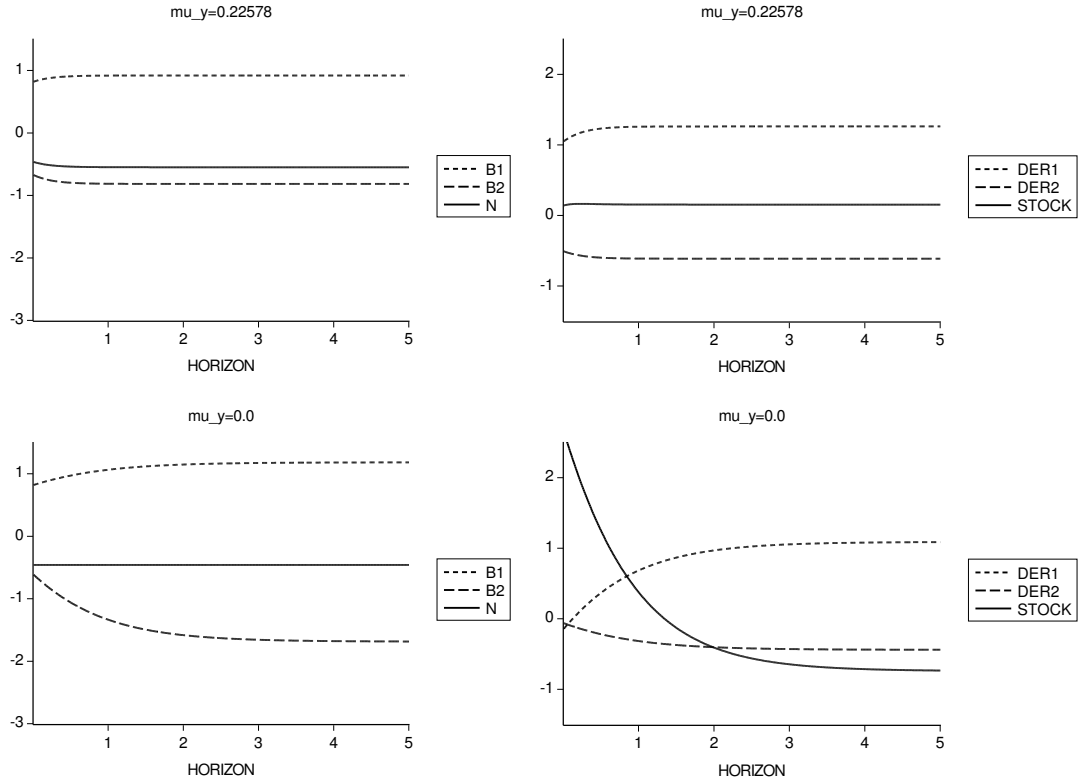


Figure 1. Optimal Risk Exposures and Asset Positions for Varying Investment Horizons

The graphs show the optimal exposures to the fundamental risk factors (left panel) and the optimal asset positions (right panel) for a varying planning horizon τ and a coefficient of risk aversion $\gamma = 3$. The upper graphs represent the benchmark case (Parametrization I in Table 2). The lower graphs represent the case $\mu_Y = 0$, i.e. the Liu and Pan (2003) economy (Parametrization II in Table 2). DER1 is a 3-month European call option with a strike price of $K = 90$, DER2 is an otherwise identical call option with strike $K = 100$. For all investment horizons, the initial value of volatility V_0 is set equal to the long-run mean \bar{v}^P , the interest rate r is 5%, and the initial stock price S_0 is set to 100.

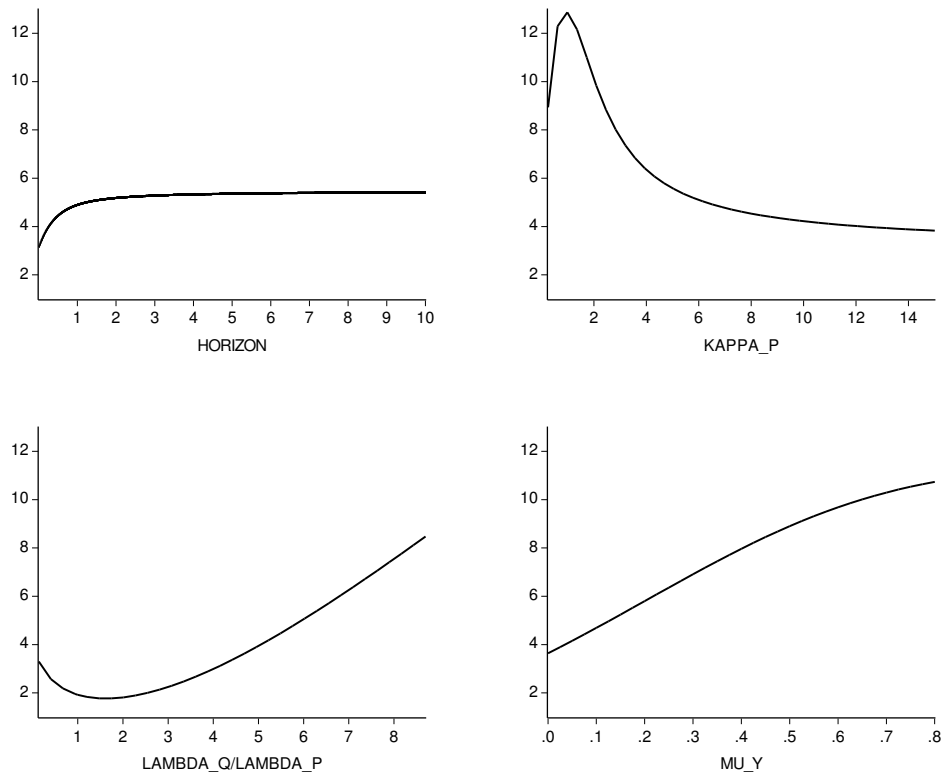


Figure 2. Portfolio Improvement from Including Derivatives [%]

The graphs show the portfolio improvement \mathcal{R}^W from including derivatives (calculated as in Liu and Pan (2003)) for varying parameters τ , κ^P , λ^Q and μ_Y . All other parameters are set to the benchmark values (Parametrization I in Table 2). The initial value of volatility V_0 is set equal to the long-run mean \bar{v}^P . Except for the upper left graph, the planning horizon τ is 10 years, the interest rate r is 5%. The coefficient of risk aversion is set to $\gamma = 3$.

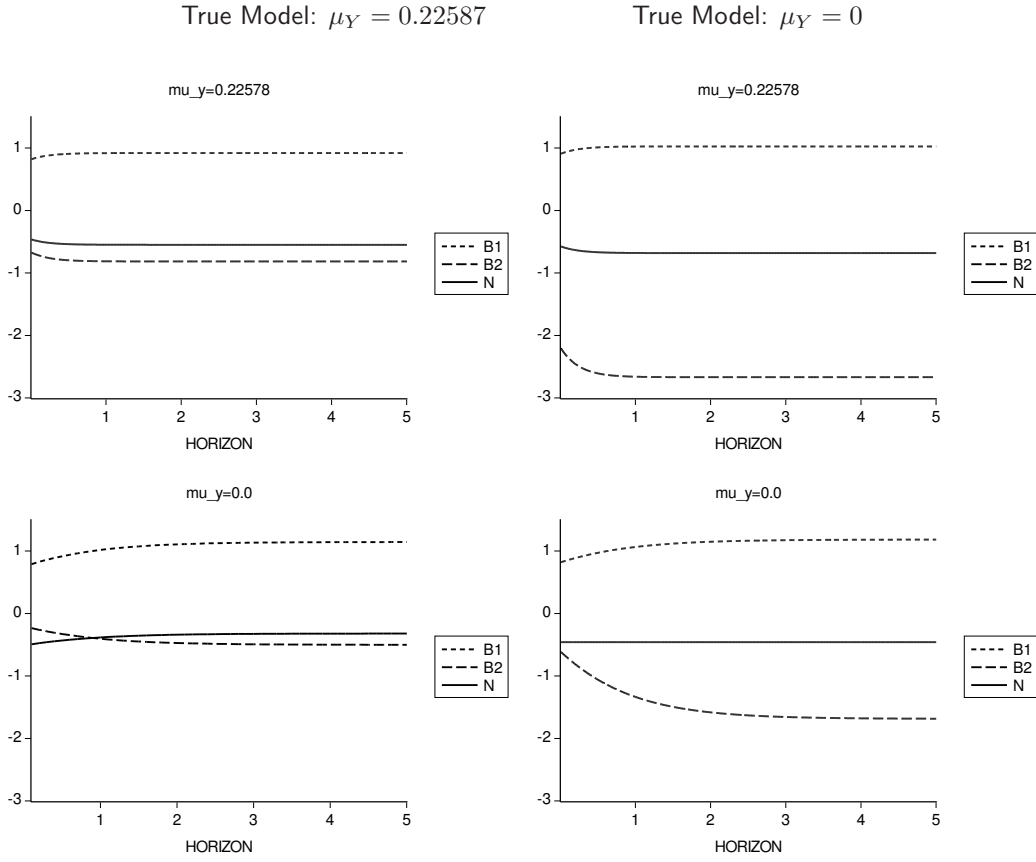


Figure 3. Realized Exposures for Varying Investment Horizons

The graphs show the realized exposures to the fundamental risk factors for an investor with varying planning horizon τ and a coefficient of risk aversion $\gamma = 3$. On the left, the true model is the model with jumps in volatility (Parametrization I in Table 2). On the right, the true model is the model without jumps in volatility (Parametrization II in Table 2). The upper graphs represent the benchmark case, when the investor relies on Parametrization I from Table 2. In the lower graphs the investor uses the model with $\mu_Y = 0.0$, i.e. the Liu and Pan (2003) economy with Parametrization II from Table 2. Traded derivatives are a European call option with a time to maturity of 3 months and strike price of $K = 90$ and an otherwise identical call option with strike $K = 100$. For all investment horizons, the initial value of volatility V_0 is set equal to the long-run mean \bar{v}^P , the interest rate r is 5% and the initial stock price S_0 is set to 100.

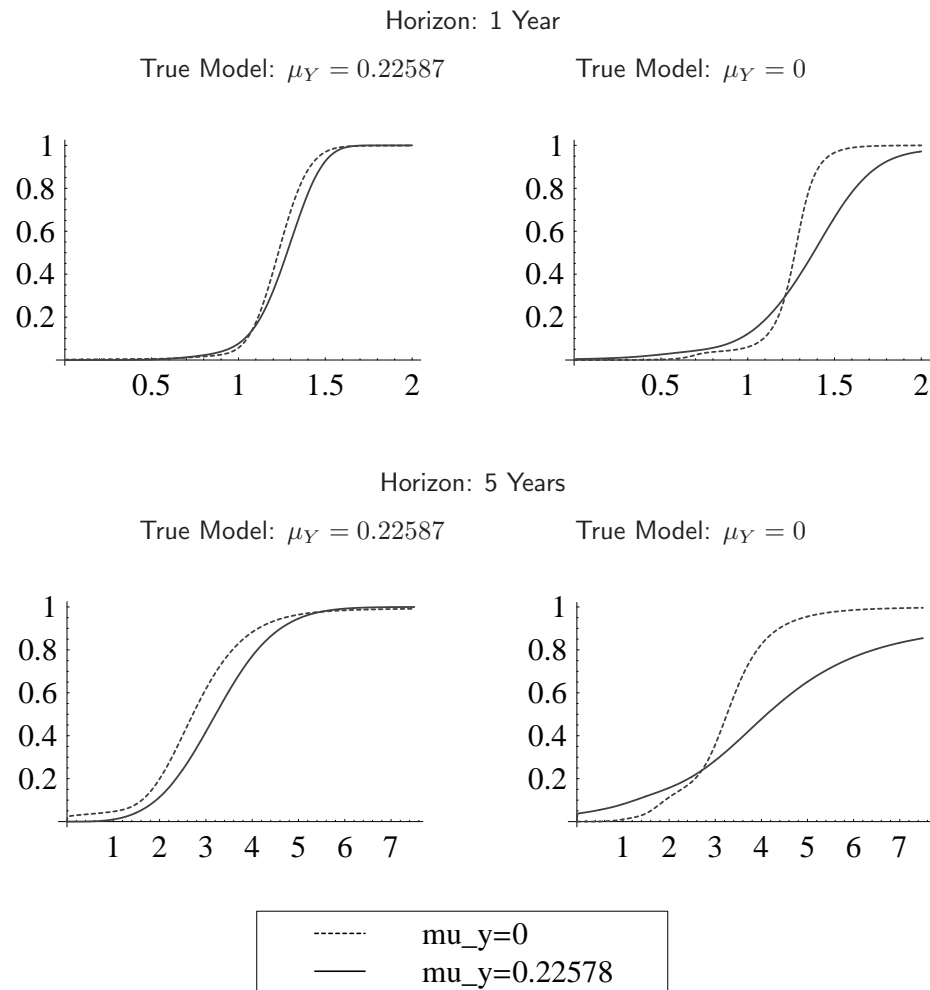


Figure 4.

Cumulative Distribution Functions of Terminal Wealth in the Presence of Model Risk

The graphs show the cumulative distribution functions of the levels of terminal wealth. On the left hand side, the true model is the model with jumps in volatility (Parametrization I from Table 2), but the investor assumes the model without jumps in volatility (Parametrization II in Table 2). On the right hand side, the true model is the model from Parametrization II, while the investor assumes Parametrization I. The coefficient of risk aversion γ is set to 3, initial wealth is set equal to 1. The starting values for the stock price and the variance are set to $S_0 = 100$ and $V_0 = \bar{v}^P$.

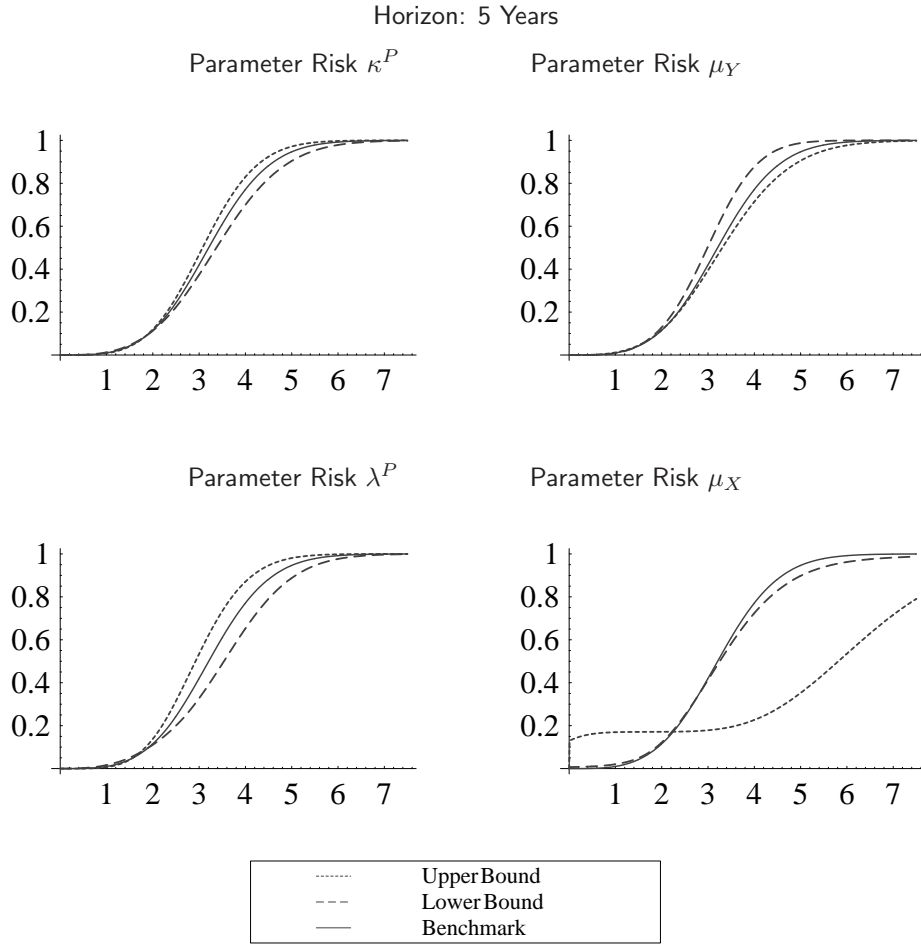


Figure 5.

Cumulative Distribution Functions of Terminal Wealth in the Presence of Parameter Risk

The graphs show the cumulative distribution functions of the levels of terminal wealth. The solid lines represent the benchmark case. The dotted and the dashed lines represent the case of parameter risk, where the parameters κ^P , μ_X , λ^P and μ_Y are varied within the empirical confidence intervals from Table 3. The dotted lines represent the case where the parameters's values equal the upper bound of the confidence interval and the dashed lines the case where they equal the lower bound. The coefficient of risk aversion γ is set to equal 3, initial wealth is set equal to 1. The starting values for the stock price and the variance are set to $S_0 = 100$ and $V_0 = \bar{v}^P$. The planning horizon τ is 5 years.

Derivatives Trading in a General Equilibrium Model With Stochastic Volatility and Jumps

Nicole Branger, Christian Schlag, Eva Schneider

This paper was presented at

- Paris International Meeting on Finance, Paris (18.12.2006 - 19.12.2006)
- Verein für Socialpolitik, Bayreuth (26.09.2006 - 29.09.2006)
- Western Finance Association, Keystone, Colorado (21.06.2006 - 24.06.2006)
- 16th Annual Derivative Securities and Risk Management Conference, Arlington, Virginia (07.04.2006 - 08.04.2006)
- Swiss Society for Financial Market Research, Zurich (07.04.2006)
- Brown Bag Seminar, Goethe University, Frankfurt am Main (07.12.2005)

Summary. We perform a general equilibrium analysis in a complete markets economy when the dividend follows a jump-diffusion process with stochastic volatility. Agents have CRRA utility, but differ with respect to their degree of risk aversion. The key output of our analysis is the structure of the investors' optimal portfolios and the volume and direction of trading between them. We find that trading in derivatives is economically significant, with a value of traded contracts of up to twenty percent of total market capitalization. In line with intuition, the less risk-averse investor holds more pure stock price risk than the more risk-averse one. Volatility derivatives, on the other hand, are special in the sense that the direction of trading depends on the exact values for the levels of risk aversion of the individual investors, not just on who is more and who is less risk-averse. We perform a general equilibrium analysis in a complete markets economy when the dividend follows a jump-diffusion process with stochastic volatility. Agents have CRRA utility, but differ with respect to their degree of risk aversion. The key output of our analysis is the structure of the investors' optimal portfolios and the volume and direction of trading between them. Trading in derivatives is economically significant, with a value of traded contracts of up to twenty percent of total market capitalization. Volatility derivatives are special in the sense that the direction of trading depends on the exact values for the levels of risk aversion of the individual investors, not just on who is more and who is less risk-averse.

1 Introduction

Heterogeneity, be it with respect to beliefs, risk aversion, or time preference, is the primary source of the desire to trade in general equilibrium models. When all investors are the same, there will obviously be no trade, and the optimal asset positions are the same for all agents in the economy.

The key contribution of our paper is an analysis of the direction and volume of trading between heterogeneous investors with different degrees of risk aversion in an economy where the dividend process exhibits stochastic volatility (SV) and jumps. The jumps can affect both the dividend level and its volatility. Trading between investors is caused by differences in their optimal exposures to these risk factors. We consider 'pure' derivatives, which provide exposure to one risk factor only. Our numerical examples show that the desire to trade can be rather strong. The value of derivative contracts outstanding reaches up to 20 percent of total market capitalization for reasonable levels of and differences in risk aversion, like levels of constant relative risk aversion equal to 2 and 4, respectively.

We perform our analysis in a standard Lucas (1978) tree economy. The dividend process is given exogenously, and investors derive utility from intermediate consumption. As stated above, the dividend exhibits SV and jumps. Stochastic volatility of dividends allows to capture changes in economic uncertainty, which occur e.g. over the business cycle. Technology shocks or catastrophe events which may change the level of dividends and/or increase economic uncertainty are introduced into the model through jump events.

We first derive the endogenous risk premia for the different risk factors and the endogenous risk-free interest rate. Second, we analyze the optimal demands of the individual investors and the resulting volume and direction of trading between them. The focus of our paper is on the impact of heterogeneity with respect to risk aversion. We thus assume the ideal setup of a complete market with symmetric information, and without model uncertainty, learning, or trading restrictions. Furthermore, we rely on standard time-additive utility functions with constant relative risk aversion.

We are not the first to analyze equilibria in economies with heterogeneous agents. Dumas (1989) considers an infinite horizon production economy with two groups of investors which differ in their level of risk aversion, but he makes the restrictive assumption that one investor type has log utility. Bhamra and Uppal (2005) analyze both complete and incomplete markets under heterogeneity, where the incompleteness is generated by

the impossibility to trade in the risk-free bond, whereas Franke and Lüders (2006) focus on the impact of a decreasing relative risk aversion of the representative investor caused by investor heterogeneity. Our paper represents a generalization by including SV and jumps and by lifting the assumption of the first two papers that one of the investors has to be myopic.

The paper closest to ours is Dieckmann and Gallmeyer (2005). They investigate optimal risk-sharing in a heterogeneous economy (one investor having log utility) and find that the less risk-averse agent purchases jump risk insurance from the more risk-averse. This may seem surprising at first, but it is plausible since the total position in jump risk (from the stock and the insurance contract together) is still higher for the less risk-averse agent. The authors obtain closed-form solutions for the market prices of risk, and price the stock numerically via Monte Carlo simulation. We structurally extend their analysis by including SV and jumps in volatility and by allowing for general degrees of risk aversion of the two investors.

The remainder of this paper is structured as follows. In Section 2 we describe the model setup and discuss the equilibrium in an economy with heterogeneous agents. We also analyze the implications of heterogeneity for the investors' optimal risk exposures. In Section 3 we study the trading volume in derivatives, generated by investor heterogeneity, and the general size of derivatives markets in our model economy. Section 4 concludes.

2 Model

2.1 Stochastic Setup

We consider a Lucas (1978) tree economy where the dividend represents aggregate endowment, and the stock is a claim to this dividend stream. The dividend follows a jump-diffusion process with stochastic volatility, and the dynamics of the dividend and its local variance are given by the following system of stochastic differential equations:

$$\begin{aligned} dD_t &= (\mu_0 + \mu_1 V_t) D_t dt + \sqrt{V_t} D_t dB_t^{(1)} + D_{t-} \left(\sum_{j,k} x^{(j)} dN_t^{(j,k)} - E^P[X] \lambda^P V_t dt \right) \quad (1) \\ dV_t &= \kappa^P (\bar{v}^P - V_t) dt + \sigma_V \sqrt{V_t} \left(\rho dB_t^{(1)} + \sqrt{1 - \rho^2} dB_t^{(2)} \right) \\ &\quad + \left(\sum_{j,k} y^{(k)} dN_t^{(j,k)} - E^P[Y] \lambda^P V_t dt \right). \end{aligned}$$

Uncertainty is generated by the independent Brownian motions $B_t^{(1)}$ and $B_t^{(2)}$ and by $M \equiv J \cdot K$ independent Poisson processes $N_t^{(j,k)}$ ($j = 1, \dots, J; k = 1, \dots, K$), each with (stochastic) intensity $\lambda^P V_t p_{jk}$. There are thus M different Poisson processes for the M different combinations of the jump sizes for the dividend level and its volatility. Equivalently, one could model the jump sizes as discrete random variables with possible realizations $x^{(j)}$ for the dividend and $y^{(k)}$ for its variance. The physical probability that a jump occurs over the next interval of length dt at all is equal to $\lambda^P V_t dt$, and given that a jump has occurred, the random jump sizes (X, Y) have realizations $(x^{(j)}, y^{(k)})$ with probabilities p_{jk} . The variance jumps have to be restricted to values $y^{(k)} \geq 0$ in order to avoid negative values for variance V_t , and analogously dividend jumps have to satisfy $x^{(j)} \geq -1$.

This setup is very general, and it enables us to model three different kinds of jumps in the economy: jumps in the dividend only, jumps in the variance only, and simultaneous jumps in both processes. Table 1 summarizes the general jump size distribution. Jumps in the dividend only can be described by pairs $(x^{(j)}, y^{(1)}) = (x^{(j)}, 0)$ for $j \geq 2$. These jumps have an individual intensity under the P -measure equal to $\lambda^P V_t p_{j1}$, so that the (total) intensity for a pure dividend jump is given by $\lambda^P V_t \sum_{j=2}^J p_{j1}$. Analogously, pure variance jumps are represented by pairs $(x^{(1)}, y^{(k)}) = (0, y^{(k)})$ for $k \geq 2$. Simultaneous jumps in the dividend and its variance are given by all other pairs $(x^{(j)}, y^{(k)})$ for $j, k \geq 2$. The desired correlation structure of dividend and variance jumps can be generated by an appropriate specification of the joint probabilities. The event $(x^{(1)}, y^{(1)}) = (0, 0)$ is assigned zero probability, since it obviously represents the case of no jump at all.

For our numerical computations below we will assume simultaneous jumps with constant jump sizes in stock and volatility. We use the parametrization in Table 2 for the dividend process, which is adapted from the estimates of Liu, Longstaff and Pan (2003) for the stock price process. We set the additional parameters μ_0 and μ_1 characterizing the drift of the dividend in Equation (1) equal to 0.01 and 2.75, respectively, and the planning horizon T equal to 1 year. Since the focus of our analysis is on trading volume in derivatives, this rather short horizon is sufficient for the purposes of our analysis. To study issues like excess volatility or return predictability, on the other hand, it would be necessary to use longer horizons, maybe even infinity.

The general dynamics of the pricing kernel in our model are given by

$$\begin{aligned}
d\xi_t = & -\xi_t \left\{ r_t dt + \eta_t^{(B1)} dB_t^{(1)} + \eta_t^{(B2)} dB_t^{(2)} \right\} \\
& + \xi_{t-} \left\{ \sum_{j,k} \left(\frac{\lambda_t^Q q_{jk}}{\lambda^P p_{jk}} - 1 \right) dN_t^{(j,k)} - \left(\frac{\lambda_t^Q}{\lambda^P} - 1 \right) \lambda^P V_{t-} dt \right\}, \quad (2)
\end{aligned}$$

where $\eta_t^{(B1)}$ is the market price of risk for one unit of $dB_t^{(1)}$ and $\eta_t^{(B2)}$ is the market price of risk for one unit of $dB_t^{(2)}$. The compensation for an exposure of α to a jump of size $(x^{(j)}, y^{(k)})$ is $\alpha \cdot (p_{jk} \lambda^P - q_{jk} \lambda_t^Q) V_{t-}$, where q_{jk} and λ^Q are the probability of a jump of size $(x^{(j)}, y^{(k)})$ and the jump intensity under the risk-neutral measure Q .

We assume a complete market where the stock, the money market account, and a sufficient number of derivatives are traded. The jump size distribution introduced above is discrete, so that a finite number of traded assets is enough to complete the market, while we are nevertheless able to study the impact of stochastic jumps.¹ Furthermore, the discrete jump size distribution in our model can certainly be specified with a fine enough grid to approximate a continuous distribution in a satisfactory fashion. In the special case with simultaneous and deterministic jumps of size j_D in the dividend and j_V in its volatility only two non-redundant derivatives are needed to complete the market, one to hedge volatility risk and the other one to hedge jumps of deterministic size.

2.2 Equilibrium

Investors are heterogeneous with respect to risk aversion. Each of the two investors is assumed to have CRRA utility, $u^{(i)}(c) = c^{1-\gamma^{(i)}}/(1-\gamma^{(i)})$ ($i = 1, 2$), with risk aversion coefficients $\gamma^{(1)} \leq \gamma^{(2)}$. The investors' objective is to maximize their respective expected life-time utility of consumption

$$E^P \left[\int_0^T e^{-\beta s} u^{(i)}(c_s^{(i)}) ds \right] \quad i = 1, 2$$

over their planning horizon T . E^P denotes the expectation under the physical measure, and β represents the constant subjective time discount rate, which is assumed to be identical for both investors.

Since the market is complete, there exists a representative investor (RI) with utility function

¹ Given that every day a very large number of different derivative contracts on the major stock market indices (like the S&P 100) are actively traded on option exchanges around the world, the assumption of market completeness does not seem too restrictive.

$$U(t, D_t) = \max_{c_t^{(1)}} \left\{ u^{(1)}(t, c_t^{(1)}) + \phi u^{(2)}(t, D_t - c_t^{(1)}) \right\}. \quad (3)$$

The constant weight ϕ depends on the distribution of initial wealth (see Duffie (2001) and Dieckmann and Gallmeyer (2005)).² Since both investors have the same subjective time discount rate, it holds that $U(t, D_t) = e^{-\beta t} U(D_t)$. In the optimum, the marginal utility of the RI satisfies

$$U_D(D_t) = u_c^{(1)}(c_t^{(1)}) = \phi u_c^{(2)}(c_t^{(2)}). \quad (4)$$

The second equality also defines the consumption sharing rule $(c^{(1)}(D_t), c^{(2)}(D_t))$. Optimal consumption is thus only a function of the dividend level. It is increasing in D_t , and one can show by differentiating both sides of Equation (4) twice with respect to D_t that the consumption $c_t^{(1)}$ of the less risk-averse investor is convex in D_t , while the consumption $c_t^{(2)}$ of the more risk-averse one is concave.

The relative risk aversion $\hat{\gamma}$ of the RI is defined as

$$\hat{\gamma}(D_t) = -\frac{U_{DD}(D_t)D_t}{U_D(D_t)}.$$

$\hat{\gamma}(D)$ depends on the dividend level and is decreasing in D_t , since

$$\frac{\partial \hat{\gamma}(D_t)}{\partial D_t} = -(\hat{\gamma}(D_t))^3 \frac{c^{(1)}(D_t) c^{(2)}(D_t)}{D_t^3} \left(\frac{1}{\gamma^{(1)}} - \frac{1}{\gamma^{(2)}} \right)^2 \leq 0, \quad (5)$$

and the RI becomes less risk-averse for higher dividend levels. Furthermore, $\hat{\gamma}(D)$ approaches $\max\{\gamma^{(1)}, \gamma^{(2)}\}$ and $\min\{\gamma^{(1)}, \gamma^{(2)}\}$ for $D_t \rightarrow 0$ and $D_t \rightarrow \infty$, respectively (see Benninga and Mayshar (2000)).

Since the market is complete, we can apply the martingale approach developed by Cox and Huang (1989) to solve the portfolio planning problem. The maximization problem of the RI can be written as

$$\max_{\{c_t, 0 \leq t \leq T\}} E^P \left[\int_0^T e^{-\beta t} U(c_t) dt \right] \quad \text{s.t.} \quad W_0 = E^P \left[\int_0^T \xi_t c_t dt \right].$$

Together with the equilibrium restriction $c_t \equiv D_t$, this yields the condition

$$e^{-\beta t} U_D(D_t) = y \xi_t, \quad (6)$$

² A simulation study by Franke and Lüders (2006) shows that the results are qualitatively very similar for different values of ϕ . In our numerical examples, we will set $\phi = 1$, so that $c^{(1)} = c^{(2)} = 1$ when $D = 2$, irrespective of the two levels of risk aversion.

where y is the Lagrange multiplier for the budget restriction of the RI. We then apply Ito to both sides of this optimality condition and use the general form of the dynamics of the pricing kernel from Equation (2). Comparing the coefficients in the two stochastic differential equations gives the market prices of risk and the interest rate.

The market prices of risk and the risk-neutral jump intensity for a jump of type $(x^{(j)}, y^{(k)})$ are

$$\eta_t^{(B1)} = \hat{\gamma}(D_t)\sqrt{V_t} \quad (7)$$

$$\eta_t^{(B2)} = 0 \quad (8)$$

$$\lambda_t^Q q_{jk} = \left(\frac{c^{(i)}(D_{t-}(1+x^{(j)}))}{c^{(i)}(D_{t-})} \right)^{-\gamma^{(i)}} \lambda^P p_{jk}. \quad (9)$$

Only those risk factors which locally affect the dividend are priced in equilibrium, implying that $\eta_t^{(B2)}$ has to be equal to zero. The same holds for jumps with $x^{(j)} = 0$ which have an effect on volatility, but not on the dividend level. The basic dividend risk factors $\sqrt{V_t}dB_t^{(1)}$ and $x^{(j)}dN_t$ (with $x^{(j)} \neq 0$) are in positive net supply. Therefore, they have to be held by the RI in equilibrium, and since the RI is risk-averse, the associated premia are positive, irrespective of the sign and size of the jumps.

The equilibrium interest rate is

$$\begin{aligned} r_t = & \beta + \hat{\gamma}(D_{t-})(\mu_0 + \mu_1 V_{t-}) - \frac{1}{2}\hat{\gamma}(D_{t-})[1 + \hat{\gamma}(D_{t-})]V_{t-} \\ & - \sum_{j,k} \left[\left(1 + x^{(j)}\right)^{-\hat{\gamma}(D_{t-})} - 1 + \hat{\gamma}(D_{t-})x^{(j)} \right] \lambda^P p_{jk} V_{t-} \\ & - \frac{1}{2} (\hat{\gamma}(D_{t-}))^3 \frac{c^{(1)}(D_{t-})}{D_{t-}} \frac{c^{(2)}(D_{t-})}{D_{t-}} \left(\frac{1}{\gamma^{(1)}} - \frac{1}{\gamma^{(2)}} \right)^2 V_{t-} \\ & - \sum_{j,k} \left[\left(\frac{c^{(i)}(D_{t-}(1+x^{(j)}))}{c^{(i)}(D_{t-})} \right)^{-\gamma^{(i)}} - \left(1 + x^{(j)}\right)^{-\hat{\gamma}(D_{t-})} \right] \lambda^P p_{jk} V_{t-}. \end{aligned} \quad (10)$$

The first four terms give the interest rate in an economy where the RI has a constant relative risk aversion equal to $\hat{\gamma}$. They capture the subjective time discount, the impact of the dividend growth rate (via intertemporal substitution), and the precautionary savings term due to diffusion risk and jump risk. The fifth and sixth term are due to the dependence of the relative risk aversion of the RI on the dividend level. His decreasing RRA induces an additional precautionary savings demand, which lowers the risk-free rate.

2.3 Stock Price and Aggregate Demand for Risk Factors

The stock price is given by the present value of future dividends, i.e.

$$S_t = E^P \left[\int_t^T \frac{\xi_s}{\xi_t} D_s ds \mid \mathcal{F}_t \right].$$

Using Equations (4) and (6) for the marginal utility of the RI to rewrite the pricing kernel, the stock price can be represented as

$$S_t = E^P \left[\int_t^T e^{-\beta(s-t)} \left(\frac{c^{(i)}(D_s)}{c^{(i)}(D_t)} \right)^{-\gamma^{(i)}} D_s ds \mid \mathcal{F}_t \right]. \quad (11)$$

In general, there is no closed-form solution for this expression, and we have to resort to numerical integration. The density of future dividends follows from the respective characteristic function (with numerical solutions also for the associated ordinary differential equations) and Fourier inversion (again by means of numerical integration). Details are given in Appendix A.

In equilibrium, the wealth of the RI is equal to the stock price. Therefore, the exposures of the stock price to the risk factors are equal to the optimal demand $\theta_t^{(B1)}$, $\theta_t^{(B2)}$, and $\theta_t^{(N,jk)}$ of the RI for these risk factors, i.e.

$$\begin{aligned} dS_t + D_t dt = S_t \left\{ r_t dt + \theta_t^{(B1)} \left(\sqrt{V_t} dB_t^{(1)} + \eta_t^{B1} \sqrt{V_t} dt \right) + \theta_t^{(B2)} \sqrt{V_t} dB_t^{(2)} \right\} \\ + S_{t-} \sum_{j,k} \theta_t^{(N,jk)} \left(dN_t^{j,k} - \lambda_t^Q q_{jk} V_t dt \right) \end{aligned} \quad (12)$$

where $\theta^{(B1)}$ and $\theta^{(B2)}$ are the demand for $\sqrt{V_t} dB_t^{(1)}$ and $\sqrt{V_t} dB_t^{(2)}$, respectively. $\theta_t^{(N,jk)}$ is the demand for a jump of type $(x^{(j)}, y^{(k)})$.

The stock price is a function of time t , the current dividend and the current local volatility. Applying Ito gives the exposures of the stock with respect to the risk factors:

$$\begin{aligned} \theta_t^{(B1)} &= \frac{\partial S_t}{\partial D_t} \frac{D_t}{S_t} + \frac{\partial S_t}{\partial V_t} \frac{1}{S_t} \sigma_V \rho \\ \theta_t^{(B2)} &= 0 + \frac{\partial S_t}{\partial V_t} \frac{1}{S_t} \sigma_V \sqrt{1 - \rho^2} \\ \theta_t^{(N,jk)} &= \frac{S(t, D_{t-}(1 + x^{(j)}), V_{t-}) - S(t, D_{t-}, V_{t-})}{S(t, D_{t-}, V_{t-})} \\ &\quad + \frac{S(t, D_{t-}(1 + x^{(j)}), V_{t-} + y^{(k)}) - S(t, D_{t-}(1 + x^{(j)}), V_{t-})}{S(t, D_{t-}, V_{t-})}. \end{aligned}$$

In the spirit of Merton (1971), the first term in each of these expressions can be regarded as the myopic demand, generated by the RI's desire to earn the risk premia, while the

second term represents the hedging demand, meant to protect the RI against unfavorable changes in the investment opportunity set.

The myopic demand for the second diffusion risk factor $\sqrt{V_t}dB_t^{(2)}$ is of course zero because of the zero market price of risk. The same holds true for jumps that happen in volatility only. For dividend diffusion risk, the myopic demand is given by

$$\frac{\partial S_t}{\partial D_t} \frac{D_t}{S_t} = 1 + \left\{ \hat{\gamma}(D_t) - E^P \left[\int_t^T \frac{\xi_s}{\xi_t} \frac{D_s}{S_t} \hat{\gamma}(D_s) ds \mid \mathcal{F}_t \right] \right\} \quad (13)$$

(see Appendix B for the proof). The right hand side is equal to the sum of the dividend risk exposure and a term that captures the deviation of the current $\hat{\gamma}$ from the expected future values, where the expectation is taken both across time and dividend levels. In a homogeneous economy $\hat{\gamma}$ would be constant, and the myopic demand would simply be equal to one. With heterogeneous investors, however, the change in risk aversion contributes a second term to the myopic demand. When the drift of dividends is sufficiently high, $\hat{\gamma}(D)$ will on average decrease over time, and the myopic demand will be larger than the dividend exposure. Similar results hold for the myopic demand to stock price jumps.

Any deviation of the stock risk exposure from the dividend risk exposure causes the stock price variance to deviate from the dividend variance. If the variance of the stock price is larger, we speak of excess volatility. Following the analysis above, parts of excess volatility may be explained by excess myopic demand. Furthermore, it might also be attributed to hedging demand.

In our model, the investment opportunity set is stochastic due to stochastic volatility. When volatility is high, the investor profits from a higher dividend drift (note that we assume $\mu_1 > 0$), while the increase in the risk of dividends reduces his utility. As we will show in the numerical example later on, the aggregate hedging demand for all three risk factors depends on the individual levels of risk-aversion and on the current dividend. In a homogeneous economy where all investors have the same level of risk aversion and are less risk-averse than the log investor, the increasing dividend drift turns out to be most important, and the investor takes advantage of this by a long position in volatility risk. When the risk aversion increases, the hedging motive becomes more important and induces the investor to take a short position in volatility. For even higher values of risk aversion, finally, the investor who has to hold one unit of the stock is most concerned about increases in risk and hedges by taking a long position in volatility. The effect on the hedging demand will be discussed in more detail at the end of the next section.

2.4 Individual Demands for Risk Factors

Trading is induced by different optimal demands of the individual investors. Thus, we first analyze the individual investors' wealth and their demand for risk factors. Investor i 's wealth follows as:

$$W_t^{(i)} = c^{(i)}(D_t) E^P \left[\int_t^T e^{-\beta(s-t)} \left(\frac{c^{(i)}(D_s)}{c^{(i)}(D_t)} \right)^{1-\gamma^{(i)}} ds \mid \mathcal{F}_t \right].$$

Like the stock price, this expression can be computed using Fourier inversion (see Appendix A). The optimal exposure of the investor with respect to the risk factors is equal to the exposure of $W_t^{(i)}$ to these risk factors, which follows from calculating partial derivatives and differences, respectively:

$$\begin{aligned} \theta_t^{(B1,i)} &= \frac{\partial W_t^{(i)}}{\partial D_t} \frac{D_t}{W_t^{(i)}} + \frac{\partial W_t^{(i)}}{\partial V_t} \frac{1}{W_t^{(i)}} \sigma_V \rho \\ \theta_t^{(B2,i)} &= 0 + \frac{\partial W_t^{(i)}}{\partial V_t} \frac{1}{W_t^{(i)}} \sigma_V \sqrt{1-\rho^2} \\ \theta_t^{(N,j,k,i)} &= \frac{W^{(i)}(t, D_{t-}(1+x^{(j)}), V_{t-}) - W^{(i)}(t, D_{t-}, V_{t-})}{W^{(i)}(t, D_{t-}, V_{t-})} \\ &\quad + \frac{W^{(i)}(t, D_{t-}(1+x^{(j)}), V_{t-} + y^{(k)}) - W^{(i)}(t, D_{t-}(1+x^{(j)}), V_{t-})}{W^{(i)}(t, D_{t-}, V_{t-})}. \end{aligned}$$

Details on the numerical computation of the partial derivatives are given in Appendix C.

In analogy to the aggregate case, the myopic demand for the second diffusion risk factor and for pure volatility jumps is zero. The myopic demand for the first diffusive risk factor again depends on the dividend elasticity of wealth (see Appendix C for computational details):

$$\begin{aligned} \frac{\partial W_t^{(i)}}{\partial D_t} \frac{D_t}{W_t^{(i)}} &= 1 + \left\{ \widehat{\gamma}(D_t) - E^P \left[\int_t^T \frac{\xi_s}{\xi_t} \frac{c^{(i)}(D_s)}{W_t^{(i)}} \widehat{\gamma}(D_s) ds \mid \mathcal{F}_t \right] \right\} \\ &\quad + E^P \left[\int_t^T \frac{\xi_s}{\xi_t} \frac{c^{(i)}(D_s)}{W_t^{(i)}} \left(\frac{\widehat{\gamma}(D_s)}{\gamma^{(i)}} - 1 \right) ds \mid \mathcal{F}_t \right]. \end{aligned} \quad (14)$$

As for the aggregate myopic demand in Equation (13), the first term on the right-hand side of Equation (14) is equal to one and thus equal to the dividend risk exposure. The second term is due to changes in the aggregate risk aversion over time. Like the RI, individual investors take these changes into account. The wealth-weighted sum of this term over the two investors equals the last term in Equation (13), i.e. the aggregate excess myopic demand. As discussed above, this component of the demand is positive for the RI, and

it is greater for the less risk-averse investor than for the more risk-averse one. Finally, the last term arises due to different risk aversions of the investors. It is positive for the less risk-averse investor, for whom a market price of risk $\hat{\gamma}(D)\sqrt{V}$ represents a rather attractive investment opportunity, and negative for her more risk-averse counterpart. The wealth-weighted sum of this component of the demand over the investors is zero.

In our model trading is generated by differences between currently given and optimal exposures to the different risk factors. Figures 3, 2, and 1 show the components of optimal demand for the two diffusions and the jump factor as a function of the dividend level for the $(\gamma^{(1)}, \gamma^{(2)})$ -combinations (2.0, 4.0), (0.8, 2.0), and (0.5, 0.8), respectively. These combinations of risk aversion levels were chosen to see whether heterogeneity has different implications depending on the absolute levels of risk aversion relative to the usual benchmark of log utility. For the numerical example, we restrict the analysis to the special case with simultaneous and deterministic jumps of size j_D in the dividend and j_V in its volatility.

The three graphs on the left show the hedging demand for the risk factors $\sqrt{V_t}dB_t^{(1)}$, $\sqrt{V_t}dB_t^{(2)}$ and dN_t , while the graphs on the right represent the myopic component of demand (which is always equal to zero for $\sqrt{V_t}dB_t^{(2)}$ and therefore not shown). The three curves in each picture represent the two individual investors' and the RI's demand. As can be seen from the scales of the graphs, the absolute value of the hedging component is always significantly smaller than the myopic demand for $B^{(1)}$ and N . The primary reason to hold these risk factors in the optimal portfolio is thus to earn the risk premium. Of course, $B^{(2)}$ is held exclusively for hedging purposes.

Myopic demand

As discussed above and stated in Equation (13), the aggregate myopic demand differs from the dividend risk exposure. However, our numerical example shows that this deviation is numerically quite small. The myopic demand for $\sqrt{V_t}dB_t^{(1)}$ is very close to 1, and that for N is more or less equal to $j_D = -0.25$, the values for the dividend exposures. An important reason for this lack of excess volatility is the relatively short horizon of $T = 1$ that we consider in our examples.

While investor heterogeneity thus has a minor impact on the aggregate myopic demand, the individual myopic demand levels differ significantly. The myopic demand $\theta^{(B1,1)}$

of the less risk-averse investor is higher than that of the more risk-averse agent. On average across the three scenarios, it amounts to roughly 150% of the dividend exposure for low levels of D_0 . In general, the myopic demands are qualitatively unaffected by whether agents are more or less risk-averse than the log investor. Apart from the absolute levels, the curves on the right-hand panels of Figures 3, 2, and 1 look very much the same. Furthermore, note that the individual myopic demand of the investor approaches one when she starts to dominate the market, that is for a very low dividend level in case of the more risk-averse investor and for a high dividend level in case of the less risk-averse investor.

For jump risk, we observe qualitatively the same result, but with opposite signs, since the aggregate exposure j_D to jump risk is negative. The less risk-averse investor 1 has an exposure which is roughly 40% greater in absolute terms than that of the RI, with her $\theta^{(N,1)}$ being between -0.3 and -0.4 .

The myopic demands of both investors decrease in absolute value for an increasing dividend level. This can be attributed to the decrease in the risk aversion of the RI, which implies decreasing risk premia, as shown, e.g., in Equation (7). The wealth-weighted average demand however, which is just the demand of the RI, is nearly constant.

Hedging Demand

The picture changes significantly when we look at the hedging component of demand. In general, both location and shape of the curves for the hedging demands now vary with the levels of risk aversion $\gamma^{(1)}$ and $\gamma^{(2)}$.

In our model, the investment opportunity set is stochastic due to the stochastic local variance V . Since V is driven by the two diffusion risk factors and the jump risk factor N , there will be a hedging demand for all three risk factors. Qualitatively, a negative demand for stock price diffusion risk and a positive demand for the other two risk factors can be interpreted as a long position in V (given that ρ is negative and j_V positive) and vice versa.

We start the discussion with the case $(\gamma^{(1)}, \gamma^{(2)}) = (0.5, 0.8)$ in Figure 3. Since both investors are less risk-averse than the log investor, we expect them to speculate on favorable changes of the investment opportunity set. An increase in volatility has two effects: the investor profits from a higher dividend drift (note that we assume $\mu_1 > 0$), but suffers a utility loss due the higher risk in dividends. As can be seen from the graphs, the first

effect dominates, and the investors take a long position in volatility. In line with intuition, the hedging demand of the less risk-averse investor, who differs more from the myopic log-investor, is more extreme. For both individual investors, the hedging demand is decreasing in the dividend level in absolute terms, reflecting that the myopic demand which creates the primary exposure to a stochastic investment opportunity set, is decreasing in absolute terms, too. The aggregate hedging demand, however, is increasing in the dividend level in absolute terms, even if the aggregate myopic demand is nearly constant. This can be attributed to the fact that the hedging demand converges to the (low) hedging demand of the more risk-averse investor for low dividend levels and to the (high) hedging demand of the less risk-averse investor for high dividend levels.

Figure 2 shows the case where one investor is less risk-averse than the log investor, while the other one is more risk-averse. Again, the less risk-averse investor speculates on changes in the investment opportunity set (in this case on a higher future dividend drift) by taking a long position in volatility risk. The more risk-averse investor, on the other hand, hedges against a lower future dividend drift by taking a short position in volatility. For both investors, the hedging demand is decreasing in absolute terms in the dividend level, following the behavior of the myopic demand. The aggregate hedging demand of the RI is the average of the individual hedging demands. As can be seen from the graphs, it even changes its sign, from a short position in volatility for low dividend levels (which is the demand of the more risk-averse investor) to a long position for high dividend levels (the demand of the less risk-averse investor).

Finally, we consider the case where both investors have a risk aversion above 1. The resulting demands are shown in Figure 1. The less risk-averse investor now has a $\gamma^{(1)} = 2$, and he hedges against a low future dividend drift by taking a short position in volatility. The behavior of the more risk-averse investor with $\gamma^{(2)} = 4$ is more involved. For high dividend levels, this investor also hedges by taking a short position in volatility. For low dividend levels, however, his hedging demand for the two diffusion risk factors changes sign, and he has a long position in the diffusion part of volatility. In these scenarios, his concern about a high dividend volatility is amplified by the concavity of his consumption in aggregate dividends, which induces partly a long position in V . The aggregate hedging demand in the diffusion risk factors is close to zero for low dividend levels and increases significantly in absolute terms for an increase in the dividend level, and thus again does not follow the behavior of the aggregate myopic demand which is rather constant.

So, overall, the exact numerical values for the two levels of risk aversion are important for the sign and the quantity of individual and aggregate hedging demand in our model. This shows that the generalization of the model to the case of (almost) arbitrary values for $\gamma^{(1)}$ and $\gamma^{(2)}$ is economically significant. The effects on the myopic component of demand, however, are not so pronounced, since the motive to earn the risk premium seems to be largely unaffected by γ , as long as investors are risk-averse.

3 Trading Volume in Derivatives

As shown in the previous section, the two investors differ in their optimal exposures, so that they will trade with each other. It is clear that basically any desired trading volume can be generated by making the two investors different enough. In our analysis, however, with values for γ , the coefficient of risk aversion, between 0.5 and 4, this should not be an issue.

We assume that the available assets are the stock, the money market account, and three pure derivatives, which have a unit exposure to one of the risk factors $\sqrt{V_t}dB_t^{(1)}$, $\sqrt{V_t}dB_t^{(2)}$, and dN_t , respectively. To give a specific example, the pure derivative on the diffusion $\sqrt{V_t}dB_t^{(1)}$ is an asset X with price dynamics $dX_t = (r_t + \eta_t^{(B1)}\sqrt{V_t})X_tdt + \sqrt{V_t}X_tdB_t^{(1)}$. This choice of traded claims is of course arbitrary, but any standard derivative, like a call or a put option, can in principle be synthesized from these basic contingent claims, since the market is complete.

The trading volume in derivatives depends on the sequence of actions in the portfolio allocation process. We assume that the investors first put all their wealth in the stock, which is the only asset in positive net supply, before they can trade in the pure derivatives, which are zero net supply assets. Consider the dividend diffusion risk first. The aggregate exposure of the stock to this factor is $\theta_t^{(B1)}$, so that from the investment in the stock, investor i has an absolute exposure of $\theta_t^{(B1)}W_t^{(i)}$. On the other hand, her desired absolute exposure is $\theta_t^{(B1,i)}W_t^{(i)}$, so to obtain this position, she has to invest the amount $(\theta_t^{(B1,i)} - \theta_t^{(B1)})W_t^{(i)}$ into the associated pure derivative. Analogously, the dollar trading volume for the claim written on $\sqrt{V_t}dB_t^{(2)}$ is $(\theta_t^{(B2,i)} - \theta_t^{(B2)})W_t^{(i)}$, and for the jump risk factor it is equal to $(\theta_t^{(N,i)} - \theta_t^{(N)})W_t^{(i)}$. To be able to compare the trading volumes for different levels of the initial dividend D_0 , we normalize the nominal trading volume by the stock price, i.e. by total market capitalization.

In the following, we focus on the position of the less risk-averse investor with risk aversion $\gamma^{(1)}$. This is, of course, sufficient since for zero net supply assets the other investor will have a position of exactly the same size, but opposite sign. Note that for very low and very high dividends the trading volumes will go to zero, since the heterogeneous economy then becomes homogeneous, without the need to trade.

The upper graph in Figure 4 shows the normalized trading volume for the first diffusion factor, $B^{(1)}$. As discussed in the previous section, the absolute levels of the myopic demand components are much higher than those for the hedging part, so it is mainly the differences in this myopic demand which generate the desire to trade. And as one would expect, the less risk-averse investor buys this claim from the more risk-averse one, since the derivative provides positive exposure to $B^{(1)}$ -risk. The numbers for trading volumes are quite impressive. In the scenarios $(\gamma^{(1)}, \gamma^{(2)}) = (2.0, 4.0)$ or $(\gamma^{(1)}, \gamma^{(2)}) = (0.8, 2.0)$ the value of contracts traded can be up to 20 percent of market capitalization for low dividends, and even for the case $(\gamma^{(1)}, \gamma^{(2)}) = (0.5, 0.8)$ it is still around 10 percent. In line with intuition, the size of the trading volume follows the size of the difference between the myopic demands of the two investors, which is also smallest for $(\gamma^{(1)}, \gamma^{(2)}) = (0.5, 0.8)$. Furthermore, note that trading volume is maximized for D_0 between 1 and 2, which is the range where the two investors are of similar importance in the economy and where the difference in the slope of the demand functions is largest.

As shown above the fractions of wealth invested in the other two risk factors are much lower, so we may expect trading volumes to be lower as well. Nevertheless, especially for low dividend levels, there is a significant desire to trade $B^{(2)}$ -risk and jump risk. The relative value of the $B^{(2)}$ -contracts traded is up to 1.8 percent of total market capitalization, which is remarkable, given that it is generated exclusively by differences in hedging demand between investors. In contrast to the $B^{(1)}$ -contract the direction of trading for $B^{(2)}$ -derivatives now depends on the specific values for $\gamma^{(1)}$ and $\gamma^{(2)}$.

For $(\gamma^{(1)}, \gamma^{(2)}) = (0.8, 2.0)$, the less risk-averse investor wants to take a long (speculative) position in $B^{(2)}$, while the more risk-averse investor wants a short position in order to hedge. In line with intuition, it is then the less risk-averse investor who buys additional units of this risk factors, thus providing insurance to the more risk-averse one. If both investors are less risk-averse than the log investor, they both want to take a long (speculative) position in $B^{(2)}$. The demand of the less risk-averse investor is the larger one, so that again, he takes a long position in this risk factor. The picture changes when both

investors have a risk aversion above one. In this case, it is the less risk-averse investor who meets his hedging demand for a short position in $B^{(2)}$ by selling additional units of the pure derivative to the more risk-averse investor. While this direction of providing insurance seems to go the wrong way round, it can be explained by the larger myopic demand of the less risk-averse investor, which increases his hedging demand beyond that of the more risk-averse investor. Furthermore, note that the hedging demand is largest in this case and not in the case where one investor is more and one is less risk-averse than the log investor. So while the direction of trade for $B^{(1)}$ -derivatives which is mainly driven by myopic demand is straightforward, things are not so clear for contracts written on diffusive volatility risk which are mainly traded due to hedging motives.

Similar to $B^{(1)}$, but in contrast to $B^{(2)}$, there is only one direction of trading for derivatives written on the jump factor. In all three cases characterized by different combinations of $\gamma^{(1)}$ and $\gamma^{(2)}$, the position of the less-risk averse agent in the pure derivative is short, i.e. she sells this contract to her more risk-averse counterpart and thus ends up with the larger (negative) exposure. Similar to the case of the $B^{(1)}$ -derivative, the economy with two agents being less risk-averse than the log investor exhibits a smaller trading volume than those where at least one of the investors has a coefficient of risk-aversion greater than 1.

4 Conclusion

In this paper we have performed a general equilibrium analysis for a Lucas (1978) tree economy with SV, jumps in dividends, and jumps in the volatility of dividends. Investor heterogeneity creates significant trading volume in derivatives, since the individual optimal exposures differ according to the respective level of risk aversion.

One of the main implications of our analysis is that there is an important difference between claims written on dividend diffusion risk or jump risk on the one side and contracts written on volatility diffusion risk on the other. While for the first two types of contingent claims it is always the less risk-averse agent who takes on additional risk in the trading process, this is not true for volatility derivatives. Here the direction of trading depends on the exact numerical values of the two coefficients of risk aversion. Contingent claims written on the *level* of dividends or stock prices are straightforward hedging instruments in the sense of protecting investors against wealth losses when the values of assets decline.

The motives to hold volatility derivatives are more complex and involve considerations about future investment opportunities.

References

- Benninga, S. and J. Mayshar, 2000, Heterogeneity and Option Pricing, *Review of Derivatives Research* 4, 7–27.
- Bhamra, H.S. and R. Uppal, 2005, The Effect of Improved Risk Sharing on Stock-Market Return Volatility, Working Paper.
- Cox, J.C. and C.F. Huang, 1989, Optimal Consumption and Portfolio Policies when Asset Prices Follow a Diffusion Process, *Journal of Economic Theory* 49, 33–83.
- Dieckmann, S. and M. Gallmeyer, 2005, The Equilibrium Allocation of Diffusive and Jump Risks with Heterogeneous Agents, *Journal of Economic Dynamics and Control* 29, 1547–1576.
- Duffie, D., 2001, *Dynamic Asset Pricing Theory*. (3rd edition, Princeton University Press Princeton).
- Dumas, B., 1989, Two-Person Dynamic Equilibrium in the Capital Market, *Review of Financial Studies* 2, 157–188.
- Dumas, B., A. Kurshev and R. Uppal, 2005, What Can Rational Investors Do About Excessive Volatility?, Working Paper.
- Franke, G. and E. Lüders, 2006, Return Predictability and Stock Market Crashes in a Simple Rational Expectations Model, Working Paper.
- Liu, J., F.A. Longstaff and J. Pan, 2003, Dynamic Asset Allocation with Event Risk, *Journal of Finance* 58, 231–259.
- Lucas, R.E., 1978, Asset Prices in an Exchange Economy, *Econometrica* 46, 1429–1445.
- Merton, R.C., 1971, Optimum Consumption and Portfolio Rules in a Continuous Time Model, *Journal of Economic Theory* 3, 373–413.

A Characteristic Functions, Stock Price and Individual Wealth

The stock price is

$$S_t = E^P \left[\int_t^T e^{-\beta(s-t)} \left(\frac{c^{(i)}(D_s)}{c^{(i)}(D_t)} \right)^{-\gamma^{(i)}} D_s ds \mid \mathcal{F}_t \right].$$

For general risk aversions, there is no closed form solution for this equation, but we have to use numerical integration. Similar to Dumas, Kurshev and Uppal (2005), to determine the density of the future dividend, we use the technique of Fourier inversion also applied when it comes to option pricing. The characteristic function of $\ln D_s$ is defined as

$$\Phi_{\ln D_s}(x; t, D_t, V_t) = E^P \left[e^{ix \ln D_s} \mid \mathcal{F}_t \right].$$

Since $\Phi_{\ln D_s}(x; t, D_t, V_t)$ is a P-martingale, we know that

$$\begin{aligned} \frac{\partial \Phi}{\partial t} + \frac{\partial \Phi}{\partial V} (\kappa^P (\bar{v}^P - V) - E^P[Y] \lambda^P V) + \frac{\partial \Phi}{\partial \ln D} \left(\mu_0 + \mu_1 V - E^P[X] \lambda^P V - \frac{1}{2} V \right) \\ + \frac{1}{2} \frac{\partial^2 \Phi}{\partial V^2} \sigma_V^2 V + \frac{1}{2} \frac{\partial^2 \Phi}{\partial (\ln D)^2} V + \frac{\partial^2 \Phi}{\partial V \partial (\ln D)} \rho \sigma_V V + E^P [\Delta \Phi] \lambda^P V \in \mathbb{B} \end{aligned}$$

where $\Delta \Phi = \Phi(x; t, D_t(1+X), V_t+Y) - \Phi(x; t, D_t, V_t)$. The standard guess for the characteristic function is

$$\Phi_{\ln D_s}(x; t, D_t, V_t) = e^{A^{cf}(s-t, x) + B^{cf}(s-t, x) V_t + ix \ln D_t}.$$

Plugging this guess into (15) and rearranging gives

$$\begin{aligned} V \left\{ ix (\mu_1 - E^P[X] \lambda^P - 0.5) - \lambda^P - 0.5x^2 + B^{cf}(-\kappa^P - E^P[Y] \lambda^P + \rho \sigma_V ix) \right. \\ \left. + 0.5(B^{cf})^2 \sigma_V^2 + E^P \left[(1+X)^{ix} e^{B^{cf} Y} \right] \lambda^P - B_\tau^{cf} \right\} \\ + \left\{ B^{cf} \kappa^P \bar{v}^P + ix \mu_0 - A_\tau^{cf} \right\} = 0 \end{aligned}$$

with A_τ^{cf} and B_τ^{cf} as derivatives w.r.t. $s-t$. Since the equality has to hold for all $V \in \mathbb{R}^+$, we get two odes for A^{cf} and B^{cf}

$$\begin{aligned} A_\tau^{cf} &= ix \mu_0 + \kappa^P \bar{v}^P B^{cf} \\ B_\tau^{cf} &= (-0.5x^2 + ix (\mu_1 - E^P[X] \lambda^P - 0.5) - \lambda^P) + (-\kappa^P - E^P[Y] \lambda^P + \rho \sigma_V ix) B^{cf} \\ &\quad + 0.5 \sigma_V^2 (B^{cf})^2 + E^P \left[(1+X)^{ix} e^{B^{cf} Y} \right] \lambda^P, \end{aligned}$$

and the initial conditions are $A^{cf}(0, x) = 0$ and $B^{cf}(0, x) = 0$. These ode's can be solved for numerically, for example using Runge-Kutta. Given the characteristic function, the density for $\ln D_s$ then follows from the inversion formula

$$\frac{1}{2\pi} \int_{-\infty}^{\infty} \Phi_{\ln D_s}(x; t, D_t, V_t) e^{-ix \ln D_s} dx.$$

The stock price can then be calculated as

$$\begin{aligned} S_t &= \int_t^T \int_{-\infty}^{\infty} e^{-\beta(s-t)} \left(\frac{c^{(i)}(D_s)}{c^{(i)}(D_t)} \right)^{-\gamma^{(i)}} D_s \\ &\quad \cdot \frac{1}{2\pi} \int_{-\infty}^{\infty} \Phi_{\ln D_s}(x; t, D_t, V_t) e^{-ix \ln D_s} dx d \ln D_s ds. \end{aligned} \quad (16)$$

Similarly, the wealth of investor i can be calculated as

$$\begin{aligned} W_t^{(i)} &= \int_t^T \int_{-\infty}^{\infty} e^{-\beta(s-t)} \left(\frac{c^{(i)}(D_s)}{c^{(i)}(D_t)} \right)^{-\gamma^{(i)}} c^{(i)}(D_s) \\ &\quad \cdot \frac{1}{2\pi} \int_{-\infty}^{\infty} \Phi_{\ln D_s}(x; t, D_t, V_t) e^{-ix \ln D_s} dx d \ln D_s ds. \end{aligned}$$

B Partial Derivative of Stock Price

The stock price is

$$S_t = E^P \left[\int_t^T \frac{u_c^{(1)}(s, c^{(1)}(D_s))}{u_c^{(1)}(t, c^{(1)}(D_t))} D_s ds \mid \mathcal{F}_t \right].$$

Rewrite as

$$u_c^{(1)}(t, c^{(1)}(D_t)) S_t = E^P \left[\int_t^T u_c^{(1)}(s, c^{(1)}(D_s)) D_s ds \mid \mathcal{F}_t \right]$$

and take partial derivatives with respect to D_t

$$\begin{aligned} &u_{cc}^{(1)}(t, c^{(1)}(D_t)) \frac{\partial c^{(1)}(D_t)}{\partial D_t} S_t + u_c^{(1)}(t, c^{(1)}(D_t)) \frac{\partial S_t}{\partial D_t} \\ &= E^P \left[\int_t^T \left\{ u_{cc}^{(1)}(s, c^{(1)}(D_s)) \frac{\partial c^{(1)}(D_s)}{\partial D_s} D_s + u_c^{(1)}(s, c^{(1)}(D_s)) \right\} \frac{\partial D_s}{\partial D_t} ds \mid \mathcal{F}_t \right]. \end{aligned}$$

For the right-hand side, we use that

$$D_s = D_t \frac{D_s}{D_t}, \quad \frac{\partial D_s}{\partial D_t} = \frac{D_s}{D_t}$$

since the ratio $\frac{D_s}{D_t}$ does not depend on D_t . Dividing by $u_c^{(1)}(t, c^{(1)}(D_t))$ gives

$$\begin{aligned} &\frac{u_{cc}^{(1)}(t, c^{(1)}(D_t))}{u_c^{(1)}(t, c^{(1)}(D_t))} \frac{\partial c^{(1)}(D_t)}{\partial D_t} S_t + \frac{\partial S_t}{\partial D_t} \\ &= E^P \left[\int_t^T \frac{u_c^{(1)}(s, c^{(1)}(D_s))}{u_c^{(1)}(t, c^{(1)}(D_t))} \left\{ \frac{u_{cc}^{(1)}(s, c^{(1)}(D_s))}{u_c^{(1)}(s, c^{(1)}(D_s))} \frac{\partial c^{(1)}(D_s)}{\partial D_s} D_s + 1 \right\} \frac{D_s}{D_t} ds \mid \mathcal{F}_t \right]. \end{aligned}$$

We now take a look at the term

$$\begin{aligned}
\frac{u_{cc}^{(1)}(s, c^{(1)}(D_s))}{u_c^{(1)}(s, c^{(1)}(D_s))} \frac{\partial c^{(1)}(D_s)}{\partial D_s} &= \frac{u_{cc}^{(1)}(s, c^{(1)}(D_s)) c^{(1)}(D_s)}{u_c^{(1)}(s, c^{(1)}(D_s))} \frac{\partial c^{(1)}(D_s)}{\partial D_s} \frac{1}{c^{(1)}(D_s)} \\
&= -\gamma^{(1)}(c^{(1)}(D_s)) \frac{c^{(1)}(D_s)}{D_s} \cdot \frac{\hat{\gamma}(D_s)}{\gamma^{(1)}(c^{(1)}(D_s))} \frac{1}{c^{(1)}(D_s)} \\
&= -\hat{\gamma}(D_s) \frac{1}{D_s}.
\end{aligned}$$

Plugging this in gives

$$\begin{aligned}
-\hat{\gamma}(D_t) \frac{S_t}{D_t} + \frac{\partial S_t}{\partial D_t} &= E^P \left[\int_t^T \frac{u_c^{(1)}(s, c^{(1)}(D_s))}{u_c^{(1)}(t, c^{(1)}(D_t))} \{1 - \hat{\gamma}(D_s)\} \frac{D_s}{D_t} ds \mid \mathcal{F}_t \right] \\
&= E^P \left[\int_t^T \frac{\xi_s}{\xi_t} \{1 - \hat{\gamma}(D_s)\} \frac{D_s}{D_t} ds \mid \mathcal{F}_t \right] \\
&= \frac{S_t}{D_t} - E^P \left[\int_t^T \frac{\xi_s}{\xi_t} \frac{D_s}{D_t} \hat{\gamma}(D_s) ds \mid \mathcal{F}_t \right].
\end{aligned}$$

Sorting terms and multiplying with D_t/S_t gives

$$\frac{\partial S_t}{\partial D_t} \frac{D_t}{S_t} = 1 + \hat{\gamma}(D_t) - E^P \left[\int_t^T \frac{\xi_s}{\xi_t} \frac{D_s}{S_t} \hat{\gamma}(D_s) ds \mid \mathcal{F}_t \right].$$

C Partial Derivative of Individual Wealth

The wealth of investor i is

$$W_t^{(i)} = E^P \left[\int_t^T \frac{u_c^{(i)}(s, c^{(i)}(D_s))}{u_c^{(i)}(t, c^{(i)}(D_t))} c^{(i)}(D_s) ds \mid \mathcal{F}_t \right].$$

Rewrite as

$$u_c^{(i)}(t, c^{(i)}(D_t)) W_t^{(i)} = E^P \left[\int_t^T u_c^{(i)}(s, c^{(i)}(D_s)) c^{(i)}(D_s) ds \mid \mathcal{F}_t \right]$$

and take partial derivatives with respect to D_t

$$\begin{aligned}
&u_{cc}^{(i)}(t, c^{(i)}(D_t)) \frac{\partial c^{(i)}(D_t)}{\partial D_t} W_t^{(i)} + u_c^{(i)}(t, c^{(i)}(D_t)) \frac{\partial W_t^{(i)}}{\partial D_t} \\
&= E^P \left[\int_t^T \left\{ u_{cc}^{(i)}(s, c^{(i)}(D_s)) \frac{\partial c^{(i)}(D_s)}{\partial D_s} c^{(i)}(D_s) + u_c^{(i)}(s, c^{(i)}(D_s)) \frac{\partial c^{(i)}(D_s)}{\partial D_s} \right\} \frac{\partial D_s}{\partial D_t} ds \mid \mathcal{F}_t \right].
\end{aligned}$$

For the right-hand side, we use that

$$D_s = D_t \frac{D_s}{D_t}, \quad \frac{\partial D_s}{\partial D_t} = \frac{D_s}{D_t}$$

since the ratio $\frac{D_s}{D_t}$ does not depend on D_t . Dividing by $u_c^{(i)}(t, c^{(i)}(D_t))$ gives

$$\begin{aligned} & \frac{u_{cc}^{(i)}(t, c^{(i)}(D_t))}{u_c^{(i)}(t, c^{(i)}(D_t))} \frac{\partial c^{(i)}(D_t)}{\partial D_t} W_t^{(i)} + \frac{\partial W_t^{(i)}}{\partial D_t} \\ &= E^P \left[\int_t^T \frac{u_c^{(i)}(s, c^{(i)}(D_s))}{u_c^{(i)}(t, c^{(i)}(D_t))} \left\{ \frac{u_{cc}^{(i)}(s, c^{(i)}(D_s))}{u_c^{(i)}(s, c^{(i)}(D_s))} \frac{\partial c^{(i)}(D_s)}{\partial D_s} c^{(i)}(D_s) + \frac{\partial c^{(i)}(D_s)}{\partial D_s} \right\} \frac{D_s}{D_t} ds \mid \mathcal{F}_t \right]. \end{aligned}$$

We now take a look at the term

$$\begin{aligned} \frac{u_{cc}^{(i)}(s, c^{(i)}(D_s))}{u_c^{(i)}(s, c^{(i)}(D_s))} \frac{\partial c^{(i)}(D_s)}{\partial D_s} &= \frac{u_{cc}^{(i)}(s, c^{(i)}(D_s)) c^{(i)}(D_s)}{u_c^{(i)}(s, c^{(i)}(D_s))} \frac{\partial c^{(i)}(D_s)}{\partial D_s} \frac{1}{c^{(i)}(D_s)} \\ &= -\gamma^{(i)} \frac{c^{(i)}(D_s)}{D_s} \cdot \frac{\hat{\gamma}(D_s)}{\gamma^{(i)} c^{(i)}(D_s)} \frac{1}{c^{(i)}(D_s)} \\ &= -\hat{\gamma}(D_s) \frac{1}{D_s}. \end{aligned}$$

Furthermore, we know that

$$\frac{\partial c^{(i)}(D_s)}{\partial D_s} = \frac{c^{(i)}(D_s)}{D_s} \cdot \frac{\hat{\gamma}(D_s)}{\gamma^{(i)}}.$$

Plugging this in gives

$$\begin{aligned} & -\hat{\gamma}(D_t) \frac{W_t^{(i)}}{D_t} + \frac{\partial W_t^{(i)}}{\partial D_t} \\ &= E^P \left[\int_t^T \frac{u_c^{(i)}(s, c^{(i)}(D_s))}{u_c^{(i)}(t, c^{(i)}(D_t))} \left\{ \frac{c^{(i)}(D_s)}{D_s} \cdot \frac{\hat{\gamma}(D_s)}{\gamma^{(i)}} - \hat{\gamma}(D_s) \frac{c^{(i)}(D_s)}{D_s} \right\} \frac{D_s}{D_t} ds \mid \mathcal{F}_t \right] \\ &= E^P \left[\int_t^T \frac{\xi_s}{\xi_t} \left\{ \frac{\hat{\gamma}(D_s)}{\gamma^{(i)}} - \hat{\gamma}(D_s) \right\} \frac{c^{(i)}(D_s)}{D_t} ds \mid \mathcal{F}_t \right]. \end{aligned}$$

Finally, sorting terms and multiplying with $D_t/W_t^{(i)}$ yields

$$\begin{aligned} \frac{\partial W_t^{(i)}}{\partial D_t} \cdot \frac{D_t}{W_t^{(i)}} &= E^P \left[\int_t^T \frac{\xi_s}{\xi_t} \cdot \frac{c^{(i)}(D_s)}{W_t^{(i)}} \cdot \frac{\hat{\gamma}(D_s)}{\gamma^{(i)}} ds \mid \mathcal{F}_t \right] \\ &+ \hat{\gamma}(D_t) - E^P \left[\int_t^T \frac{\xi_s}{\xi_t} \cdot \frac{c^{(i)}(D_s)}{W_t^{(i)}} \hat{\gamma}(D_s) ds \mid \mathcal{F}_t \right]. \end{aligned}$$

	$Y = y^{(1)} \equiv 0$	$Y = y^{(2)}$	\dots	$Y = y^{(K)}$
$X = x^{(1)} \equiv 0$	$p_{11} = 0$	p_{12}	\dots	p_{1K}
$X = x^{(2)}$	p_{21}	p_{22}	\dots	p_{2K}
\vdots	\vdots	\vdots	\ddots	\vdots
$X = x^{(J)}$	p_{J1}	p_{J2}	\dots	p_{JK}

Table 1. Jump Size Distribution

The table shows the structure of the jump size distribution in our model. X is the random jump size in the dividend, Y is the size of a variance jump, where we assume $Y \geq 0$. The event $X = 0, Y = 0$ is assigned a zero probability in the joint distribution of X and Y , since it represents the event that no jump has occurred.

μ_0	μ_1	j_D	λ^P	κ^P	\bar{v}^P	σ_V	ρ	j_V
0.010	2.750	-0.250	1.840	5.300	0.020	0.225	-0.570	0.226

Table 2. Parameter Values for Numerical Computations

The table summarizes the parametrization used for the numerical computations. The parameter values are adapted from Liu, Longstaff and Pan (2003). The time discount rate β is set to equal 0.05. V_0 is set to equal its long-run mean \bar{v}^P . The planning horizon is 1 year.

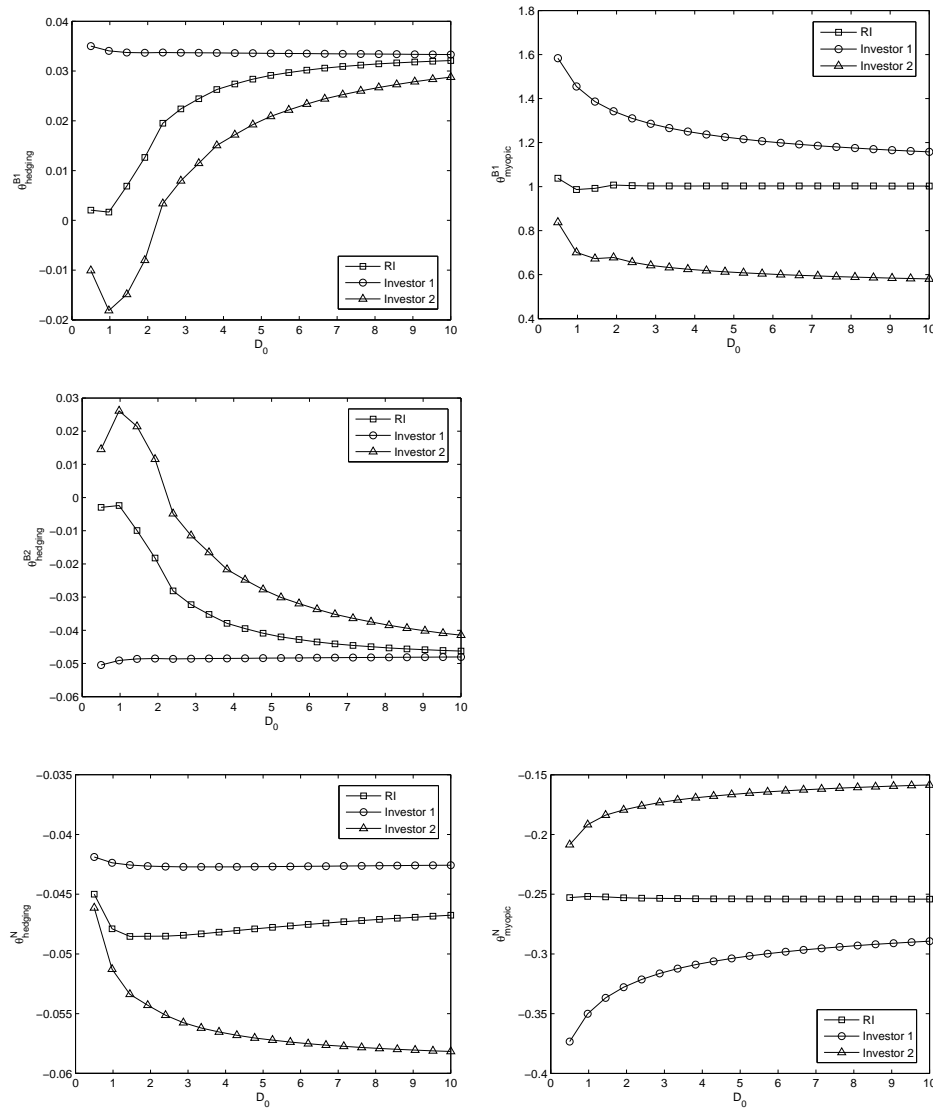


Figure 1. Demand for Risk Factors ($\gamma^{(1)} = 2.0, \gamma^{(2)} = 4.0$)

The graphs show the optimal demand for the risk factors of the RI and the two investors. The parameters are taken from Table 2.

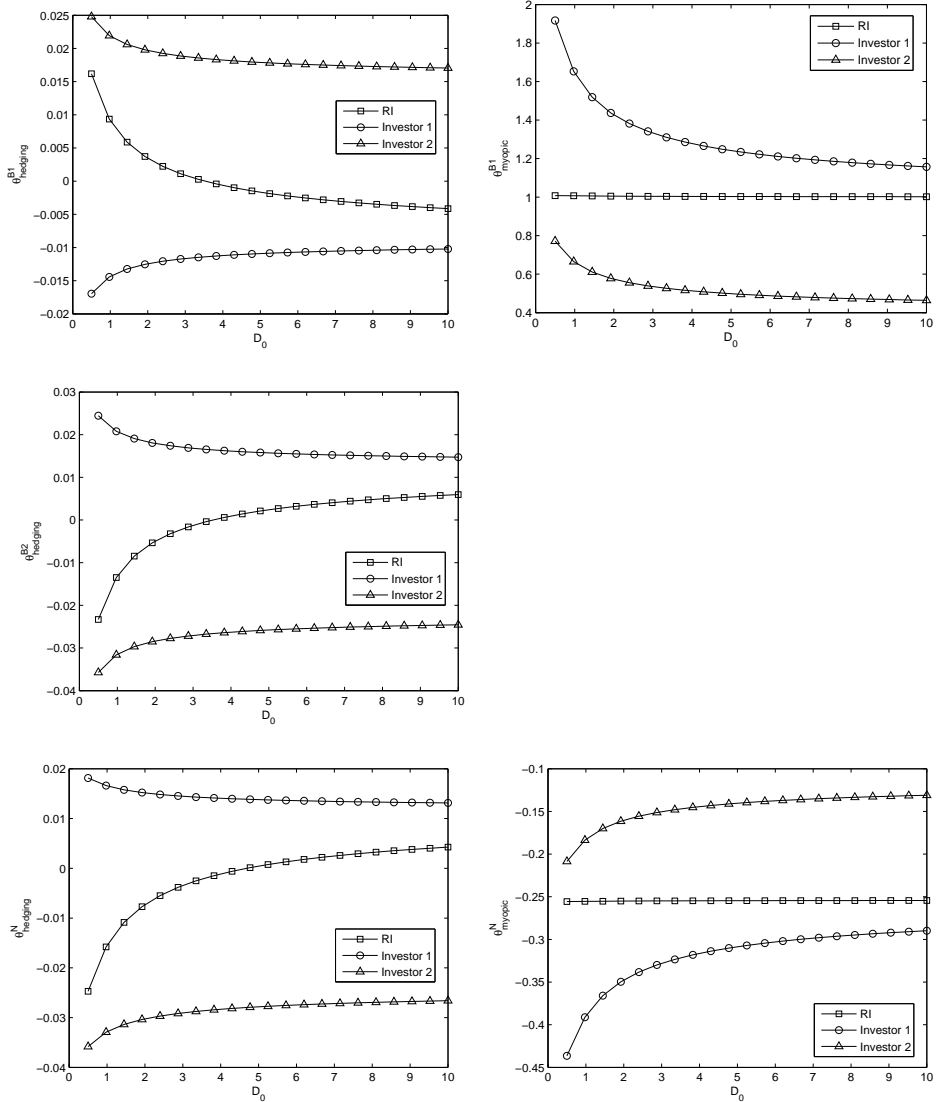


Figure 2. Demand for Risk Factors ($\gamma^{(1)} = 0.8, \gamma^{(2)} = 2.0$)

The graphs show the optimal demand for the risk factors of the RI and the two investors. The parameters are taken from Table 2.

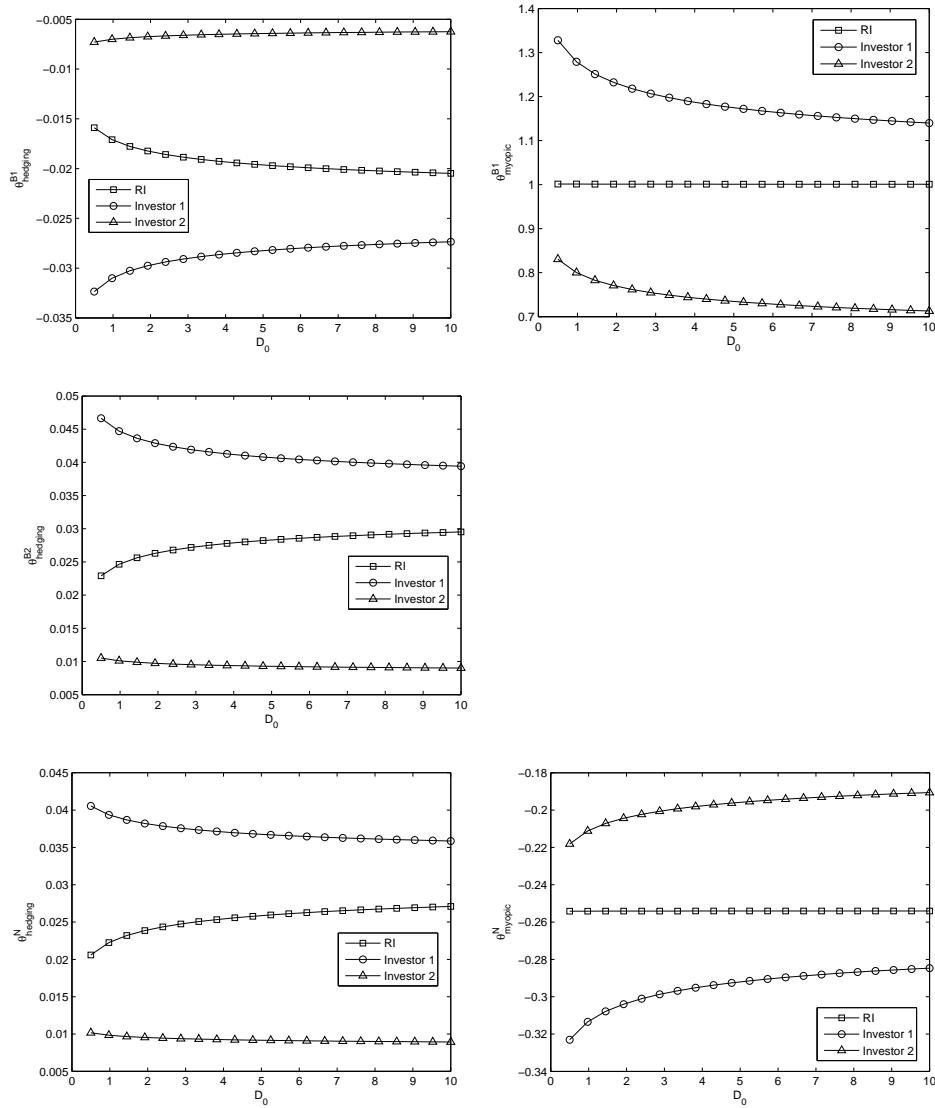


Figure 3. Demand for Risk Factors ($\gamma^{(1)} = 0.5, \gamma^{(2)} = 0.8$)

The graphs show the optimal demand for the risk factors of the RI and the two investors. The parameters are taken from Table 2.

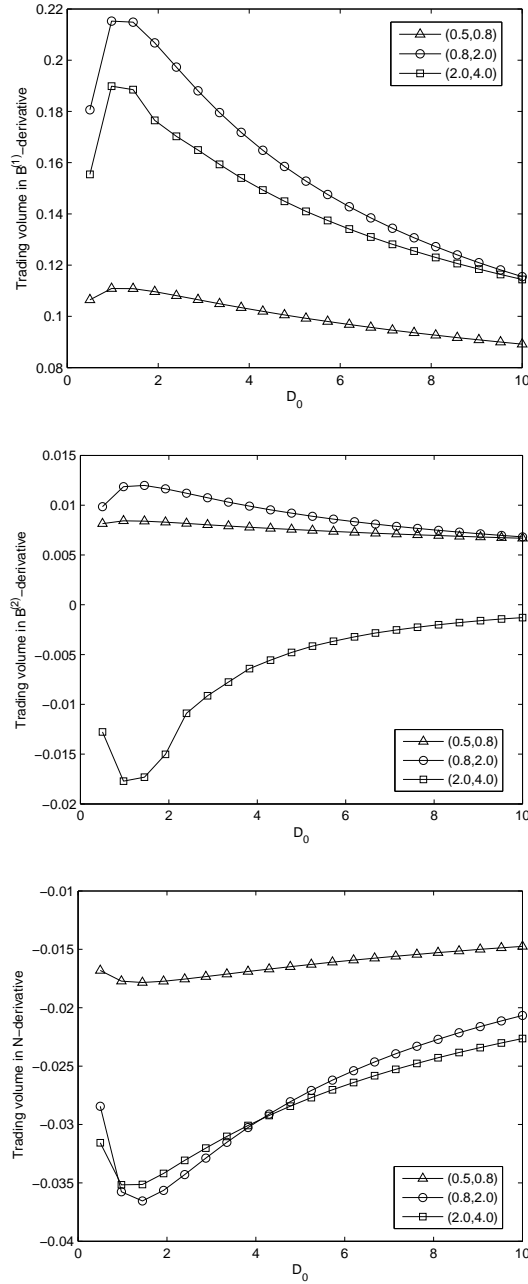


Figure 4. Trading Volume in Derivatives

The graphs show the trading volume in the pure derivatives, relative to total market capitalization, as a function of the dividend level from the less risk-averse agent's perspective. The three curves represent the different combinations of the two levels of risk aversion, $\gamma^{(1)}$ and $\gamma^{(2)}$. The upper graph shows the relative trading volume in the claim with a unit exposure to $\sqrt{V_t}dB_t^{(1)}$, the middle and lower graph show the analogous volume for the claims on $\sqrt{V_t}dB_t^{(2)}$ and on dN_t . The parameters are taken from Table 2.

Continuous-time Volatility Component Models: Option Pricing and Asset Allocation

Eva Schneider

The paper was presented at

- Deutsche Gesellschaft für Finanzwirtschaft, Dresden (28.09.2007 - 29.09.2007)
- Brown Bag Seminar, Goethe University, Frankfurt am Main (27.06.2007)

Summary. This paper analyzes continuous-time volatility component models and their application in option pricing and asset allocation. A focus of the paper is to assess the economic consequences of model mis-specification with regard to volatility components.

A multi-factor stochastic volatility model allows the slope, the level and the curvature of the volatility smile to change even when the local variance remains constant. Concerning asset allocation the optimal portfolio composition becomes state-dependent. We provide a general methodology to compute the utility loss resulting from model mis-specification, and show that the utility loss from ignoring volatility components is less important than the one from model mis-specification concerning jumps.

1 Introduction

1.1 Motivation

In many empirical studies, models with multiple volatility components are shown to provide a better fit to the observed stock price data than one-factor models. Nevertheless, very few papers analyze the implications of these model specifications for option pricing and asset allocation. The paper aims at filling this gap by comparing the multi-factor model of Bates (2000) (excluding jumps) and the stochastic long-run mean model (SLRM) of Duffie, Pan and Singleton (2000) to the standard stochastic volatility model of Heston (1993). We also analyze the impact of model mis-specification concerning volatility components in the portfolio planning problem.

First, after deriving closed-form solutions for the option price, we look in detail at the properties of the smile and especially at the time-variation of the smile. Then we compare the optimal portfolio position and the indirect utility in an incomplete market across the three models.

1.2 Literature

This paper is mostly related to the literature analyzing the impact of volatility components. There are only very few papers considering the modeling of volatility components in continuous-time. The most prominent paper is certainly the paper of Bates (2000) who introduces a two-factor stochastic volatility model including jumps in the stock price. Via Fourier inversion, he derives a closed-form option pricing formula, and then mainly focusses on the empirical estimation of the model. The same holds for Chernov, Gallant, Ghysels and Tauchen (2003) who compare the empirical performance of different volatility specifications, but do not consider their impact on the smile dynamics or asset allocation. A recent paper by Christoffersen, Heston and Jacobs (2007) analyzes the model of Bates (2000) (excluding jumps) in more detail and shows that the model explains several empirical facts. In particular, the authors show that it can generate the observed smile dynamics and that it implies independence of the slope of the smile from the level of volatility.

Other authors introducing volatility component models are Duffie, Pan and Singleton (2000) and Chacko and Viceira (2003). Both papers emphasize the convenient empirical properties, but none of them analyzes in detail the implications on option prices or asset allocation. Duffie, Pan and Singleton (2000) present a stochastic volatility model where the long-run mean of the stochastic volatility follows itself a CIR process. Chacko and Viceira (2003) estimate a stochastic volatility model via 'Spectral GMM', and state that the differences in estimation results they find with changing data frequency can be explained by the existence of multiple volatility components. Since their model specification does not fall into the affine class and lacks therefore many desirable properties, we decided not to include their model in our analysis.

There is a wide range of papers dealing with volatility component models in discrete time. Two of the most recent ones are Adrian and Rosenberg (2005) and Christoffersen, Jacobs and Wang (2005). Both emphasize the empirical performance of these models in explaining stock market data, while none of them discusses their implications on smile dynamics or asset allocation.

1.3 Contribution

Although the empirical performance of models with volatility components is widely confirmed in the literature, their properties in terms of option pricing and in particular asset allocation are rarely discussed.

Our analysis shows that in case of the SLRM model, the smile has properties as in the Heston (1993) model, but, contrary to this, the level of smile may change even if local volatility does not change (but the long-run mean). The Bates (2000) model can be considered as a one-factor model with stochastic speed of mean-reversion, stochastic volatility of variance and stochastic stock-volatility correlation. This implies the empirically well supported property that the slope, the level and the curvature of the smile change even if local volatility remains constant.

The main contribution of the paper is in the dimension of asset allocation. As for option prices, the SLRM model does not provide a significant modification compared to the results obtained with a one-factor Heston (1993) model. In contrast, the Bates (2000) model is a significant extension of the Heston (1993) model concerning portfolio planning. In addition to the stochastic correlation, the model specification implies an expected excess return on the stock which is not constant per unit of variance. As a result, the model does not have a closed-form solution for the indirect utility and the optimal stock position, although it falls in the class of affine models as defined in Duffie, Pan and Singleton (2000). In this paper we solve for the optimal stock position numerically via the method of finite differences.

In the last step, we consider the impact of model mis-specification on the indirect utility of an investor. To do so, we present a general approach how to compute the indirect utility in case of model mis-specification via the method of finite differences. This methodology can be applied in complete and incomplete markets and allows to avoid a time-consuming Monte Carlo simulation. The utility losses from model mis-specification concerning volatility components are moderate, especially compared to the results from the literature in case of jump mis-specification.

2 Models with Volatility Components

2.1 Model Setup

This paper analyses and compares two multi-component stochastic volatility models proposed in the literature to the standard one-component Heston (1993) model. Since one purpose of this paper is to encourage the use of these multiple volatility component models, we focus on the most popular ones: the stochastic long-run mean (SLRM) model of Duffie, Pan and Singleton (2000) and the two factor model of Bates (2000)¹. These models have the advantage to fall in the affine class of Duffie, Pan and Singleton (2000), so that there are closed-form solutions for many pricing problems.

In the following, we present and discuss briefly the three models considered in this paper: the two models with volatility components and for comparison the one-factor Heston (1993) model.

One-factor stochastic volatility (Heston (1993))

Besides the dynamics of the stock price, the Heston (1993) model specifies the \mathbb{P} -dynamics of the (stochastic) local variance V :

$$\begin{aligned}\frac{dS_t}{S_t} &= \mu_t dt + \sqrt{V_t} dW_t \\ dV_t &= \kappa(\theta - V_t)dt + \sigma\sqrt{V_t}dW_t^V\end{aligned}$$

with $Corr(dW_t^V, dW_t) = \rho$. V thus follows a CIR process with speed of mean-reversion κ , long-run mean θ and volatility σ . For option pricing, the processes have to be specified under the \mathbb{Q} -measure. We assume that the premium W is such that $\eta\sqrt{V_t}$ is earned per unit of $\sqrt{V_t}dW_t$. Analogously, the risk premium for W^V is $\xi\sqrt{V_t}$ per unit of $\sqrt{V_t}dW_t^V$.

Stochastic long-run mean (SLRM, Duffie, Pan and Singleton (2000))

The dynamics of the stock price and of the local variance are very similar to the Heston model, but the model specifies an additional process such that the long-run mean of variance follows its own CIR process:

¹ We consider the Bates (2000) model excluding jumps to focus on the impact of the volatility components. Properties of this model are also discussed in Christoffersen, Heston and Jacobs (2007).

$$\begin{aligned}\frac{dS_t}{S_t} &= \mu_t dt + \sqrt{V_t} dW_t \\ dV_t &= \kappa(\bar{V}_t - V_t) dt + \sigma_V \sqrt{V_t} dW_t^V \\ d\bar{V}_t &= \kappa_{\bar{V}}(\theta_{\bar{V}} - \bar{V}_t) dt + \sigma_{\bar{V}} \sqrt{\bar{V}_t} dW_t^{\bar{V}}\end{aligned}$$

with, as the only non-zero correlation, $\text{Corr}(dW_t^V, dW_t) = \rho_V$. The change of measure to obtain the \mathbb{Q} -dynamics is again realized via the specification of the local risk compensation. $\eta_V \sqrt{V_t}$ is earned per unit of $\sqrt{V_t} dW_t$, $\xi_V \sqrt{V_t}$ per unit of $\sqrt{V_t} dW_t^V$ and $\xi_{\bar{V}} \sqrt{\bar{V}_t}$ per unit of $\sqrt{\bar{V}_t} dW_t^{\bar{V}}$. This model has been introduced in Duffie, Pan and Singleton (2000) and is known to fall into the class of affine models.

Multi-factor stochastic volatility (Bates (2000) without jump components)

This model assumes that the stock price dynamics is driven by two independent stochastic volatility components:

$$\begin{aligned}\frac{dS_t}{S_t} &= \mu_t dt + \sqrt{V_{1t}} dW_{1t} + \sqrt{V_{2t}} dW_{2t} \\ dV_{1t} &= \kappa_1(\theta_1 - V_{1t}) dt + \sigma_1 \sqrt{V_{1t}} dW_{1t}^V \\ dV_{2t} &= \kappa_2(\theta_2 - V_{2t}) dt + \sigma_2 \sqrt{V_{2t}} dW_{2t}^V.\end{aligned}$$

The Wiener processes of the variance dynamics, however, may be correlated with the stock price via $\text{Corr}(dW_{1t}^V, dW_{1t}) = \rho_1$ and $\text{Corr}(dW_{2t}^V, dW_{2t}) = \rho_2$. We assume that $\eta_i \sqrt{V_{it}}$ is the compensation per unit of $\sqrt{V_{it}} dW_{it}$ ($i = 1, 2$) and $\xi_i \sqrt{V_{it}}$ per unit of $\sqrt{V_{it}} dW_{it}^V$ ($i = 1, 2$).

To understand the properties of this model, it is useful to regard the model as a one-factor model with variance dynamics

$$dV_t = d(V_{1t} + V_{2t}) = [\kappa_1 \theta_1 - \kappa_1 V_{1t} + \kappa_2 \theta_2 - \kappa_2 V_{2t}] dt + \sigma_1 \sqrt{V_{1t}} dW_{1t}^V + \sigma_2 \sqrt{V_{2t}} dW_{2t}^V.$$

The (weighted) sum of two independent normal Wiener processes dW_{1t}^V and dW_{2t}^V is itself normally distributed and the process is therefore equal in distribution to

$$dV_t = d(V_{1t} + V_{2t}) = \kappa_V [\theta_V - V_t] dt + \sigma_V \sqrt{V_t} dB_t$$

with

$$\begin{aligned}
\theta_V &= \theta_1 + \theta_2 \\
\kappa_V &= \frac{\kappa_1(\theta_1 - V_{1t}) + \kappa_2(\theta_2 - V_{2t})}{(\theta_1 - V_{1t}) + (\theta_2 - V_{2t})} \\
\sigma_V &= \sqrt{\frac{\sigma_1^2 V_{1t} + \sigma_2^2 V_{2t}}{V_{1t} + V_{2t}}} \\
\text{Corr} \left(\frac{dS_t}{S_t}, dV_t \right) &= \frac{V_{1t}\sigma_1\rho_1 + V_{2t}\sigma_2\rho_2}{\sigma_V V_t} = \frac{\frac{V_{1t}}{\sqrt{V_{1t}+V_{2t}}}\sigma_1\rho_1 + \frac{V_{2t}}{\sqrt{V_{1t}+V_{2t}}}\sigma_2\rho_2}{\sqrt{\sigma_1^2 V_{1t} + \sigma_2^2 V_{2t}}}.
\end{aligned}$$

This representation allows a direct comparison with the Heston model. The long-run mean of variance θ_V corresponds to the sum of the two individual long-run means of the variance processes. The speed of mean-reversion κ_V is a weighted average of the individual mean-reversion speeds where the weights are the deviations of the individual variances from their respective long-run means $\theta_i - V_{it}$ ($i = 1, 2$).² The variance of variance σ_V^2 is also a weighted average of the individual variances. Here, the weights are the local levels of the variance components. Speed of mean-reversion, variance of variance and also stock-volatility correlation are thus stochastic and time-varying. For the special case $\sigma_1 = \sigma_2 = \sigma_V$, the correlation is a weighted average of individual correlations where the weights are the local levels of the variances.

2.2 Comparison of Model Properties

In the following, we compare several properties of the models which will be important for the later analysis. First, consider the local variance of stock return implied by the three models. In case of the Bates model, the local variance of the stock return is the sum of two components, $\text{Var}(dS_t/S_t) = (V_{1t} + V_{2t}) dt$, in the other two models it consists of one component, $\text{Var}(dS_t/S_t) = V_t dt$, only. Since local variance is one of the main drivers of option prices, we facilitate the comparison of the models by setting $V_t = V_{1t} + V_{2t}$ for the later analysis.

From the literature on option pricing we know that the stock-volatility correlation plays a special role. It accounts for the so called 'leverage effect', the fact that when the stock price decreases, volatility tends to increase at the same time. As discussed before, the Heston and the SLRM model have the standard feature of constant stock-volatility

² Contrary to the individual variance components the speed of mean-reversion may be negative and thus the total variance temporarily diverges from its long-run mean.

correlation. In the Bates model on the other hand the stock-volatility correlation may change over time within the same parametrization due to changing V_1 and V_2 and this time variation of correlation induces a model-consistent time-variation of the smile.

The SLRM model has a constant stock-volatility correlation but unlike the Bates (2000) model it has a stochastic long-run mean. However, in contrast to stock-volatility correlation and local variance, the impact of the long-run mean of variance may be of second-order importance for option pricing and asset allocation.

In asset allocation, the most important driver of the portfolio composition are the expected excess returns earned on the different assets. In all of the above models, the expected excess return on the stock is linked to the local level of variance. In the Heston and the SLRM model $\mu_t - r = \eta V_t$, in the Bates model $\mu_t - r = \eta_1 V_{1t} + \eta_2 V_{2t}$. The expected excess return per unit of stock-variance, however, is constant in the Heston and the SLRM model, but stochastic in the case of Bates:

$$\frac{\mu_t - r}{V_t} = \frac{\eta_1 V_{1t} + \eta_2 V_{2t}}{V_{1t} + V_{2t}}.$$

In general, $\eta_1 \neq \eta_2$, so that the expected excess return per unit of variance depends on the local levels of the variance components. We will see that, as a consequence, the optimal portfolio allocation will not only be time- but also state-dependent.

3 Option Pricing

3.1 Option Valuation

All three models fall in the affine class, so we can apply the approach described in Bakshi and Madan (2000) and Duffie, Pan and Singleton (2000) to price standard call and put options on the stock.³ The price of a call option with strike K and maturity T is given by

$$C_t = S_t \Pi_1 - K e^{-r(T-t)} \Pi_2 \tag{1}$$

with

³ The multi-component model proposed in Chacko and Viceira (2003), e.g., is non-affine, and the price of a call option can thus only be computed by the method of finite differences or Monte Carlo simulation.

$$\begin{aligned}\Pi_1 &= \frac{1}{2} + \frac{1}{\pi} \int_0^\infty \Re \left[\frac{\varphi(u-i, T-t, S_t, \dots) e^{-iu \ln K}}{iu S_t} \right] du \\ \Pi_2 &= \frac{1}{2} + \frac{1}{\pi} \int_0^\infty \Re \left[\frac{\varphi(u, T-t, S_t, \dots) e^{-iu \ln K}}{iu e^{-r(T-t)}} \right] du\end{aligned}$$

where $\Re[x]$ denotes the real part of x and $\varphi(u, T-t, S_t, \dots)$ is the Fourier transform of the state price density given by

$$\varphi(u, T-t, S_t, \dots) = E^Q \left[e^{-r(T-t)} e^{iu \ln S_T} \right].$$

Besides the integration variable u , the Fourier transform depends on the time to maturity of the option, the current stock price and the current values of the state variables of the model. The Fourier transform differs across the models and in some cases closed-form solutions exist. Details are given in Appendix A.

3.2 Smile Dynamics

At a single point in time, most empirical properties of the option smile can be explained by models with one-factor stochastic volatility and jumps. On the other hand, one also observes that the shape of the smile changes over time, a fact that usually cannot be easily explained in standard option pricing models. In these models, a change of the smile shape can only be generated by changing the parameters of the pricing model which is obviously inconsistent with the model assumption of constant parameters.

These smile changes which are also discussed in Christoffersen, Heston and Jacobs (2007), have different characteristics. The smile may change from upward to downward sloping, and vice versa, its level is time-varying and in the course of time, the curvature of the smile may be more or less pronounced. Importantly, this is often observed although local variance has not changed.

Figure 1 shows that the SLRM model can explain some of these smile dynamics. In this figure, option smiles for options with 6 and 12 months to maturity are plotted for different levels of the local long-run mean \bar{V}_t of variance. It is important to note that, contrary to the variance level itself, this change in the long-run mean of variance is not directly observable in the market. An increase or decrease in the local long-run mean of variance may occur while local variance does not change. For all maturities, a change of the local long-run mean induces an approximately parallel shift of the smile which is

the stronger the longer the time to maturity. The level of smile thus changes even if local volatility remains constant. Altogether, however, the ability of the SLRM model to explain the observed smile dynamics is rather limited.

The Bates model can explain much better the empirically observed smile dynamics. Figure 2 plots option smiles for different levels of local variances V_{1t} and V_{2t} , holding total variance constant for options with 6 and 12 months to maturity. For the two variance dynamics, all but one of the parameters are set equal to focus on the smile dynamics induced by stochastic stock-variance correlation (left graphs), stochastic volatility of variance (middle graphs) and stochastic speed of variance mean-reversion (right graphs). In the left graphs, we can see that, in particular for long maturity options, the smile changes from primarily downward sloping to upward sloping the more weight is locally contributed by the variance with negative correlation. The middle graphs show that, in particular for short maturity options, the smile becomes the steeper the more weight is locally contributed by the variance with lower volatility. And the level of the smile is the lower, the more weight is locally contributed by the variance with lower speed of mean-reversion (left graphs). The Bates model thus explains nicely the empirical observation that the shape of the smile changes over time, independently of the volatility level.

4 Portfolio Planning

In this section we consider asset allocation in models with volatility components. We assume that our investor derives utility from terminal wealth. First, we compute the optimal portfolio strategies in an incomplete market where only stock and money market account are traded.⁴ In the second step we assess the impact of model mis-specification concerning volatility components, i.e. we compute the utility loss suffered by an investor assuming the one-factor Heston (1993) model when a volatility component model is the true data generating process. Thereby, we present a general method to compute the utility loss under model mis-specification, either with a closed-form solution or via numerical methods.

The investor is assumed to have CRRA utility with a coefficient of risk aversion γ and an investment horizon of T . His objective is thus

⁴ The results for a complete market can be found in Appendix B. A comparison to the results for an incomplete market allows to assess the value of trading derivatives as e.g. in Liu and Pan (2003).

$$\max_{\phi} E[U(Y_T)] = E \left[\frac{Y_T^{1-\gamma}}{1-\gamma} \right]$$

subject to the budget constraint

$$\frac{dY_t}{Y_t} = \phi_t \frac{dS_t}{S_t} + (1 - \phi_t)r dt$$

with ϕ as percentage investment in the stock and initial wealth Y_0 given.

In the following we present and discuss the optimal stock positions in the different models. The optimal positions in the complete market are presented in Appendix B.

Heston

In this one-factor stochastic volatility model the optimal stock position can be derived as a special case from the results in Liu, Longstaff and Pan (2003). A percentage investment of size ϕ in the stock leads to the following dynamics of wealth

$$dY_t = rY_t dt + \phi_t Y_t (\eta V_t dt + \sqrt{V_t} dW_t).$$

The approach via the HJB-equation yields the optimal stock position as

$$\phi_t = \frac{\eta}{\gamma} + \rho \sigma H(\tau) \quad (2)$$

with $\tau = T - t$. The function H and the indirect utility J can be solved in closed-form (see Appendix C). As usual, the optimal stock position consists of a myopic part (first summand) and a hedging component (second summand). It is important to note that this optimal stock position is only time-dependent (through $H(\tau)$), but not state-dependent. This is due to the fact that the market price of volatility risk is assumed to be proportional to the local level of volatility such that the risk premium earned per unit of stock-variance is constant and equal to η .

SLRM

In this model, an investment in the stock leads to a local exposure to stock price risk, but not to an exposure to volatility or long-run mean volatility risk. The dynamics of wealth are therefore structurally identical to the one in the one-factor stochastic volatility case:

$$dY_t = rY_t dt + \phi_t Y_t (\eta_V V_t dt + \sqrt{V_t} dW_t)$$

with ϕ as the fraction invested in the stock. Again, the optimal stock position can be derived via the HJB equation and leads to

$$\phi_t = \frac{\eta V}{\gamma} + \rho \sigma_V H(\tau)$$

with $\tau = T - t$. The indirect utility J and the function H can be solved in closed-form (see Appendix C). The stock is exposed to one risk factor only, and this factor is assumed to be uncorrelated to stochastic long-run mean risk, but correlated to stochastic volatility risk (correlation ρ). Therefore the optimal stock position contains a hedging demand for stochastic volatility risk but not for stochastic long-run mean risk. Note that the optimal position looks very similar to the one in the Heston (1993) model, differences come from the different parameters and the slightly different PDE to be satisfied by the function $H(\tau)$.

Bates

In this two-factor model, an investment in the stock leads to an exposure to the two independent risk factors dW_{1t} and dW_{2t} and the wealth follows the dynamics

$$dY_t = rY_t dt + \phi_t Y_t ((\eta_1 V_{1t} + \eta_2 V_{2t}) dt + \sqrt{V_{1t}} dW_{1t} + \sqrt{V_{2t}} dW_{2t})$$

with ϕ as the fraction invested in the stock. Each of the two factors is correlated (through correlations ρ_1 and ρ_2) to the stochastic investment opportunity set. The optimal stock position therefore contains two hedging components:

$$\phi_t = \frac{1}{\gamma} \left[\eta_1 \frac{V_{1t}}{V_{1t} + V_{2t}} + \eta_2 \frac{V_{2t}}{V_{1t} + V_{2t}} \right] + \rho_1 \sigma_1 \frac{V_{1t}}{V_{1t} + V_{2t}} \frac{g_1}{g} + \rho_2 \sigma_2 \frac{V_{2t}}{V_{1t} + V_{2t}} \frac{g_2}{g}.$$

with g_i ($i = 1, 2$) denoting the derivative of g w.r.t. variance component i . The function g follows from the indirect utility of the investor defined as

$$J(t, Y_t, V_{1t}, V_{2t}) = \frac{Y_t^{1-\gamma}}{1-\gamma} g(T-t, V_{1t}, V_{2t}) \quad (3)$$

Although the Bates model is included in the affine model class, we cannot give a more specific expression for the function g , but only note that it will be a function of the investor's planning horizon $T - t$ and the state variables V_1 and V_2 . Interestingly and in contrast to the two models above, the indirect utility J , the function g , and thus also the optimal portfolio ϕ cannot be solved in closed form. Although this model is affine and there exist closed-form solutions for the option prices, the optimal asset allocation in

the case of an incomplete market has to be solved numerically (Details on this numerical computation are presented in the following section and in Appendix C).

Another interesting point is that the optimal stock position is now state-dependent. First, the myopic demand is stochastic since the risk compensation per unit of stock-variance changes stochastically depending on the exact decomposition of total variance into the two variance components. Second, the state-dependence of the hedging demand is generated by the stochastic stock-volatility correlation. Hence, each component individually would make the optimal stock position state-dependent.

4.1 Numerical Example

Before presenting the results of the optimal portfolio composition, we first discuss some details on the numerical computation.

Computational Details

For all models, we solve the arising PDEs numerically. In the cases where closed-form solutions exist, the numerical values are indistinguishable in case of a sufficient number of discretization steps (usually about 10,000 Euler steps).

In case of the Bates model in an incomplete market, no closed-form solution for the asset allocation exists. Therefore, we solve for the function g and its derivatives by applying the method of finite differences to the HJB equation. When using the standard guess (3) for the indirect utility, g follows the PDE

$$\begin{aligned} -g' = & -(1 - \gamma) \left[r + \phi_t(\eta_1 V_{1t} + \eta_2 V_{2t}) + \frac{1}{2}\gamma(1 - \gamma)\phi_t^2(V_{1t} + V_{2t}) \right] g \\ & - [\kappa_1(\theta_1 - V_{1t}) + (1 - \gamma)\sigma_1\rho_1\phi_t V_{1t}] g_1 - \frac{1}{2}\sigma_1^2 V_{1t} g_{11} \\ & - [\kappa_2(\theta_2 - V_{2t}) + (1 - \gamma)\sigma_2\rho_2\phi_t V_{2t}] g_2 - \frac{1}{2}\sigma_2^2 V_{2t} g_{22} \end{aligned}$$

with boundary condition $g(0, V_{1t}, V_{2t}) = 1$ and g_i and g_{ii} ($i = 1, 2$) denoting the first and second derivatives with respect to variance component i , respectively. The approach is similar to the one proposed in Brennan, Schwartz and Lagnado (1997). Nevertheless, some changes in the boundary conditions and the advances in computational speed allow to improve the accuracy of the results.

To solve the PDE in the three dimensions $T - t$, V_1 and V_2 , we apply an ADI finite difference approximation on a grid with 4000 points in time direction and 200 points in

either variance direction. The emerging system of equations is solved via exact LU decomposition. The partial derivatives inside the grid are discretized using central difference approximations. The variance components range from 0 to 0.1 with a resulting step size of 0.0005. Due to the state dependence of ϕ , one has to iterate on this variable using values of the partial derivatives from the previous time step as proposed in Brennan, Schwartz and Lagnado (1997). For sufficiently small time steps, however, ϕ changes only to a very small extent from one step to the other and the iteration becomes therefore dispensable. We further impose the boundary conditions $g_{ii} = 0$ for V_{it}^{min} and V_{it}^{max} ($i = 1, 2$). To check the accuracy of the procedure, we applied the numerical procedure in case of the SLRM model where a closed-form solution of the optimal position exists. The deviation of the numerically computed indirect utility from its closed-form counterpart was less than 1%. The procedure was therefore considered to yield sufficiently precise results.

Asset Allocation Results

In the following we discuss the resulting optimal portfolio composition in the different models. Under the assumption of an incomplete market, the investor invests the fraction of wealth ϕ in the stock and the remainder in the money market account.

First, we discuss the optimal position in the Bates model. Figure 3 shows that, in contrast to the other models, the investor's optimal stock position is state-dependent. The graphs plot the optimal stock position as a function of local variance V_{1t} when total variance $V_t = V_{1t} + V_{2t}$ is restricted to be equal to 0.04. In this example, all but one parameter are the same for the two variance processes. In the benchmark case (solid line) they are thus perfectly symmetric and the investment is state-independent. In the left graph, we assume the market prices of risk η of the two variance components to be different, but the long-run expected excess return ($\theta_1\eta_1 + \theta_2\eta_2$) is held constant at 10%. In this case, $\rho_1 = \rho_2 = 0$, so there is no hedging demand and in the benchmark case where $\eta = \eta_1 = \eta_2 = 2.5$ we have an optimal position in the stock of $\phi = \eta/\gamma = 2.5/3 = 0.833$ for all V_{1t} . Here, state-dependence can only come from the myopic demand. For $\eta_1 > \eta_2$, the (locally) expected excess return on the stock, and thus also the investment in the stock, is the larger the larger V_{1t} is relative to V_{2t} . The reverse holds for $\eta_1 < \eta_2$. For the special case $V_{1t} = V_{2t} = 0.02$, $\phi = \frac{0.02}{0.04} \frac{\eta_1 + \eta_2}{\gamma} = 0.833$, which corresponds to the benchmark case.

In the right graph, the market prices of risk of the two processes are equal, but the correlations are assumed to be different. Since $\eta_1 = \eta_2 = 2.5$, the myopic part of the stock

demand is constant and equal to $2.5/3.0=0.833$ and thus all state-dependence comes from the hedging demand. The state-dependence generated by the hedging demand only is much smaller than the one generated by myopic demand (note the scaling of the graphs). We assume an investor with $\gamma > 1$, so g_i/g will be negative (for a discussion see e.g. Branger, Schlag and Schneider (2007)). For $\rho_1 > \rho_2$, the hedging demand decreases in V_{1t} increasing (relative to V_{2t}), the reverse holds for $\rho_1 < \rho_2$. For $V_{1t} = V_{2t} = 0.02$, the stock position is larger than in the benchmark case. This is due to the fact that g_i is convex in ρ_i and thus, for the same absolute correlation, but different sign, the two do not offset each other but there is still a positive hedging demand. A similar result can be obtained for the case of differences in variance of variance $\sigma_1 \neq \sigma_2$.

In a next step, we compare the optimal stock position across the different models. To make the models comparable, we use again the results from our calibration exercise in Table 1. Note that besides the \mathbb{Q} -parameters, we need assumptions on the risk premia to derive the optimal asset allocation. Therefore, we set the long-run expected excess return on the stock equal to 10% which results in $\eta = 2.17$ for the one-factor Heston model, $\eta_1 = \eta_2 = 2.17$ in the Bates model (assuming the same risk compensation for each factor) and $\eta_V = 2.5$ in the SLRM model.

The optimal stock position as a function of the investment horizon is shown in the left graph of Figure 4. For the given calibration, the investment in the stock is larger for the SLRM model than for the other two models for all investment horizons. This is due to the larger myopic demand induced by the higher risk compensation per unit of risk $\eta_V = 2.5$. Due to the hedging demand, the optimal stock position is the higher the longer the investment horizon. This impact of the hedging demand is largest for the Bates model and can be explained as follows. The higher the local variances, the larger the expected excess return on the stock. Shocks in the variance are, however, highly negatively correlated to shocks in the stock price and the investor can hedge a decrease in the expected excess return caused by a decrease in local variance with a long position in the stock. As a result, the investor hedges by shifting wealth from states with high variance to states with low variance, i.e. from states with good investment opportunities to states with bad investment opportunities. In the other two models, a position in the stock gives exposure to one other state variable only. The covariance, although negative, is lower in absolute value than for the Bates model and hedging is thus more difficult.

In the right graph of Figure 4, the special feature of the Bates model becomes apparent. For the Heston model and the SLRM model the stock position is state-independent and only depends on the investment horizon. In contrast, the stock position in the Bates model decreases in the relative importance of V_1 for our parametrization. This state-dependence comes from hedging demand only, since by assuming the same market prices of risk for both volatility components the myopic part does not change. The lower the local variance component V_1 , the more weight is shifted to the component V_2 with the higher covariance $\sigma_2\rho_2$ with the stock. Therefore the hedging demand and consequently the optimal position in the stock increases.

Compared to other model specifications, the Bates model thus implies some interesting properties concerning the optimal stock position in an incomplete market. The question we want to answer in the next section is whether the resulting differences in the optimal asset allocation are economically important, and in particular, how large is the utility loss suffered by an investor in case of model mis-specification.

4.2 Impact of Model Mis-Specification

Another point of interest in asset allocation is to assess the impact of model mis-specification on the utility of the investor. For example, consider the following setup: The true model is a model with two volatility components. However, the investor ignores volatility components and assumes a one-factor Heston model to be the true data generating process. It is then interesting to compute the utility loss suffered by this investor when the true model is either the SLRM model or the Bates model.

Similarly, many other types of model mis-specification are conceivable and we aim to provide a general methodology to compute the utility in those cases. For the sake of simplicity, we assume that the market is incomplete and thus, that the portfolio of the investor consists only of a position in the stock and the money market account. However, the methodology is just as well applicable in complete markets.

Computation of the utility loss

We measure the utility loss via the difference in certainty equivalent wealth:

$$\mathcal{R}^{\mathcal{Y}} = \frac{1}{T}(\ln(\mathcal{Y}) - \ln(\widehat{\mathcal{Y}})) \quad (4)$$

where \mathcal{Y} and $\widehat{\mathcal{Y}}$ solve $J_0 = \mathcal{Y}^{1-\gamma}/(1-\gamma)$ and $\widehat{J}_0 = \widehat{\mathcal{Y}}^{1-\gamma}/(1-\gamma)$, with J_0 and \widehat{J}_0 as indirect utility under the correct and under the mis-specified model, respectively.

In general, the indirect utility obtained with strategy ϕ is defined as today's expected utility of terminal wealth

$$J_0^\phi = E \left[U(Y_T^\phi) \right].$$

In case the investor uses the optimal strategy ϕ^* , it follows

$$J_0 = \max_{\phi} E \left[U(Y_T^\phi) \right].$$

On the other hand, when he uses a suboptimal strategy $\widehat{\phi}$, the investor obtains the indirect utility

$$\widehat{J}_0 = E \left[U(Y_T^{\widehat{\phi}}) \right] \leq J_0.$$

It is important to note that under both the optimal and the suboptimal strategy, the indirect utility is defined as the conditional \mathbb{P} -expectation of the utility of terminal wealth and as such is a \mathbb{P} -martingale. From this results the condition that the indirect utility has no drift under \mathbb{P} , and together with the boundary condition $J_T^\phi = Y_T^{1-\gamma}/(1-\gamma)$ we can derive (at least numerically) the indirect utility in both cases. For the optimal strategy, this condition yields the well-known HJB equation. In case of the suboptimal strategy, the PDE is structurally the same as the HJB equation but replacing J and ϕ with \widehat{J} and $\widehat{\phi}$.

Under certain conditions, this PDE can be solved in closed-form. The main condition is that the share invested in the risky asset has to be state-dependent. So either we need a constant investment opportunity set for the true model or all asset positions taken under the assumed model need to be state-independent. An example in the literature where a closed-form solution for the mis-specified case can be derived is Liu, Longstaff and Pan (2003). This is the case despite the fact that they have a stochastic investment opportunity set, because they allow for investments in linear claims (stock and money market account) only. In contrast, Branger, Schlag and Schneider (2007) work in a complete markets and derive optimal exposures to the different risk factors in the optimal and in the mis-specified case. However, the realized exposures depend on the sensitivities of the traded claims which themselves are in general state-dependent. This is exactly what makes a closed-form solution of the PDE in their case impossible. As one of the main contributions of the paper we show that \widehat{J} and $\widehat{\phi}$ can be found numerically via the method of finite differences.

With regard to our two models, the computation of the suboptimal indirect utility in the SLRM model results in the numerical solution of ODEs. In the Bates model, at every node of the finite difference grid, we plug in the (state- and time-dependent) position of the investor under model mis-specification and solve backwards to obtain the numerical value of the indirect utility. Principally, the case of the complete market, i.e. where we solve for exposures to risk factors instead of asset positions, can be solved by the same procedure. At every node, we have to proceed in two steps: first, we compute the seemingly optimal exposure under model mis-specification. Second, we transfer these seemingly optimal exposures into realized exposures by using the (state- and time-dependent) sensitivities of the traded assets. Finally, these state-dependent realized exposures are plugged in the discretized PDE which we can solve backwards to obtain the corresponding indirect utility.

The method of finite differences thus allows us to compute the indirect utility of suboptimal strategies without having to rely on closed-form solutions. One has to note however, that when the true (but not the assumed) model is driven by a jump process, default (and therefore a utility loss of 100%) becomes possible. In this case, it is therefore more reasonable to consider other statistics like e.g. the distribution of terminal wealth (see Branger, Schlag and Schneider (2007)).

Numerical Example

In this section, we apply the described procedure to our models. The investor ignores the fact that the model has two volatility components and instead assumes the Heston model with the parametrization from Table 1 to be true. He computes the (seemingly) optimal stock position $\hat{\phi}$ via Equation (2). This position is only time- but not state-dependent. To compute the indirect utility \hat{J}_t obtained under model mis-specification, we plug the investor's stock position $\hat{\phi}$ into the HJB equation of the true data generating process (again with the parametrization of Table 1).

In case of the SLRM model as the true model, the indirect utility can be solved in closed-form. It has the general form

$$\hat{J}_t(V_t, \bar{V}_t) = \frac{Y_t^{1-\gamma}}{1-\gamma} \exp\{\gamma \hat{h}(T-t) + \gamma \hat{H}(T-t)V_t + \gamma \hat{H}(T-t)\bar{V}_t\}. \quad (5)$$

The ODEs to be satisfied by the functions $\hat{h}(T-t)$, $\hat{H}(T-t)$ and $\hat{H}(T-t)$ are derived as described before:

$$\begin{aligned}
(\widehat{H})' &= \frac{1-\gamma}{\gamma}\eta_V\widehat{\phi} - \frac{1}{2}(1-\gamma)\widehat{\phi}^2 + ((1-\gamma)\rho_V\sigma_V\widehat{\phi} - \kappa_V)\widehat{H} + \frac{1}{2}\gamma\sigma_V^2\widehat{H}^2 \\
(\widehat{H})' &= \kappa_V\widehat{H} - \kappa_{\widehat{V}}\widehat{H} + \frac{1}{2}\gamma\sigma_{\widehat{V}}^2\widehat{H}^2 \\
\widehat{h}' &= \frac{1-\gamma}{\gamma}r + \kappa_{\widehat{V}}\theta_{\widehat{V}}\widehat{H}
\end{aligned}$$

subject to the boundary conditions $\widehat{H}(0) = \widehat{H}(0) = \widehat{h}(0) = 0$.

The resulting utility loss from assuming a Heston model is shown in the upper-left graph of Figure 5. Although there are pronounced differences between the optimal and the seemingly optimal position (see left graph of Figure 4), the utility loss from model mis-specification is rather small ($\mathcal{R}^{\mathcal{Y}}$ less than 15 basis points p.a.).

For comparison, we repeat the same exercise when the investor assumes a model without stochastic volatility, in this case a Black and Scholes (1973) dynamics. With a stock risk premium of 2.5 and a risk aversion of $\gamma = 3.0$ the investor perceives a constant stock position of $2.5/3=0.833$ to be optimal. In the upper-right graph of Figure 5 one can see that the utility loss in this case is even smaller than in case of Heston (1993) model. This can be explained by the smaller difference in the stock position between the BS and the SLRM case than between the Heston and the SLRM case (compare the BS stock position $\widehat{\phi} = 0.833$ with the values in Figure 4).

When the Bates model is true, the indirect utility has to be computed numerically via the method of finite differences. As in the optimal case, we compute the indirect utility under model mis-specification by solving numerically for \widehat{g} in

$$\widehat{J}_t = \frac{Y^{1-\gamma}}{1-\gamma}\widehat{g}(T-t, V_{1t}, V_{2t}).$$

To do this, we use the same discretization scheme as in the optimal case, but we plug in the seemingly optimal $\widehat{\phi}$ from Equation (2) at every node.

By assuming the Heston model, this stock position is not state-dependent as in the optimum, but only time-dependent. Although Figure 4 shows that there are only small differences between the optimal and the seemingly optimal exposure (at least for the values of the state variables considered in this graph), the investor suffers an economically significant utility loss of 20 to 30 basis points per year (see lower-left graph of Figure 5). This loss decreases in V_1 (and increases in V_2). To get the intuition, note that in this graph the total local variance is held constant at 0.04, so the larger V_1 relative to V_2 , the smaller the utility loss. This result is confirmed by the right graph of Figure 4. The larger

V_1 relative to V_2 , the smaller the difference between the optimal Bates and the seemingly optimal Heston portfolio.

Again we consider the case of an assumed Black and Scholes (1973) model for comparison. As shown in the upper-right graph of Figure 5, with less than 6 basis points the utility loss is smaller than with the Heston (1993) mis-specification. Thus, for many states, an underestimation of the optimal stock position (as with assumed Heston model) seems to be worse than the opposite mistake as with the assumed Black and Scholes model. This is in sharp contrast to results from the literature for the case of mis-specification of jumps, where an overestimation of the optimal stock position may lead to a default of the investor and thus to a significant loss in utility. The utility loss is the larger, the larger V_1 relative to V_2 . This is confirmed by comparing the BS-position in stock (constantly 0.833) with the optimal position in the Bates model: The larger the relative importance of V_1 , the larger the deviation of the BS stock position compared to the optimal stock position in the Bates model.

A comparison with the results of Branger, Schlag and Schneider (2007) shows that, in line with intuition, the utility loss in case of volatility component mis-specification is in general smaller than in case of model mis-specification concerning jumps. As for option pricing, the Heston model is much closer to the SLRM model and no significant utility losses are obtained. In contrast, a mis-specification concerning multiple variance factors as in the Bates model induces larger losses in utility.

5 Conclusion

In this paper we have analyzed different aspects of volatility component models and compared them to the results obtained in usual one-factor models. Hereby, we focused on the economic (and technical) differences concerning option pricing and asset allocation and the impact of model mis-specification.

For option prices and the resulting smile dynamics, the inclusion of volatility components in the form of a stochastic long-run mean does not provide an important added value compared to a single-factor model. Except for the fact that the volatility smile may change its level although local volatility remains constant, the SLRM model primarily impacts options with very long maturity. In contrast, the inclusion of multiple volatility factors as in the Bates (2000) model significantly enhances the empirical fit of the smile

dynamics. In particular, we observe a stochastic correlation, a stochastic speed of mean-reversion and a stochastic volatility of variance and the model can thus explain twisting, steepening and parallel shifts of the smile within the same parametrization.

For asset allocation, again the SLRM does not provide a significant modification compared to the results obtained with the Heston model. In contrast, the Bates model represents a significant extension. In addition to the stochastic correlation, the model specification implies a stochastic expected excess return of the stock per unit of variance which makes the optimal stock position not only time-, but also state-dependent. From a technical point of view, it is interesting to note that although the model falls into the class of affine models as defined in Duffie, Pan and Singleton (2000) it does not have a closed-form solution for the indirect utility and/or the optimal stock position. Concerning model mis-specification, i.e. assuming an investor ignoring volatility components, the utility losses are negligible when the true model is the SLRM model, but economically important when the true data generating process follows a Bates model. Nevertheless, compared to the results of the literature concerning the utility losses in case of jump mis-specification, the utility losses are rather moderate.

Technically, this paper shows how the finite difference method can generally be applied to compute utility losses from model mis-specification in other models, no matter if the market is assumed to be complete or incomplete.

References

- Adrian, T. and J. Rosenberg, 2005, Stock Returns and Volatility: Pricing the Short-Run and Long-Run Components of Market Risk, Working Paper.
- Bakshi, G. and D. Madan, 2000, Spanning and Derivative-Security Valuation, *Journal of Financial Economics* 55, 205–238.
- Bates, D.S., 2000, Post-'87 Crash Fears in the S&P Futures Option Market, *Journal of Econometrics* 94, 181–238.
- Black, F. and M. Scholes, 1973, The Pricing of Options and Corporate Liabilities, *Journal of Political Economy* 81, 637–654.
- Branger, N., C. Schlag and E. Schneider, 2007, Optimal Portfolios When Volatility can Jump, forthcoming *Journal of Banking and Finance*.

- Brennan, M. J., E.S. Schwartz and R. Lagnado, 1997, Strategic Asset Allocation, *Journal of Economic Dynamics and Control* 21, 1377–1403.
- Chacko, G. and L.M. Viceira, 2003, Spectral GMM estimation of continuous-time processes, *Journal of Econometrics* 116, 259–292.
- Chernov, M., A. R. Gallant, E. Ghysels and G. Tauchen, 2003, Alternative models for stock price dynamics, *Journal of Econometrics* 116, 225–257.
- Christoffersen, P., S. Heston and K. Jacobs, 2007, The Shape and the Term Structure of the Index Smirk: Why Multifactor Stochastic Volatility Models Work So Well, Working Paper.
- Christoffersen, P., K. Jacobs and Yintian Wang, 2005, Option Valuation with Long-run and Short-run Volatility Components, Working Paper.
- Duffie, D., J. Pan and K. Singleton, 2000, Transform Analysis and Asset Pricing for Affine Jump Diffusions, *Econometrica* 68, 1343–1376.
- Heston, S.L., 1993, A Closed-Form Solution for Options with Stochastic Volatility with Applications to Bond and Currency Options, *Review of Financial Studies* 6, 327–343.
- Liu, J., F.A. Longstaff and J. Pan, 2003, Dynamic Asset Allocation with Event Risk, *Journal of Finance* 58, 231–259.
- Liu, J. and J. Pan, 2003, Dynamic Derivatives Strategies, *Journal of Financial Economics* 69, 401–430.

A Fourier Transforms of State Price Density

Heston

A closed-form solution for the Fourier transform of the state price density is derived in Heston (1993). In our notation it is given by

$$\varphi(u, T-t, S_t, V_t) = \exp\{A(T-t, u) + B(T-t, u)V_t + iu \ln S_t\}$$

where the functions $A(T-t, u)$ and $B(T-t, u)$ solve the following system of differential equations

$$\begin{aligned} A'(\cdot, u) &= iur + \kappa\theta B(\cdot, u) \\ B'(\cdot, u) &= -0.5iu - 0.5u^2 + (\rho\sigma iu - \kappa - \sigma\xi)B(\cdot, u) + 0.5\sigma^2 B^2(\cdot, u) \end{aligned}$$

with boundary conditions $A(0, u) = 0$ and $B(0, u) = 0$. As described in Heston (1993), the system of differential equations can be solved in closed-form.

SLRM

The Fourier transform of the state price density in the SLRM model can be derived as

$$\varphi(u, T-t, S_t, V_t, \bar{V}_t) = \exp\{A(T-t, u) + B(T-t, u)V_t + C(T-t, u)\bar{V}_t + iu \ln S_t\}$$

where the functions $A(T-t, u)$, $B(T-t, u)$ and $C(T-t, u)$ solve the following system of differential equations

$$\begin{aligned} A'(\cdot, u) &= iur + \kappa_{\bar{V}}\theta_{\bar{V}}C(\cdot, u) \\ B'(\cdot, u) &= -0.5iu - 0.5u^2 + (\rho_V\sigma_V iu - \kappa_V - \sigma_V\xi_V)B(\cdot, u) + 0.5\sigma_V^2 B^2(\cdot, u) \\ C'(\cdot, u) &= \kappa_V B(\cdot, u) - (\kappa_{\bar{V}} + \sigma_{\bar{V}}\xi_{\bar{V}})C(\cdot, u) + 0.5\sigma_{\bar{V}}^2 C^2(\cdot, u) \end{aligned}$$

with boundary conditions $A(0, u) = 0$, $B(0, u) = 0$ and $C(0, u) = 0$. The system of differential equation is solved numerically.

Bates

The Fourier transform of the state price density in the Bates model results as a special case from the closed-form solution in Bates (2000). It is given as

$$\varphi(u, T-t, S_t, V_t, \bar{V}_t) = \exp\{A(T-t, u) + B(T-t, u)V_{1t} + C(T-t, u)V_{2t} + iu \ln S_t\}$$

where the function $A(T-t, u)$, $B(T-t, u)$ and $C(T-t, u)$ solve the following system of differential equations

$$\begin{aligned} A'(\cdot, u) &= iur + \kappa_1\theta_1B(\cdot, u) + \kappa_2\theta_2C(\cdot, u) \\ B'(\cdot, u) &= -0.5iu - 0.5u^2 + (\rho_1\sigma_1iu - \kappa_1 - \sigma_1\xi_1)B(\cdot, u) + 0.5\sigma_1^2B^2(\cdot, u) \\ C'(\cdot, u) &= -0.5iu - 0.5u^2 + (\rho_2\sigma_2iu - \kappa_2 - \sigma_2\xi_2)C(\cdot, u) + 0.5\sigma_2^2C^2(\cdot, u) \end{aligned}$$

with boundary conditions $A(0, u) = 0$, $B(0, u) = 0$ and $C(0, u) = 0$. The system of differential equations can be solved in closed form. Details are given in Bates (2000).

B Indirect Utility J in the Complete Market

In this section, we assume the existence of a complete market, i.e. we assume that the stock, the money market account and a sufficient number of derivatives are traded. The solution follows the approach introduced in Liu and Pan (2003). In this complete market, all risk factors can be traded separately. In a first step, the optimal exposures to the different risk factors are derived, before in a second step one transfers these optimal exposures into fractions of wealth to be invested in the traded assets using the sensitivities of these assets.

As in the incomplete market, the investor is assumed to have CRRA utility with a coefficient of risk aversion γ and has the objective

$$\max_{\Theta} E[U(Y_T)] = E \left[\frac{Y_T^{1-\gamma}}{1-\gamma} \right]$$

where Θ contains the exposures to all the risk factors of the assumed dynamics and depends therefore on the model setup.

Heston

In the one-factor Heston model, one derivative needs to be traded to complete the market. The optimal exposure then can be calculated as a special case of the Liu and Pan (2003) results. With θ and θ^V as fractions of wealth invested in the risk factors $\sqrt{V_t}dW_t$ and $\sqrt{V_t^V}dW_t^V$, we obtain the following wealth dynamics:

$$\begin{aligned} dY_t &= rY_t dt \\ &+ Y_t \theta_t \left(\eta V_t dt + \sqrt{V_t} dW_t \right) \\ &+ Y_t \theta_t^V \left(\xi V_t dt + \sqrt{V_t^V} dW_t^V \right). \end{aligned}$$

With the guess

$$J(t, Y_t, V_t) = \frac{Y_t^{1-\gamma}}{1-\gamma} \exp\{\gamma h(T-t) + \gamma H(T-t)V_t\}$$

for the indirect utility, the optimal portfolio can be derived from the HJB equation:

$$\begin{aligned} \theta_t &= \frac{\eta}{\gamma} + \rho \sigma H(\tau) \\ \theta_t^V &= \frac{\xi}{\gamma} + \sqrt{1-\rho^2} \sigma H(\tau) \end{aligned}$$

with $\tau = T - t$ and where the indirect utility J and the function $H(\tau)$ can be solved in closed form. The result is quite standard. There are two risk factors to invest in and the stochastic investment opportunity set induces a hedging demand which depends on the investment horizon of investor through $H(\tau)$.

Plugging the optimal exposures back in the HJB equation leads to two ODEs for h and H with boundary conditions $H(0) = 0$ and $h(0) = 0$

$$\begin{aligned} (H)' &= \frac{1-\gamma}{2\gamma^2}(\eta^2 + \xi^2) + \left(\frac{1-\gamma}{\gamma}\sigma(\eta\rho + \xi\sqrt{1-\rho^2}) - \kappa\right)H + \frac{1}{2}\sigma^2 H^2 \\ h' &= \frac{1-\gamma}{\gamma}r + \kappa\theta H \end{aligned}$$

which can be solved in closed-form. Details are given in Liu and Pan (2003).

SLRM

In the SLRM model, two derivatives need to be traded to complete the market, one risky asset for each risk factor. The wealth dynamics then follows as

$$\begin{aligned}
 dY_t &= rY_t dt \\
 &\quad + Y_t \theta_t \left(\eta_V V_t dt + \sqrt{\bar{V}_t} dW_t \right) \\
 &\quad + Y_t \theta_t^V \left(\xi_V V_t dt + \sqrt{\bar{V}_t} dW_t^V \right) \\
 &\quad + Y_t \theta_t^{\bar{V}} \left(\xi_{\bar{V}} \bar{V}_t dt + \sqrt{\bar{V}_t} dW_t^{\bar{V}} \right)
 \end{aligned}$$

with θ , θ^V and $\theta^{\bar{V}}$ as fractions of wealth invested in $\sqrt{\bar{V}_t} dW_t$, $\sqrt{\bar{V}_t} dW_t^V$ and $\sqrt{\bar{V}_t} dW_t^{\bar{V}}$, respectively. As before, the guess

$$J(t, Y_t, V_t, \bar{V}_t) = \frac{Y_t^{1-\gamma}}{1-\gamma} \exp\{\gamma h(T-t) + \gamma H(T-t)V_t + \gamma \bar{H}(T-t)\bar{V}_t\}$$

for the indirect utility allows the derivation of the optimal risk exposures

$$\begin{aligned}
 \theta_t &= \frac{\eta_V}{\gamma} + \rho_V \sigma_V H(\tau) \\
 \theta_t^V &= \frac{\xi_V}{\gamma} + \sqrt{1 - \rho_V^2} \sigma_V H(\tau) \\
 \theta_t^{\bar{V}} &= \frac{\xi_{\bar{V}}}{\gamma} + \sigma_{\bar{V}} \bar{H}(\tau)
 \end{aligned}$$

with $\tau = T - t$ and where again, J and H can be computed in closed-form by solving

$$\begin{aligned}
 (H)' &= \frac{1-\gamma}{2\gamma^2} (\eta_V^2 + \xi_V^2) + \left(\frac{1-\gamma}{\gamma} (\eta_V \rho_V \sigma_V + \xi_V \sqrt{1 - \rho_V^2} \sigma_V) - \kappa_V \right) H + \frac{1}{2} \sigma_V^2 H^2 \\
 (\bar{H})' &= \frac{1-\gamma}{2\gamma^2} \xi_{\bar{V}}^2 + \kappa_{\bar{V}} H + \left(\frac{1-\gamma}{\gamma} \xi_{\bar{V}} \sigma_{\bar{V}} - \kappa_{\bar{V}} \right) \bar{H} + \frac{1}{2} \sigma_{\bar{V}}^2 \bar{H}^2 \\
 h' &= \frac{1-\gamma}{\gamma} r + \kappa_{\bar{V}} \theta_{\bar{V}} \bar{H}
 \end{aligned}$$

with boundary conditions $H(0) = 0$, $\bar{H}(0) = 0$ and $h(0) = 0$. The system of differential equations is solved numerically. There are three risk factors to invest in and the stochastic investment opportunity set induces a hedging demand in all of them. Since the correlation between the Wiener processes in V_t and \bar{V}_t is assumed to be zero, 'cross-hedging' is not possible and each optimal exposure has only one hedging component. The optimal positions are time- but not state-dependent.

Bates

To complete the market, three traded derivatives are needed to invest individually in each of the four risk factors. The wealth dynamics are then

$$\begin{aligned}
dY_t &= rY_t dt \\
&+ \sum_{i=1}^2 Y_t \theta_t^i \left(\eta_i V_{it} dt + \sqrt{V_{it}} dW_t^i \right) \\
&+ \sum_{i=1}^2 Y_t \theta_t^{iV} \left(\xi_i V_{it} dt + \sqrt{V_{it}} dW_t^{Vi} \right)
\end{aligned}$$

with θ^i and θ^{Vi} as fractions invested in $\sqrt{V_{it}}dW_t^i$ and $\sqrt{V_{it}}dW_t^{Vi}$, $i = 1, 2$, respectively.

The optimal portfolio follows with

$$J(t, Y_t, V_{1t}, V_{2t}) = \frac{Y_t^{1-\gamma}}{1-\gamma} \exp \{ \gamma h(T-t) + \gamma H^1(T-t)V_{1t} + \gamma H^2(T-t)V_{2t} \}$$

as guess for the indirect utility:

$$\begin{aligned}
\theta_t^i &= \frac{\eta_i}{\gamma} + \rho_i \sigma_i H^i(\tau) \\
\theta_t^{iV} &= \frac{\xi_i}{\gamma} + \sqrt{1 - \rho_i^2} \sigma_{iV} H^i(\tau)
\end{aligned}$$

where $i = 1, 2$ and $\tau = T - t$. Here h , H^1 and H^2 solve the following ODEs

$$\begin{aligned}
H^{i'} &= \frac{1-\gamma}{2\gamma^2} (\eta_i^2 + \xi_i^2) + \left[\frac{1-\gamma}{\gamma} \sigma_i (\eta_i \rho_i + \xi_i \sqrt{1 - \rho_i^2}) - \kappa_i \right] H^i + \frac{1}{2} \sigma_i^2 (H^i)^2, i = 1, 2 \\
h' &= \frac{1-\gamma}{\gamma} r + \kappa_1 \theta_1 H^1 + \kappa_2 \theta_2 H^2
\end{aligned}$$

with boundary conditions $h(0) = 0$, $H^1(0) = 0$ and $H^2(0) = 0$. The system of differential equations can be solved in closed-form (compare to the results in Liu and Pan (2003)). Contrary to the case of an incomplete market, the optimal portfolio position can thus be derived in closed-form and is only time- but not state-dependent.

C Indirect Utility J in the Incomplete Market

Heston

The indirect utility J is given by

$$J(t, Y_t, V_t) = \frac{Y_t^{1-\gamma}}{1-\gamma} \exp \{ \gamma h(T-t) + \gamma H(T-t)V_t \}$$

where H solves

$$\begin{aligned}
H' &= \frac{1-\gamma}{2\gamma^2} \eta^2 + \left(\frac{1-\gamma}{\gamma} \sigma \rho \eta - \kappa \right) H + \frac{1}{2} ((1-\gamma)\rho^2 + \gamma)\sigma^2 H^2 \\
h' &= \frac{1-\gamma}{\gamma} r + \kappa \theta H
\end{aligned}$$

with the boundary conditions $H(0) = 0$ and $h(0) = 0$. The system of differential equations is solved numerically.

SLRM

The indirect utility J is given by

$$J(t, Y_t, V_t, \bar{V}_t) = \frac{Y_t^{1-\gamma}}{1-\gamma} \exp\{\gamma h(T-t) + \gamma H(T-t)V_t + \gamma \bar{H}(T-t)\bar{V}_t\}$$

where H solves

$$\begin{aligned} H' &= \frac{1-\gamma}{2\gamma^2} \eta_V^2 + \left(\frac{1-\gamma}{\gamma} \sigma_V \rho_V \eta_V - \kappa_V \right) H + \frac{1}{2} ((1-\gamma)\rho_V^2 + \gamma)\sigma_V^2 H^2 \\ \bar{H}' &= \kappa_V H - \kappa_{\bar{V}} \bar{H} + \frac{1}{2} \gamma \sigma_{\bar{V}}^2 \bar{H}^2 \\ h' &= \frac{1-\gamma}{\gamma} r + \kappa_{\bar{V}} \bar{\theta} \bar{H} \end{aligned}$$

with the boundary conditions $H(0) = 0$, $\bar{H}(0) = 0$ and $h(0) = 0$. The system of differential equations is solved numerically.

Bates

The indirect utility J is given by

$$J(t, Y_t, V_{1t}, V_{2t}) = \frac{Y_t^{1-\gamma}}{1-\gamma} g(T-t, V_{1t}, V_{2t})$$

where g solves

$$\begin{aligned} -g' &= -(1-\gamma) \left[r + \phi_t (\eta_1 V_{1t} + \eta_2 V_{2t}) + \frac{1}{2} \gamma (1-\gamma) \phi_t^2 (V_{1t} + V_{2t}) \right] g \\ &\quad - [\kappa_1 (\theta_1 - V_{1t}) + (1-\gamma) \sigma_1 \rho_1 \phi_t V_{1t}] g_1 - \frac{1}{2} \sigma_1^2 V_{1t} g_{11} \\ &\quad - [\kappa_2 (\theta_2 - V_{2t}) + (1-\gamma) \sigma_2 \rho_2 \phi_t V_{2t}] g_2 - \frac{1}{2} \sigma_2^2 V_{2t} g_{22} \end{aligned}$$

and

$$\phi_t = \frac{1}{\gamma} \left[\eta_1 \frac{V_{1t}}{V_{1t} + V_{2t}} + \eta_2 \frac{V_{2t}}{V_{1t} + V_{2t}} \right] + \frac{\rho_1 \sigma_1}{\gamma} \frac{V_{1t}}{V_{1t} + V_{2t}} \frac{g_1}{g} + \frac{\rho_2 \sigma_2}{\gamma} \frac{V_{2t}}{V_{1t} + V_{2t}} \frac{g_2}{g}$$

with the boundary condition $g(0, V_{1T}, V_{2T}) = 1$. The differential equation cannot be solved in closed form. It is therefore solved by the method of finite differences.

	V_1	κ_1	θ_1	σ_1	ρ_1	V_2	κ_2	θ_2	σ_2	ρ_2
Heston	0.040	3.650	0.046	0.263	-0.675					
SLRM	0.040	4.500		0.300	-0.600	0.040	0.500	0.040	0.100	
Bates	0.025	3.068	0.038	0.105	-0.900	0.015	1.839	0.008	0.403	-0.744

Table 1. Calibrated Q-Parameters

The table summarizes the results of the calibration. In case of the stochastic long-run mean model (SLRM) V_1 and the corresponding parameters refer to the local variance, V_2 and the corresponding parameters to the local long-run mean. The market prices of risk were chosen such that the long-run expected excess return on the stock equals 10%, i.e. $\eta = 2.17$ in the model of Heston (1993), $\eta_1 = \eta_2 = 2.17$ in the model of Bates (2000), $\eta_V = 2.5$ and $\xi_V = -2.0$ in the SLRM model.

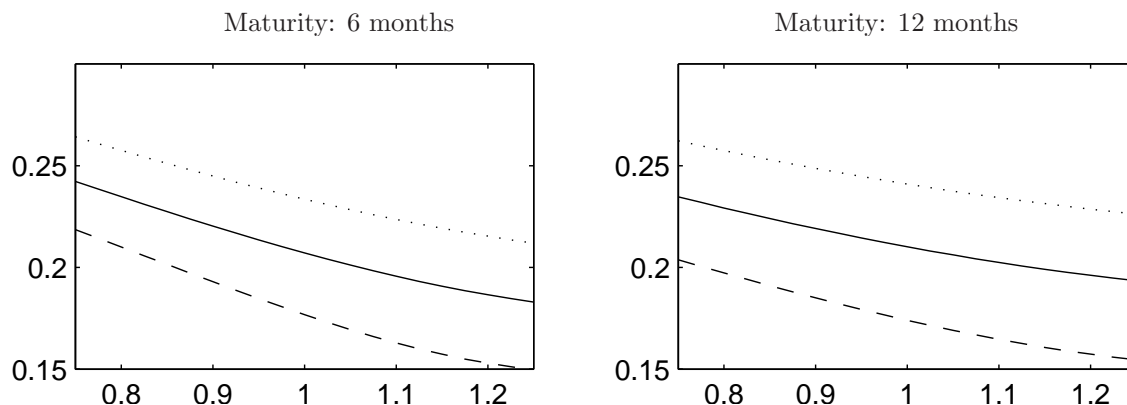


Figure 1. Smile Dynamics in the SLRM-Model

The figure shows the dynamics of the IV smile induced by a shift in the local long-run mean of variance \bar{V}_t in the SLRM-Model. In the left graph, the maturity of the options is 6 months, in the right graph 12 months. The solid lines represent the case where the local long-run mean of variance \bar{V} is equal to the local variance, the dashed lines the case where it is 50% lower than the local variance and the dotted lines where it is 50% higher. The parametrization is from Table 1. The interest rate is 5%, the current stock price is 100.

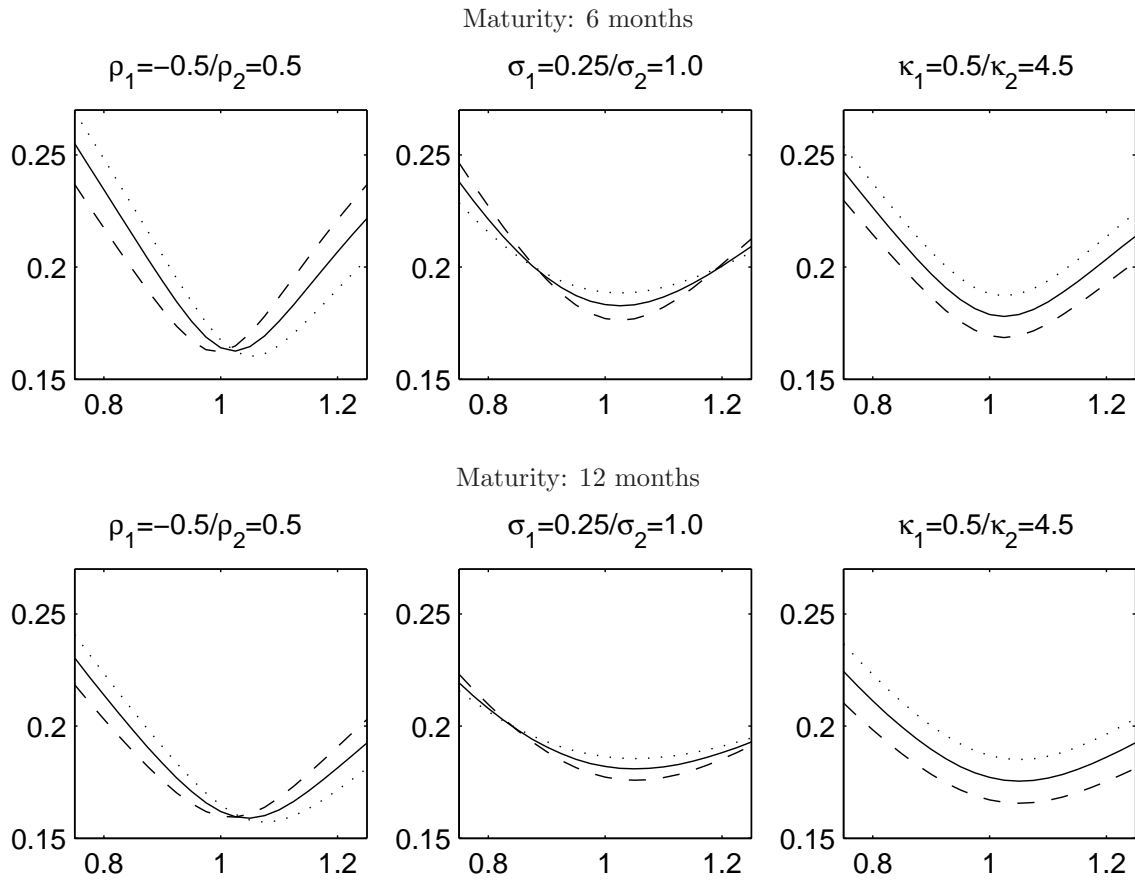


Figure 2. Smile Dynamics in the Model of Bates (2000)

The figure shows the possible dynamics of the IV smile induced by different variance compositions in the Bates (2000) model. In the upper graphs, the maturity of the options is 6 months, in the lower graphs 12 months. The solid lines represent the case where each of the local variance components accounts for 50%, the dashed lines the case where the variance component V_1 accounts for 25% of total variance and the dotted lines where V_1 accounts for 75% of total variance. In the benchmark case, $V_t = V_{1t} + V_{2t} = 0.04$, $\rho_1 = \rho_2 = 0.0$, $\kappa_1 = \kappa_2 = 1.5$, $\theta_1 = \theta_2 = 0.02$, $\sigma_1 = \sigma_2 = 0.75$, $r = 0.05$ and $S_0 = 100$ and one of the parameters ρ , σ and κ is varied for the two variances.

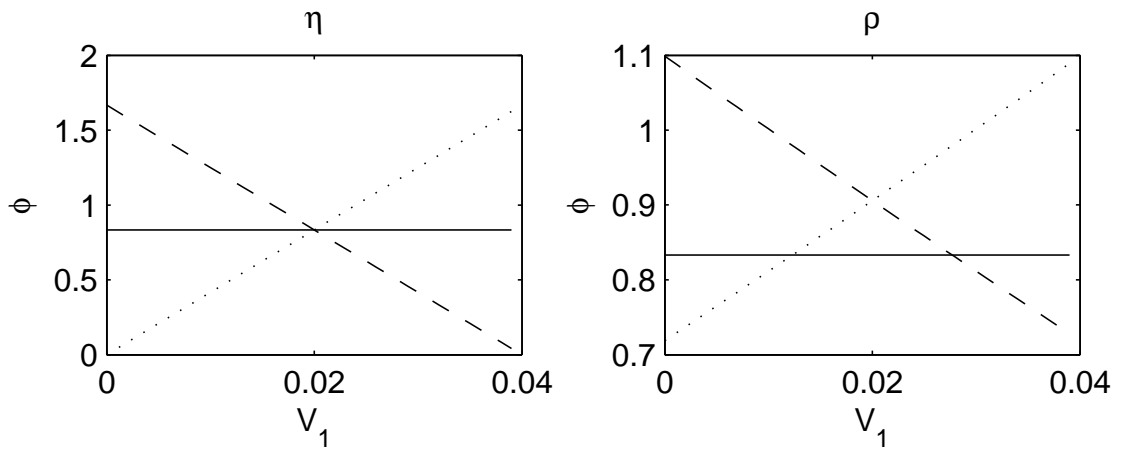


Figure 3. Optimal Stock Position in the Model of Bates (2000)

The figure shows the optimal stock position ϕ in the Bates (2000) model as a function of local variance V_{1t} . The solid lines represent the benchmark case where the parameters of the dynamics of the two variance processes are perfectly symmetric. Here, $\rho_1 = \rho_2 = 0.0$, $\kappa_1 = \kappa_2 = 1.5$, $\theta_1 = \theta_2 = 0.02$, $\sigma_1 = \sigma_2 = 0.75$, $\eta_1 = \eta_2 = 2.5$, $r = 0.05$ and $S_0 = 100$. In the left graph, the dashed line represents the case where the parameter $\eta_1 = 5.0$ ($\eta_2 = 0.0$) and the dotted line the case where $\eta_1 = 0.0$ ($\eta_2 = 5.0$). In the right graph, the dashed line represents the case where the parameter $\rho_1 = -0.5$ ($\rho_2 = 0.5$) and the dotted line the case where $\rho_1 = 0.5$ ($\rho_2 = -0.5$). The investment horizon is 5 years, the investor has a risk aversion of $\gamma = 3$.

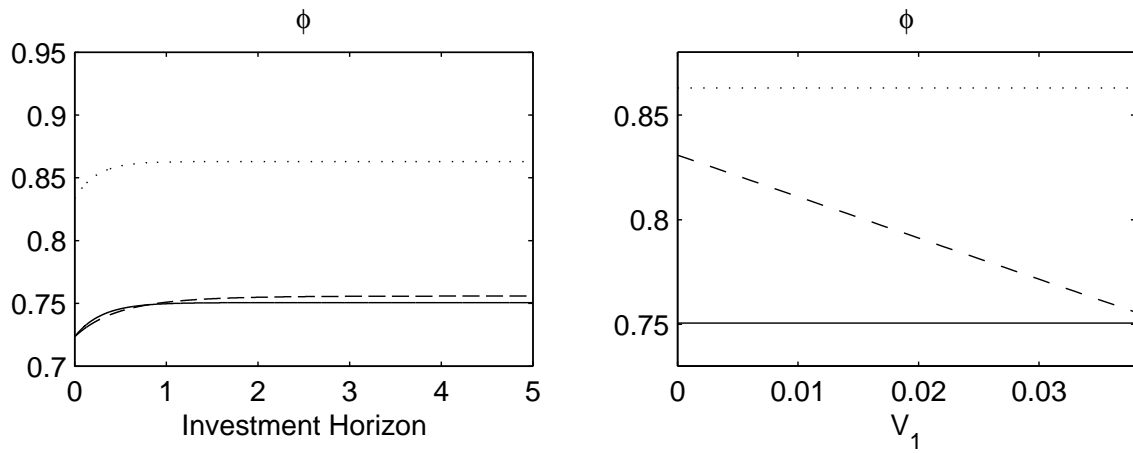


Figure 4. Comparison of Stock Positions

The figure shows the optimal stock position ϕ in the different models as a function of the investment horizon (left graph) and as a function of local variance V_1 (right graph). The solid lines are the optimal positions in the model of Heston (1993), the dashed lines in the model of Bates (2000) and the dotted lines in the SLRM model. The parameters are taken from Table 1. In the left graph, local variance levels are set to their long-run mean. In the right graph, the investment horizon is 5 years, the investor has a risk aversion of $\gamma = 3$.

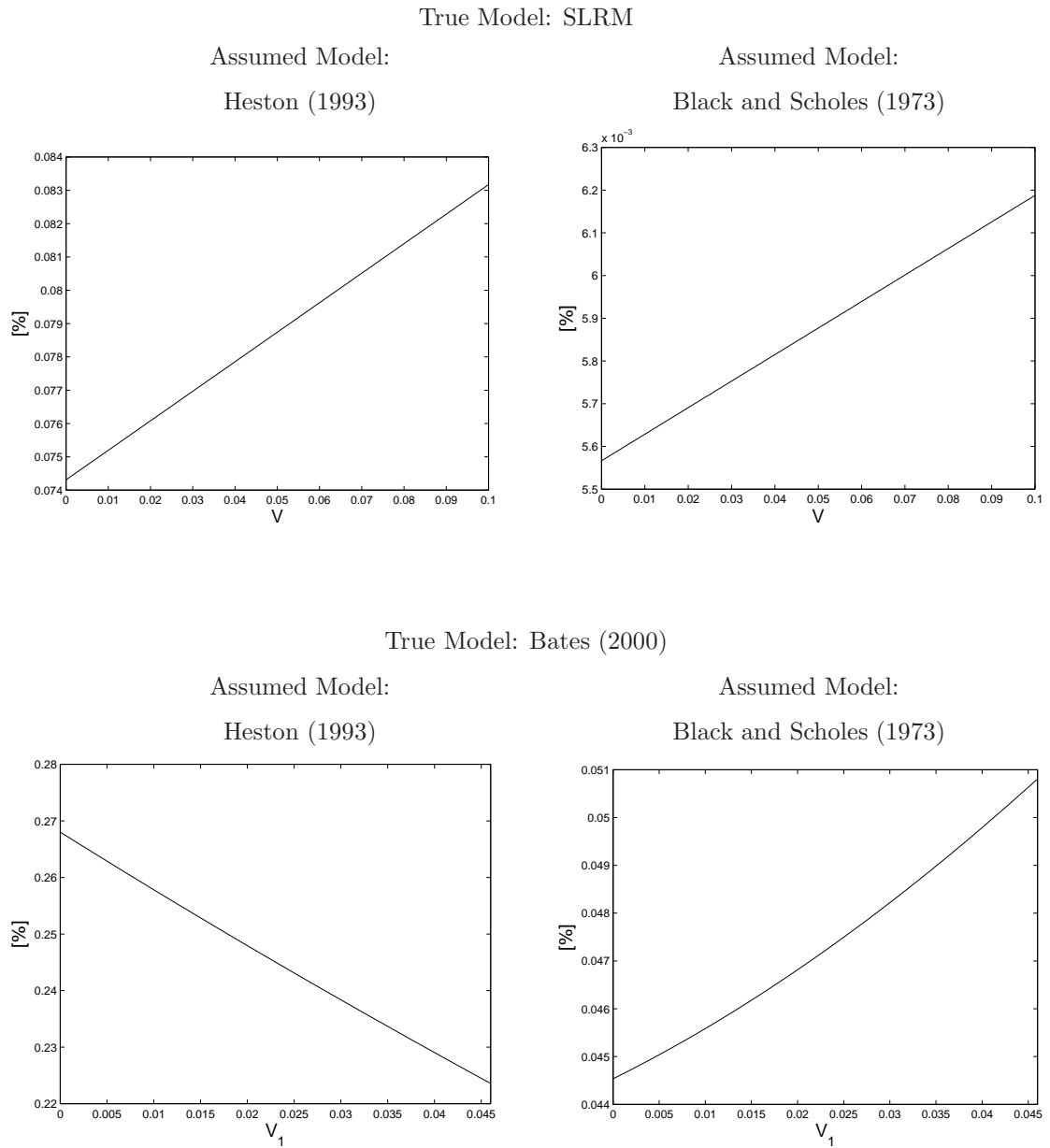


Figure 5. Utility Loss from Model Mis-Specification

The figure shows the utility loss (measured by the quantity \mathcal{R}^y defined in Equation (4)) as a function of the state variables. In the upper graphs, the true model is the SLRM model, in the lower graphs, the true model is the Bates model. In the left graph, the investor assumes the Heston model to be true, in the right, he assumes the model of Black and Scholes (1973). In the upper graphs, \bar{V} is set to its long-run mean 0.04. In the lower graphs, V_1 is varied, but the sum of $V_1 + V_2$, is restricted to equal 0.04. The parametrization is taken from Table 1. The interest rate is 5%, the current stock price is 100. The investor's planning horizon is 5 years, his risk aversion is $\gamma = 3$.

Hedging in the Presence of Microstructural Noise

David Horn, Eva Schneider, Grigory Vilkov

Summary. In order to use an option pricing model for dynamic hedging an investor will have to calibrate it to a cross-section of option prices. Microstructural noise in option prices results in a set of indistinguishable parametrizations which may give rise to different hedging errors. In our simulation study for the Heston (1993) model, we identify the parameters most important for hedging and show which set of strikes and time to maturity is relevant for the identification of certain parameters. In our empirical study we show that different but indistinguishable parametrizations w.r.t. prices may induce large differences in hedging performance.

1 Introduction

An investor setting up a dynamic hedging strategy will first have to identify a stochastic process for the underlying. Having chosen the appropriate model, the investor will have to calibrate this model to a cross-section of empirical option prices. With the calibrated model the investor can then proceed to calculate the weights of the replicating portfolio. The identification and calibration of the model are of great importance, since a wrong model will result in wrong hedging weights and larger and more volatile hedging errors. When using empirical data to identify and calibrate the model at least two problems arise. First, there is only limited data available. Usually only for very liquid index options we have a broad range of option prices available. For other types of underlyings, the limited number of available option prices at a particular point in time can make the identification and calibration very difficult. Second, the prices we observe on option markets are noisy. When we speak of noise in option prices we mean that we believe in one true (frictionless) option price but this price cannot be observed due to the bid- and ask-spread. Several reasons for noisy option prices have been suggested: bid-ask spread in the underlying, different

interest rates for borrowing and lending, non-synchronous observations or rounding to the nearest tick size (see Hentschel (2003)).

The existence of a bid-ask spread complicates the identification and calibration of a model in the following ways. Identification becomes more difficult since two structurally different models that yield option prices, which differ by less than the bid-ask spread, cannot be distinguished anymore (see Dennis and Mayhew (2004)). The same problem applies to the calibration. Even if we knew the true model, two different parametrizations could not be distinguished from another if they produce option prices differing by less than the bid-ask spread. Not only can two parametrizations result in different option prices, but they can also result in different hedging weights in a hedge portfolio. They will thus also yield different hedge errors. In the present paper we want to focus on this second issue. Hence, this paper tries to answer the following research questions: What are the most sensitive parameters for calibration and hedging? Which parameters are the most important to identify a model correctly? Which subset of prices (with respect to strike price and time to maturity) is especially relevant for the identification of certain parameters? Can we rely on cross-sectional information or do we have to use time series information? And finally: Can we verify the theoretical results for the previous questions empirically?

In order to answer these questions we will perform both a simulation analysis in the stochastic volatility framework of Heston (1993) and an empirical study. In the simulation we will generate European option prices in the Heston (1993) model under a fixed parametrization which represents the true model. Then we will identify the parameter range leading to an indistinguishable cross-sectional fit for an investor who calibrates the Heston model to the generated dataset. This means that we ignore model risk and solely focus on parameter risk. In the empirical part of this paper we will calibrate the model of Heston (1993) to option prices of several single stocks and the S&P 100 and identify the indistinguishable parametrizations for the observed bid-ask spread. We find that a parametrization with a good cross-sectional fit does not necessarily have to have good hedging properties and that there are economically important differences in the hedging performance of these indistinguishable parametrizations.

We contribute to the existing literature in the following ways: First, we identify the parameters which prices and greeks are most sensitive to. Second, we show which information (number of strikes, number of maturities) is important for the correct identification of

certain parameters. Third, we show which parameters are the most important to identify correctly for the purpose of hedging. Fourth, we measure parameter risk using empirical option prices.

2 Literature Review

Besides the papers looking at the sensitivities of option prices to model parameters, there are only few which consider the impact of parameter risk. These papers mainly focus on volatility mis-estimation. Hentschel (2004) provides a thorough analysis of the error in implied volatility estimation induced by measurement errors in the input variables and by truncation, i.e. when low option prices are missing in the calibration. He works in the model of Black and Scholes (1973) and shows that the resulting error is the larger the more the options are OTM or ITM and that due to the truncation error, the confidence interval may not even contain the correct volatility. Figlewski (2004) estimates the volatility by using a simple average of squared returns or via an exponentially-weighted moving average. He then performs a simulation analysis of estimation errors for the computation of the value at risk. For the data generating process, he assumes the dynamics given in Black and Scholes (1973), Heston (1993), Bakshi, Cao and Chen (1997) and Eraker, Johannes and Polson (2003). The standard estimation technique of the value at risk is shown to lead to significant errors in the estimation of tail probabilities.

In contrast to these papers, we estimate parameters in the true model and do not take volatility as a simple estimate from time series but calibrate the model to option prices. As our base model, we use the empirically well supported stochastic volatility model of Heston (1993).

Another strand of literature related to our work is concerned with model mis-specification. Here, the mis-specification does not relate to the model parameters but to the whole model class. Dennis and Mayhew (2004) study the impact of noise in option prices on parameter or model estimation and try to answer the question if, given the noise in option prices, one can distinguish between different models. Schoutens, Simons and Tistaert (2003) calibrate several models to a cross section of European options and compare the resulting prices of exotic options. An and Suo (2003) test several models by looking at the hedging errors of strategies for exotic derivatives.

The closest paper to ours is the paper by He, Kennedy, Coleman, Forsyth, Li and Vetzal (2006). The authors assume a jump-diffusion model with a local volatility function as the true data-generating process. When calibrating the model, jump parameters are harder to estimate than the local volatility function since a large surface of parameters yields sufficiently small estimation errors. However, the hedging performance is not largely affected by the estimation problems. Both dynamic variance-minimizing hedges and semi-static hedges perform well for the set of instrument options. In our paper, we focus on mis-estimation of stochastic volatility parameters (not jump parameters) and in addition to a simulation study, we perform an empirical analysis.

3 Motivation

3.1 Parameter Risk in the Heston Model

As stated in the introduction, we want to focus on parameter risk. We therefore assume that the structural type of the model is known. Also, to keep the analysis as simple as possible, we will examine a stochastic volatility model and exclude additional sources of risk, such as multiple volatility components or jumps in the stock price or in volatility. We choose stochastic volatility since this seems to be the most important improvement over the model of Black and Scholes (1973). In particular we will use the model of Heston (1993). This model assumes the following risk-neutral dynamics for the underlying stock S and its local variance V :

$$\begin{aligned} dS_t &= rS_t dt + \sqrt{V_t} S_t dW_t^S \\ dV_t &= \kappa(\theta - V_t) dt + \sigma_v \sqrt{V_t} dW_t^V \end{aligned}$$

where r is the riskless rate of return, κ is the speed of mean reversion, θ is the long run mean of local variance V , σ_v is the 'volatility of variance' parameter and the correlation between the two Wiener processes is described by the parameter $\rho dt = E[dW^S dW^V]$. The Heston model is essentially an incomplete market model. A closed form solution for option prices can be derived via Fourier inversion (see Heston (1993)). For hedging purposes all claims can be replicated with a stock, the money market account and one instrument option.

At date t , the interest rate r and the stock price S can be observed. The speed of mean-reversion κ , the long-run mean of variance θ , and the volatility of variance σ_v all

have to be estimated from a cross section of option prices. The local level of variance V plays a special role since it is theoretically assumed to be a state variable but for practical purposes is usually estimated from empirical option prices like a model parameter.

The starting point for our analysis is the fact that several parameter combinations can provide a similar fit to a given cross section of option prices. Microstructural noise in option prices can then make two parametrizations virtually indistinguishable. If the focus of the investor is the pricing of plain vanilla options, each of these indistinguishable parametrizations might be acceptable. However, when the pricing of exotic options or hedging is considered, different parametrizations might lead to significantly different outcomes. That is, even if the investor knows the true model he will not only incur a hedging error due to discrete trading, but also an additional hedging error due to the fact that he picks a parametrization which is not the true one. This of course raises the question of what the true parametrization is in the presence of a bid-ask spread in option prices. For the rest of the paper we will assume that the true parametrization is the one which would persist if there were no bid-ask-spread, i.e. the parametrization in a world without noise in option prices.

To get a feel for the importance of parameter risk for hedging consider a dynamic delta-vega hedge. For the case of continuous trading and noiseless option prices it is possible to devise a strategy with zero hedging error. The investor trying to hedge a short position in a call then has to solve the following problem: Find the quantities w_s , w_m , w_i of the stock S , the money market account M , and the instrument option C^I subject to the constraints

$$\begin{aligned} C^T &= w_s \cdot S + w_m \cdot 1 + w_i C^I \\ C_S^T &= w_s \cdot 1 + w_m \cdot 0 + w_i C_S^I \\ C_V^T &= w_s \cdot 0 + w_m \cdot 0 + w_i C_V^I, \end{aligned}$$

where subscripts denote partial derivatives. The first condition makes the replicating portfolio self-financing, the second one delta-neutral and the third one vega-neutral. Note that the weights of this hedging strategy will depend on the derivatives of the instrument and the target option with respect to S and V , which are model and parameter dependent. The correct estimation of the sensitivities will thus be crucial for the performance of the hedging strategy.

3.2 Parameter Sensitivity of Option Prices and Greeks

The purpose of this section is to give a first intuition about the relative importance of different parameters for pricing and hedging. In particular we will ask two questions: First, which parameters have the largest impact on option prices? Since the calibration of option pricing models is usually done by fitting observed prices, a parameter with little influence on the option price can easily be misestimated. Second, which parameters have the largest impact on the greeks of the option price? The performance of a dynamic hedge depends heavily on the use of the correct sensitivities.

To answer these two questions we plot the price, delta and vega in the Heston model as a function of moneyness for different parameter levels. Differences in the reaction of prices and greeks to the change of a parameter can then be used to draw some first conclusions regarding the effect of misestimation on hedging performance. Since we expect the effects to be strongest for long-term options we analyze an option with a maturity of 0.9 years.

We start with the analysis of the effect of the parameter changes on prices and on the volatility smile. The sensitivities of the option price to its parameters are depicted in Figure 1. We see that a variation of κ and σ_v has little effect, while the impact of ρ is a little stronger. Note that there is an inverse effect for ITM and OTM options. The parameters with the strongest influence on the option price are θ and V_0 . Except for the case of ρ the sensitivities are highest for ATM options. The plots of the sensitivities of the smile give essentially the same findings. However, it becomes clearer that κ and σ_v seem to have influence only on ATM options. Again the plots show that θ and V_0 have a strong effect for all moneyness levels and that the influence of ρ is weakest for ATM options and becomes stronger the deeper the options are ITM or OTM.

This is in line with intuition, since local variance and long-term mean of variance are the most important drivers of option prices, while the other parameters exhibit only a second-order impact. Due to its asymmetric payoff structure, an OTM option increases in value for more positive stock-variance correlation where simultaneous increases or decreases of the stock price and its local variance are more likely to occur. On the other hand, its price decreases the more negative the correlation. Overall we can say that mis-estimation is most likely for the parameters κ and σ_v . Mis-estimation is less likely if ATM options are used. An exception here is the estimation of ρ for which we would advise to

use OTM or ITM options for calibration. Since ITM options often lack liquidity, OTM options seem to be most appropriate for the calibration.

Figure 3 shows the sensitivity of the Heston delta with respect to the various parameters. Again we find only little influence of κ and σ_v . Except for ρ the sensitivities are highest for OTM and ITM options, and the effect is reversed when moving from ITM to OTM options. For ρ , the influence is strongest for ATM options and becomes weaker the deeper the option is ITM or OTM.

The sensitivity of vega is depicted in Figure 4. Here we see that ρ and σ_v have little, θ and V_0 moderate influence on the Heston vega. In contrast to delta we see that κ has a very strong effect on vega. In total we find that delta reacts most strongly to changes in θ , ρ and V_0 , while vega reacts most strongly to changes in κ , θ and V_0 .

To sum up the results of this preliminary analysis, we find that when parameters are estimated through a calibration to observed prices, a mis-estimation of κ is likely. This can result in strong differences in vega. In contrast, although a mis-estimation of σ_v is likely, this will not affect delta or vega severely. For ρ , a mis-estimation is likely when calibrating the model only to ATM options. This simple analysis already shows that if several parametrizations provide a satisfactory fit in the presence of microstructural noise, these different parametrizations can lead to very different deltas and vegas, which will in turn affect the composition of our hedging portfolio. The question arises to what extent this carries over to hedging performance.

In the following sections we will analyze the effect of microstructural noise on the hedging performance in more detail.

4 Design of the Study

In this section the general design of our simulation analysis is explained. An investor setting up a dynamic delta-vega hedge for a short position in a target call will first estimate the parameters of his model from a cross section of option prices. The objective of his calibration routine will be to find a parametrization Ψ which fits observed option prices best. In the Heston model the investor will have to estimate the parameters vector $\Psi = (\kappa, \theta, \sigma_v, \rho, V_t)$. Several approaches to the calibration of a model are possible. For example, one could employ the minimization of the relative or absolute squared pricing error or the

minimization of the squared implied volatility difference. In this paper we will assume that the investor minimizes the sum of squared absolute pricing errors as in Bakshi, Cao and Chen (1997). This means his minimization problem is of the form

$$\min_{\Psi} \sum_{i=1}^N \left(C_i^{Market} - C_i^{Model}(\Psi) \right)^2,$$

where $i = 1, \dots, N$ is the index for the options used in the calibration. Furthermore, we will assume that option prices are noisy. One implication of this assumption is that a perfect identification of the parametrization is no longer possible. In fact all parametrizations having a pricing error smaller than the bid-ask spread may be true. To find parametrizations which cannot be distinguished in the presence of noisy option prices we implement the following procedure.

For our simulation study, we first assume one benchmark parametrization (Θ) to be the true parametrization, i.e. the parametrization which would persist in a world without noisy option prices. Based on this parametrization, we then compute a set of observable 'market' option prices.¹ Then, we compute the surface of pricing errors for all conceivable parametrizations. We restrict our analysis to the misestimation of two parameters at a time while all other parameters are correctly identified. This procedure has the advantage that it is a conservative approach in that all but two parameters are correctly estimated. We denote by $\tilde{\Theta}_{(x,y)}$ the parametrization where all but two parameters (x, y) are equal to the parameters in Θ . So for each possible parameter combination (x, y) we compute the sum of squared pricing errors between the true options prices $C_i(\Theta)$ and prices $C_i(\tilde{\Theta}_{(x,y)})$ ($i = 1, \dots, N$) calculated in the Heston model using the parametrization $\tilde{\Theta}_{(x,y)}$. By plotting the results we obtain a three-dimensional surface, where one parameter is varied along the x-axis, the other one along the y-axis, and the objective function is plotted in z-direction. An often used measure for the total calibration error is the root mean squared error (RMSE). We denote the RMSE by $\Xi_{(x,y)}$:

¹ The benchmark parametrization is taken from Bakshi, Cao and Chen (1997), Table III, 'All Options', SV-Model. The interest rate is set to 5%, the stock price is 100. The initial variance equals its long-run mean. For the benchmark case 'all options', we consider a cross section of $N = 28$ option prices with maturities of 1 month, 3 months, 6 months and 12 months and moneyness levels in steps of 0.05 from 0.85 to 1.15. For 'ATM options' we use $N = 28$ options with some maturity, but moneyness levels in steps of 0.01 from 0.97 to 1.03, for 'short-term options' $N = 26$ options with maturities of 1 month and 2 months and moneyness levels in steps of 0.02 from 0.88 to 1.12.

$$\Xi_{(x,y)} = \sqrt{\frac{1}{N} \sum_{i=1}^N \left(C_i(\Theta) - C_i(\tilde{\Theta}_{(x,y)}) \right)^2}.$$

An investor calibrating a model will not be able to distinguish between certain parametrizations if a bid-ask spread (BA) is present. In our study the set of indistinguishable parametrizations $M_{(x,y)}$ is defined as follows.

$$M_{(x,y)} = \left\{ \tilde{\Theta}_{(x,y)} \mid \Xi_{(x,y)} \leq \frac{BA}{2} \right\}.$$

We thus assume that all parametrizations which result in an RMSE smaller than the upper bound $BA/2$ are not distinguishable from each other given the observed option prices. In the graphs shown in the appendix all parametrizations in the set $M_{(x,y)}$ lie inside the marked bounds. The identification of these sets of indistinguishable parametrizations now allows us to assess the impact on hedging performance caused by the misestimation of parameters.

After calibrating the model to empirical data, the investor sets up a hedge portfolio. Our aim is to identify the difference in performance between the optimal hedge (based on the true parametrization Θ) and the hedges based on all parametrizations within the set $M_{(x,y)}$ for each parameter combination (x, y) . The hedging error based on parametrization $\tilde{\Theta}_{(x,y)}$ is defined as the deviation of the hedge portfolio from the value of the target option after the next time step of length Δt :

$$\epsilon(\tilde{\Theta}_{(x,y)}) = C_{t+\Delta t}^T - w_s(\tilde{\Theta}_{(x,y)})S_{t+\Delta t} - w_m(\tilde{\Theta}_{(x,y)})e^{r\Delta t} - w_i(\tilde{\Theta}_{(x,y)})C_{t+\Delta t}^I,$$

where $C_{t+\Delta t}^T$ and $C_{t+\Delta t}^I$ are the realized market prices of the target and the instruments option, respectively, at time $t + \Delta t$. For our simulation under the P-measure, we assume that all risk premia are zero and thus the P-measure equals the Q-measure. This makes the average hedging error of all strategies equal to zero and allows to focus solely on the distribution.

The hedging performance under parametrization $\tilde{\Theta}_{(x,y)}$ is measured by the standard deviation of hedging errors over all observations $j = 1, \dots, M$.

$$\sigma(\tilde{\Theta}_{(x,y)}) = \sqrt{\frac{1}{M-1} \sum_{j=1}^M \epsilon^2(\tilde{\Theta}_{(x,y)})}.$$

The larger this value the worse the hedging performance. The hedging errors for the true parametrization are taken as a benchmark. Due to discrete trading the hedging errors for

this strategy will not be equal to zero and the standard deviation of the hedging error follows as $\sigma(\Theta)$. We correct the standard deviation of hedging errors under parameter risk by this unavoidable standard deviation due to discretization and measure the performance loss due to parameter risk as:

$$\Upsilon_{(x,y)} = \frac{\sigma(\tilde{\Theta}_{(x,y)}) - \sigma(\Theta)}{C_0^T}.$$

We perform a one-day delta-vega hedge. We hedge an OTM target call with a moneyness (strike/ S_t) of 1.1 and a maturity of 0.2 years. The hedge portfolio consists of the stock, the money-market account and an instrument option. The instrument option is an ATM call with a maturity of 0.2 years. We perform 10,000 simulation runs with 10 steps per day. After performing the simulations we again draw a three-dimensional surface, where one parameter is varied along the x-axis, the other one along the y-axis and the percentage hedging error is plotted in z-direction. We thus have two plots for each parameter combination: one for the objective function and one for the hedging errors. In order to highlight the effect of microstructural noise on the hedging performance in each plot we mark the subarea of objective function values and hedging errors for the set of indistinguishable parametrizations $M_{(x,y)}$. The hedging errors within the marked subarea result from parametrizations indistinguishable from a noisy cross-section of option prices. All hedging errors in this set are hedging errors which have to be added to the discretization error and stem from the parameter risk induced by the bid-ask-spread in the option price.

5 Simulation Results

5.1 Pricing and Hedging Performance

In this section we will present and interpret the results of our simulation study. Figures 5 to 8 in the appendix show for each combination of two parameters (x, y) of the Heston model the area of indistinguishable parametrizations $M_{(x,y)}$ when the model is calibrated to noisy option prices (marked area in left surface plots). We also show graphs illustrating how different the resulting hedging performance for each set of parametrizations can be. That is we show the area of possible performance losses for indistinguishable parametrizations (marked area in right surface plots). We perform this analysis for a calibration to all options ('all'), for a calibration only to ATM options ('atm') and for a calibration only

to short maturity options ('short').² The latter two analyses are done to show how a 'thin' market aggravates the results found for the case of a deeper market where a wide spectrum of moneyness levels and maturities is available. The underlying problem here is that on the one hand parameter identification is easier when the whole range of strikes and maturities is used and that a mis-estimation of parameters is more likely when only short maturity or only ATM options are used. On the other hand, the use of highly liquid short maturity or ATM options may be preferable due to a lower bid-ask spread and the resulting better identification of the true model with more precise option prices.

The numerical results are based on a bid-ask spread of 10% which lies well within the empirical spread observation. For options on the S&P100 individual stocks the average bid-ask spreads between 1996 and 2003 sorted by delta buckets are depicted in Table 1. They are lowest with about 3% for deep ITM options and largest with up to 42% for deep OTM options. For ATM options the average bid-ask spread is around 7%.

We start our interpretation of the graphs with the parameter combination (σ_V, κ) in Figure 5. For the case 'all' (upper row) we find that for a given bid-ask spread the identification of κ is more difficult than the identification of σ_V . The marked area in the graph shows that κ can vary roughly between 0 and 5, while σ_V can only deviate by a relatively small amount from its true value. For the 'atm' (lower row) case we immediately see that identification of the true parameter combination becomes extremely difficult. Almost all parameter combinations of σ_V and κ are possible.

For the parameter combination (σ_V, θ) in Figure 6 we see that both parameters are quite easy to identify in the 'all' (upper row) case. The area of indistinguishable parametrizations also increases in the 'atm' (lower row) case although not as drastically as in the previous case. An interesting result is that in the 'atm' case the form and curvature of the surface of the objective function is very different from the surface of the hedging performance. In particular the smallest values of the objective function are on a straight line along the true value of θ while the smallest values of the performance loss function are on a straight line along the true value of σ_V . Also note that the performance loss function is strongly increasing in σ_V from the point of the minimum of $\mathcal{Y}_{(\sigma_V, \theta)}$ onwards. This means that in the calibration procedure a mis-estimation of σ_V is likely to be compensated by a correct identification of θ , but this could result in large performance losses.

² Since for all parameter combinations the results for the cases 'all' and 'short' are almost the same, we henceforth only report the results for the case 'all'.

The parameter combination (V_0, σ_V) is probably the one easiest to identify (see Figure 7). The area of indistinguishable parameters is extremely small. Again the identification becomes worse when only ATM options (lower row) are used. It seems that V_0 is more important for prices and hence slightly easier to identify. In the plots for the combination (θ, κ) in Figure 8 we see that for small values of κ the identification of θ becomes very difficult. The higher κ , the easier the identification of θ .

Since similar results hold for the other parameter combinations, the graphs are not shown. Note, however, that in accordance with the results in Section 3 it is always very important to use OTM options to identify ρ .

In summary, we find that in general pricing performance is a good proxy for hedging performance. A notable exception here is the parameter combination (σ_V, θ) where the surface of the objective function is very different from the surface of the hedging performance in the 'atm' case. Furthermore, V_0 is the most important parameter for pricing and hedging as expected. A correct identification should be easy, but a mis-estimation will have serious consequences for the hedging performance. We find that σ_V and ρ are of particular importance: For σ_V an increase in hedging error is steeper than the increase in the objective function. This means that a mis-estimation of this parameter has a large impact on hedging errors. For ρ we find that a calibration is very difficult if only ATM options are used. This could result in very high performance losses. Consequently in order to identify ρ , it is of first order importance to use OTM options. We also find a cross effect between θ and κ . For very low values of κ the identification of θ is very difficult and the closer θ is to its true value, the more difficult identification of κ becomes. Finally, most effects are more pronounced when calibration is done using ATM options only. That is, the performance loss can become a lot higher when using only ATM options. Although ATM options may have lower bid-ask spreads and prices are therefore more precise, we find that the less liquid OTM options contain important information (concerning the tails of the distribution) necessary to identify ρ .

5.2 Hedging and Microstructural Noise

After having identified the qualitative effects in our simulation study, we next want to show the quantitative effects. In particular we want to answer the following questions: How large is the maximum possible size of the performance loss for different sizes of the bid-ask spread? Although ATM options have a lower bid-ask spread and the price information

is therefore more precise, does a calibration to these options, only, result in significantly worse hedging performance? In order to answer these questions we plot the maximum performance loss $\max \mathcal{Y}_{(x,y)}$ as a function of the mean bid-ask spread over options used for calibration for three different cases: all options, atm options and short-maturity options. These graphs give a feel for the quantitative impact of parameter risk on hedging in a worst case scenario. This means we show how large the performance loss can possibly get when the investor cannot distinguish between different parametrizations due to a given bid-ask spread.

The results are depicted in Figure 9. First of all note that since we restrict the parameter range to reasonable values³, \mathcal{Y} seems to converge to an upper bound in some graphs. However without the restriction on the parameter set, it could increase even further. For example in the case (κ, ρ) the upper bound on \mathcal{Y} in the case 'atm' is obtained for $\kappa = 10$ and $\rho = 0$. Without the restricted parameter range, both parameters could possibly be estimated larger and then \mathcal{Y} would be larger. Also note that the stepwise behavior of the functions is a result of the parameter grid we chose for the calibration.

When comparing the graphs for the different calibrations, we make the following observations: First, for an average bid-ask spread of 5% the investor may suffer from a performance loss of more than 2% (case σ_V, ρ) when the investor calibrates to 'all' options and up to 11% (case σ_V, ρ) when the investor calibrates to 'atm' options. For an average bid-ask spread of 30%, the maximum performance loss lies in a range between 7% (case θ, ρ) and 16% (case σ_V, V_0) when the investor calibrates to 'all' options. In the case of 'atm' options the maximum performance loss becomes even higher and is within a range of 11% (case κ, ρ) and 30% (cases ρ, V_0 and σ_V, ρ). So we see that the lowest performance loss is obtained when calibration is done using 'all' options, while the largest performance loss results for 'atm' options and the performance loss for 'short'-maturity options is in between. The hedging performance for 'short'-maturity options is, however, only marginally worse than the hedging performance for the calibration to 'all options'. This means that for dynamic hedging it is of huge importance to use a wide range of moneyness levels while the range of maturities seems to be less relevant. The use of OTM options for calibration allows the investor to accept a higher bid-ask spread and still achieve a similar hedging performance. As can be seen in the graphs, in most cases

³ The parameters were restricted to be in the following intervals: $\kappa \in [0, 10]$, $\sigma_V \in [0, 1]$, $\theta \in [0, 0.1]$, $\rho \in [-1, 0]$ and $V_0 \in [0, 0.1]$.

a calibration to ATM options with a bid-ask spread of 5% results in a similar hedging performance as a calibration to 'all' options or 'short'-maturity options with a bid-ask spread of more than 20%.

Regarding the relative importance of the particular parameters of the Heston model we find the following numeric results: performance losses resulting from a calibration to 'all' options are largest when σ_V is one of the parameters subject to mis-estimation. i.e. identification is difficult and mis-estimation may lead to large performance losses, because σ_V has only a small impact on prices, but has a large impact on hedging errors. A similar result holds for the parameter ρ for which already our introductory analysis has indicated that OTM options are extremely important for the calibration. As can be seen in the graphs, when ρ is one of the parameters subject to mis-estimation, the maximum performance loss increases sharply when only 'atm' options are used for calibration.

6 Empirical Illustration

6.1 Design of the Study

To support the economic relevance of our simulation results, we assess the impact of parameter risk on hedging errors empirically.

Theoretically, indistinguishable parametrizations are those for which the calibrated option prices lie within the bid-ask spread. Finding empirically the worst case scenario, i.e. the parametrization which yields the worst hedging performance among all indistinguishable parametrizations is computationally infeasible. To keep our analysis as simple as possible we therefore take a conservative approach and perform three different calibrations: to the bid-, ask- and mid-prices. Additionally, we again calibrate our prices to the Heston model which seems to provide a sufficient complexity to reflect our empirical data, while being analytically tractable at the same time. Of course, there may be other risk factors like jumps in the true stock dynamics, especially for the index options. However, this is not the focus of our analysis, we do not want to state that the Heston model is the true model to describe the data. Rather, we intend to show that assuming one model there may be several equally well parametrizations which still yield different hedging performances.

At each trading day in our data set, we perform the following steps. First, we calibrate the Heston model to the empirically observed (bid, ask and mid) option prices. These are

all call options traded on that day on the specific underlying available in the Option Metrics database. Second, we build the hedge portfolio. We set up the Heston delta-vega and, for comparison, also the Heston delta hedge for each of the three parametrizations. This is done for all call options traded on that and the following day. Third, to assess the differences in hedging performance, we compute the hedging errors after one day. For both the construction and the evaluation of the hedge portfolio, we use mid-prices and thus do not focus on either short- or long-positions.

The hedging performance is then judged according to the standard deviation of hedging errors, differences between the parametrizations are statistically tested with an F -Test and the non-parametric test of Ansari-Bradley (AB).

6.2 Data Description

We use Option Metrics to select all call options on the S&P100 index and two individual stocks (Cisco, and AT&T) in the time frame from 2000 to 2004.

First, we take all calls with times to maturity from 14 to 180 days. We eliminate option price observations for dates with zero open interest, with zero bid prices or with missing implied volatility or delta. We also take out deep ITM and far OTM options (with moneyness smaller than 0.8 and larger than 1.2), as the lack of liquidity in those options may distort the results.

After applying these filters we are left with the number of observations as shown in Table 2. From these numbers we can see that we have on average 15 option prices observed on each date for individual securities and 64 options for S&P100.

In the following we treat each underlying separately. On each date we select the option to be used as the instrument for hedging. To do so we first select the options with remaining time to maturity closest to the average time to maturity for all options observed on a given date. From this group of options we then select the one closest to the ATM level.

6.3 Results

Table 3 summarizes the results. In addition to the results from the Heston model, we include the hedging errors obtained from a Black-Scholes delta hedge based on implied volatility.

In the table the standard deviation of the hedging errors (relative to the initial value of the option) is depicted as a measure of hedging performance. The point of interest for our analysis is when the hedging performance is significantly different if the hedge is based on different parametrizations. To confirm the visible differences, we perform a statistical test for the difference in variance of hedging errors based on the ask- and the bid-calibration. Under the assumption of normally distributed hedging errors, a two-sided *F*-Test is performed for the null of equal variances. The non-parametric AB test tests the null that hedging errors of bid- and ask-calibration come from the same distribution against the alternative that they come from distributions with same median but different variances. To increase the power of the AB-test, we first normalize our data by subtracting the medians. The results are sorted by the moneyness of the target option.

The general results are as expected. The standard deviations of the hedging errors in case of the delta-vega hedge are much smaller than in case of the simple delta hedge. They are largest for OTM options and smallest for ITM options. Surprisingly, but in line with practitioners' experience is the very good performance of the Black-Scholes delta hedge. Often it outperforms the delta-vega hedge, although this hedge uses an additional instrument. For both statistical tests, the variances of Black-Scholes delta hedging error are significantly different from Heston delta hedging errors. This does not necessarily mean that the Heston hedge is generally worse, but reveals a mistake often arising in the measurement of hedging performance. There is a mismatch between the objective of our hedge and the performance measure. Whereas in our objective we want to set delta and vega of our portfolio equal to zero, the performance measure prefers hedges with low standard deviations. The Black-Scholes hedge portfolio as built in our example often seems to be closer to the minimum-variance hedge than the Heston delta-vega hedge.

Looking at the results for Cisco in Panel A, the standard deviation of relative hedging errors is larger for the Black-Scholes hedge than for the Heston hedge, in particular for the delta-vega hedge. When the Heston model is used, a delta-vega hedge decreases the standard deviation of about 0.02 over all options compared to the simple Heston delta hedge. For different moneyness levels, the hedging performance is best for ITM options and worst for OTM options. In case of OTM options, a simple Black-Scholes hedge has a lower standard deviation than the Heston delta-vega hedge. The differences in hedging performance of the calibrations may be of important size: It is more than 0.1 for all options and more than 0.2 for OTM options. The differences in results of the bid- and

ask-calibrations are statistically significant in case of the F-Test (to the 5% level), but not significant in case of the AB-Test. The differences are largest for OTM options where the hedging performance for different calibrations differs in more than 20% of option value.

In case of the S&P100 index in Panel B, the standard deviations are much larger than for the other securities, especially for OTM options. As before, the standard deviation of relative hedging errors is largest for OTM options and smallest for ITM options. On average over all options, the performance of the Black-Scholes delta hedge is better than the performance of the Heston hedge. This is mainly due to the bad performance of the Heston hedge for OTM options. Between the parametrizations, differences of about 0.01 for ATM up to 0.05 for OTM options are observed. They are in most cases statistically significant. Especially for OTM options, the differences in the standard deviation between the parametrizations arise to 5 percentage points.

The results for AT&T are depicted in Panel C of Table 3. For the Heston model, the delta-vega hedge is much better than the simple delta hedge and the standard deviation of hedging errors decreases of about 0.03 on average over all options. As before, the performance of the hedge is best for ITM and worst for OTM options. The differences between the parametrizations may arise up to 0.01 for ATM and OTM options. They are in many cases statistically significant.

In summary, the differences in hedging performance of the parametrizations are economically and statistically significant. Especially for OTM options, the already large standard deviation of the hedging errors of about 24% of the option value may nearly double to about 45%. For ITM and ATM options the standard deviation differs in less than 0.01 which is small in absolute value but relative to the total standard deviation of on average 0.05 still significant.

Compared to the controlled simulation analysis, this empirical study is influenced by many external factors. Most importantly, since our study is based on the Heston model, it is certainly subject to model risk - the fact that our assumed stochastic volatility model is not the true data-generating process. The more surprising is the fact that even in this simple study parameter risk is shown to significantly impact the hedging performance.

7 Conclusion

The presence of microstructural noise in option prices makes the calibration of an option pricing model difficult. Even if the investor is sure about the structural type of the model, he will not be able to identify the true parametrization. As we have shown for the case of the Heston model, this is in particular true for the parameters of second-order importance like κ or σ_v . Another parameter difficult to estimate is ρ for which it is extremely important to have OTM option prices at hand. For calibration, a wide range of moneyness levels is therefore much more important than a wide range of maturities.

In a second step, however, finding the correct parametrization is not an objective in itself. The investor always has to take into account for what purpose he needs a calibration. In this paper we have focussed on the impact of different parametrizations on the hedging performance. We have also shown that σ_v and ρ are not only difficult to identify, but also that a mis-estimation of these parameters may have severe consequences for the hedging performance. Further, the link of the size of the average bid-ask spread to the average hedging performance allowed us to put the need of OTM option prices for calibration in numbers: To have only ATM options with a bid-ask-spread of 5% available is as good as having options with a wide range of moneyness levels with a bid-ask-spread of 20%! The most important parameters to identify correctly for hedging purposes are again σ_v and ρ .

Already our simple empirical study could confirm the theoretical results of the simulation analysis. In terms of standard deviation of hedging errors, the differences between the parametrization arose to 20% relative to the target option value for OTM options. The results of our paper illustrate the difficulties arising from microstructural noise and highlight the importance of parameter risk for hedging. Further research in this field seems necessary.

References

- An, Y. and W. Suo, 2003, The Performance of Option Pricing Models on Hedging Exotic Options, Working Paper.
- Bakshi, G., C. Cao and Z. Chen, 1997, Empirical Performance of Alternative Option Pricing Models, *Journal of Finance* 52, 2003–2049.
- Black, F. and M. Scholes, 1973, The Pricing of Options and Corporate Liabilities, *Journal of Political Economy* 81, 637–654.

- Dennis, P. and S. Mayhew, 2004, Microstructural Biases in Empirical Tests of Option Pricing Models, EFA 2004 Maastricht Meetings Paper No. 4875.
- Eraker, B., M. Johannes and N. Polson, 2003, The Impact of Jumps in Volatility and Returns, *Journal of Finance* 58, 1269–1300.
- Figlewski, S., 2004, Estimation Error in the Assessment of Financial Risk Exposure, Working Paper.
- He, C., J.S. Kennedy, T. Coleman, P.A. Forsyth, Y. Li and K. Vetzal, 2006, Calibration and Hedging under Jump Diffusion, *Review of Derivatives Research* 9, 1–35.
- Hentschel, L., 2003, Errors in Implied Volatility Estimation, *Journal of Financial and Quantitative Analysis* 38, 779–810.
- Hentschel, L., 2004, Option Hedging in the Presence of Measurement Errors, Working Paper.
- Heston, S.L., 1993, A Closed-Form Solution for Options with Stochastic Volatility with Applications to Bond and Currency Options, *Review of Financial Studies* 6, 327–343.
- Schoutens, W., E. Simons and J. Tistaert, 2003, A Perfect Calibration! Now What?, Working Paper.

Δ^{BS} interval	Bid-Ask Spread
[-1.0,-0.8)	0.03
[-0.8,-0.6)	0.05
[-0.6,-0.4)	0.07
[-0.4,-0.2)	0.14
[-0.2, 0.0]	0.42

Table 1. Bid-Ask Spreads on S&P100 Individual Stock Put Options

The table shows the average percentage spreads of put options on S&P100 individual stocks from 1996 to 2003 as a function of the Δ^{BS} interval. Δ^{BS} is the Black-Scholes delta based on implied volatility.

Underlying	Number of Observations	Number of Options	Number of Days	Avg. Number of Observations per Day
Cisco	13,850	434	1,248	11
AT&T	10,128	337	1,244	8
S&P100	80,301	2,141	1,248	64

Table 2. Data Description

Panel A: Cisco					
	Calibration	Moneyness Range			
		0.8 to 0.95	0.95 to 1.05	1.05 to 1.2	All Options
Delta (rel.)	Bid	0.0963	0.2728	0.5701	0.1570
	Mid	0.0952	0.2684	0.5629	0.1557
	Ask	0.0945	0.2679	0.5530	0.1499
Delta-Vega (rel.)	Bid	0.0503	0.0844	0.2509	0.1638
	Mid	0.0506	0.0827	0.2419	0.1583
	Ask	0.0521	0.0905	0.4543	0.2874
BS-Hedge (rel.)		0.0915	0.2369	0.3853	0.2694
F-Test (p-value)	Delta	19.82%	36.80%	3.91%	0.17%
	Delta-Vega	1.21%	0.05%	0.00%	0.00%
AB-Test (p-value)	Delta	3.19%	0.67%	16.48%	0.41%
	Delta-Vega	51.16%	34.95%	74.17%	88.38%
Panel B: S&P100					
	Calibration	Moneyness Range			
		0.8 to 0.95	0.95 to 1.05	1.05 to 1.2	All Options
Delta (rel.)	Bid	0.0295	0.1343	0.6946	0.4523
	Mid	0.0294	0.1257	0.5975	0.3903
	Ask	0.0294	0.1306	0.6420	0.4188
Delta-Vega (rel.)	Bid	0.0188	0.0721	0.5133	0.3317
	Mid	0.0195	0.0683	0.4630	0.2995
	Ask	0.0190	0.0713	0.5013	0.3240
BS-Hedge (rel.)		0.0370	0.0897	0.3011	0.2010
F-Test (p-value)	Delta	66.09%	0.00%	0.00%	0.00%
	Delta-Vega	0.00%	0.00%	0.00%	0.00%
AB-Test (p-value)	Delta	82.91%	0.00%	0.00%	0.00%
	Delta-Vega	18.29%	0.13%	14.88%	6.82%
Panel C: AT&T					
	Calibration	Moneyness Range			
		0.8 to 0.95	0.95 to 1.05	1.05 to 1.2	All Options
Delta (rel.)	Bid	0.0349	0.0968	0.2411	0.1570
	Mid	0.0349	0.0926	0.2330	0.1517
	Ask	0.0355	0.0924	0.2234	0.1461
Delta-Vega (rel.)	Bid	0.0283	0.0681	0.1997	0.1287
	Mid	0.0286	0.0688	0.1913	0.1238
	Ask	0.0292	0.0667	0.1882	0.1218
BS-Hedge (rel.)		0.0398	0.0870	0.1959	0.1300
F-Test (p-value)	Delta	32.76%	5.55%	0.00%	0.00%
	Delta-Vega	7.50%	40.14%	0.08%	0.00%
AB-Test (p-value)	Delta	85.64%	11.86%	3.10%	8.25%
	Delta-Vega	94.32%	45.90%	89.91%	60.71%

Table 3. Standard Deviations of Hedging Errors

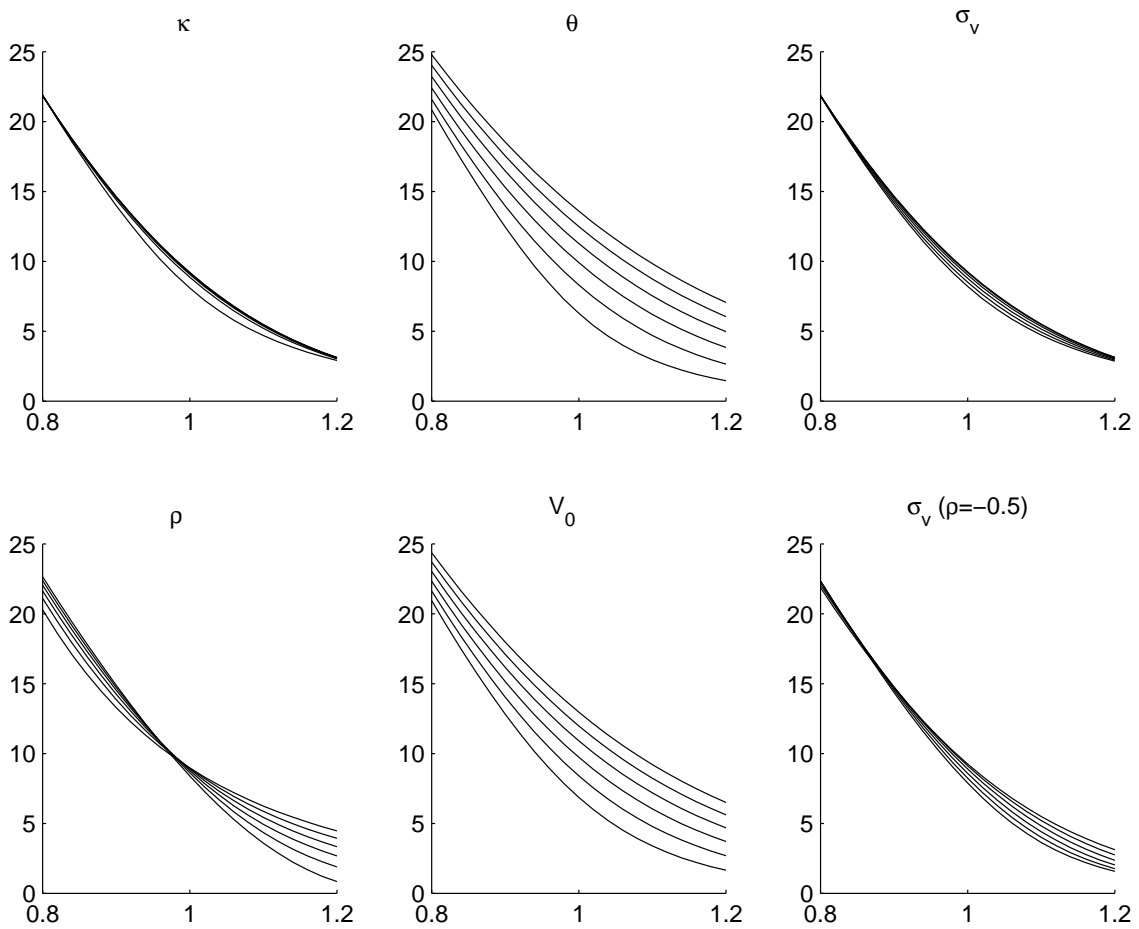


Figure 1. Sensitivity of Call Price

The graphs show the sensitivities of a call price in the Heston (1993) model as a function of moneyness. In each graph one parameter is varied within a certain range while all others are held constant. The base case and the parameter ranges were chosen as follows: $\kappa = 2.0$ [0.1; 10.0], $\theta = 0.06$ [0.01; 0.2], $\sigma_v = 0.5$ [0.01; 0.9], $\rho = 0.0$ [-1.0; 1.0], $V_0 = 0.06$ [0.01; 0.2]. The current stock price equals 100 and the interest rate is 0.0%.

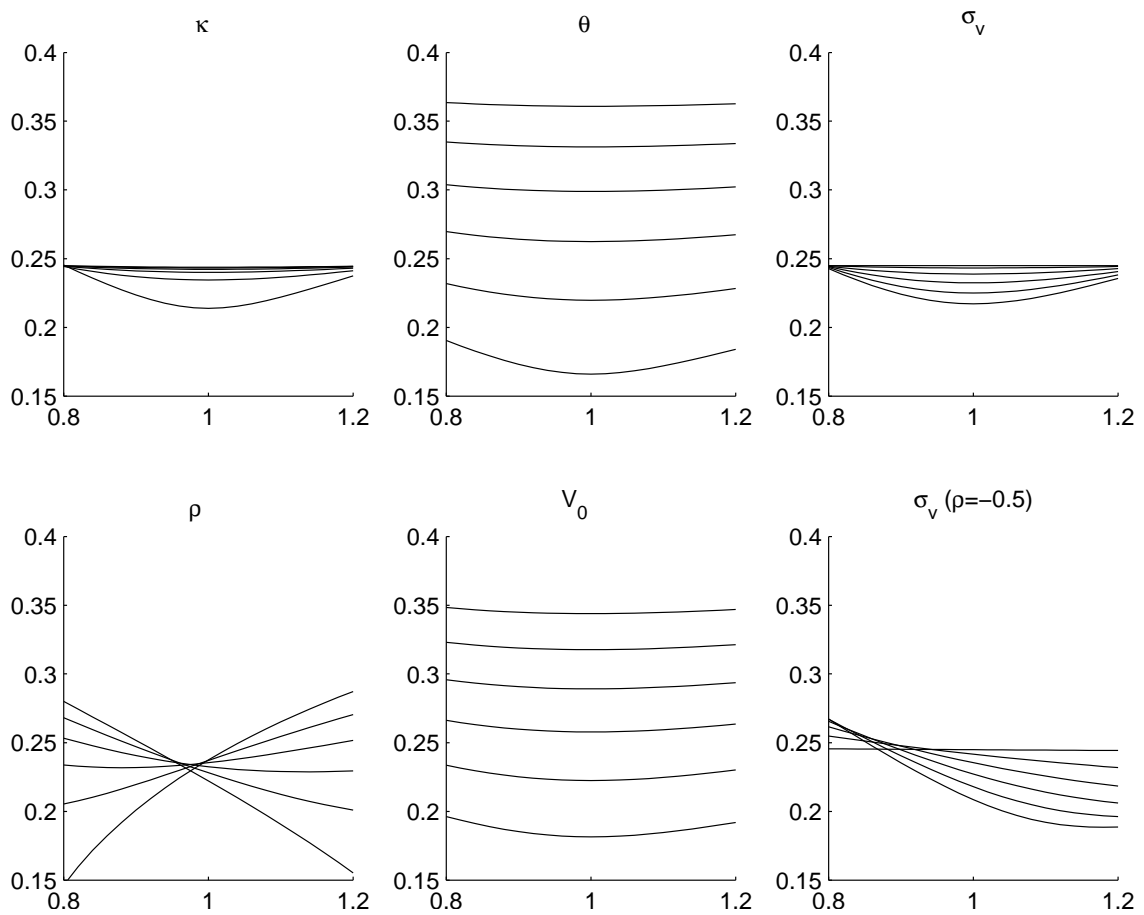


Figure 2. Sensitivity of IV-Smile

The graphs show the sensitivities of the IV-Smile in the Heston (1993) model. In each graph one parameter is varied within a certain range while all others are held constant. The base case and the parameter ranges were chosen as follows: $\kappa = 2.0$ [0.1; 10.0], $\theta = 0.06$ [0.01; 0.2], $\sigma_v = 0.5$ [0.01; 0.9], $\rho = 0.0$ [-1.0; 1.0], $V_0 = 0.06$ [0.01; 0.2]. The current stock price equals 100 and the interest rate is 0.0%.

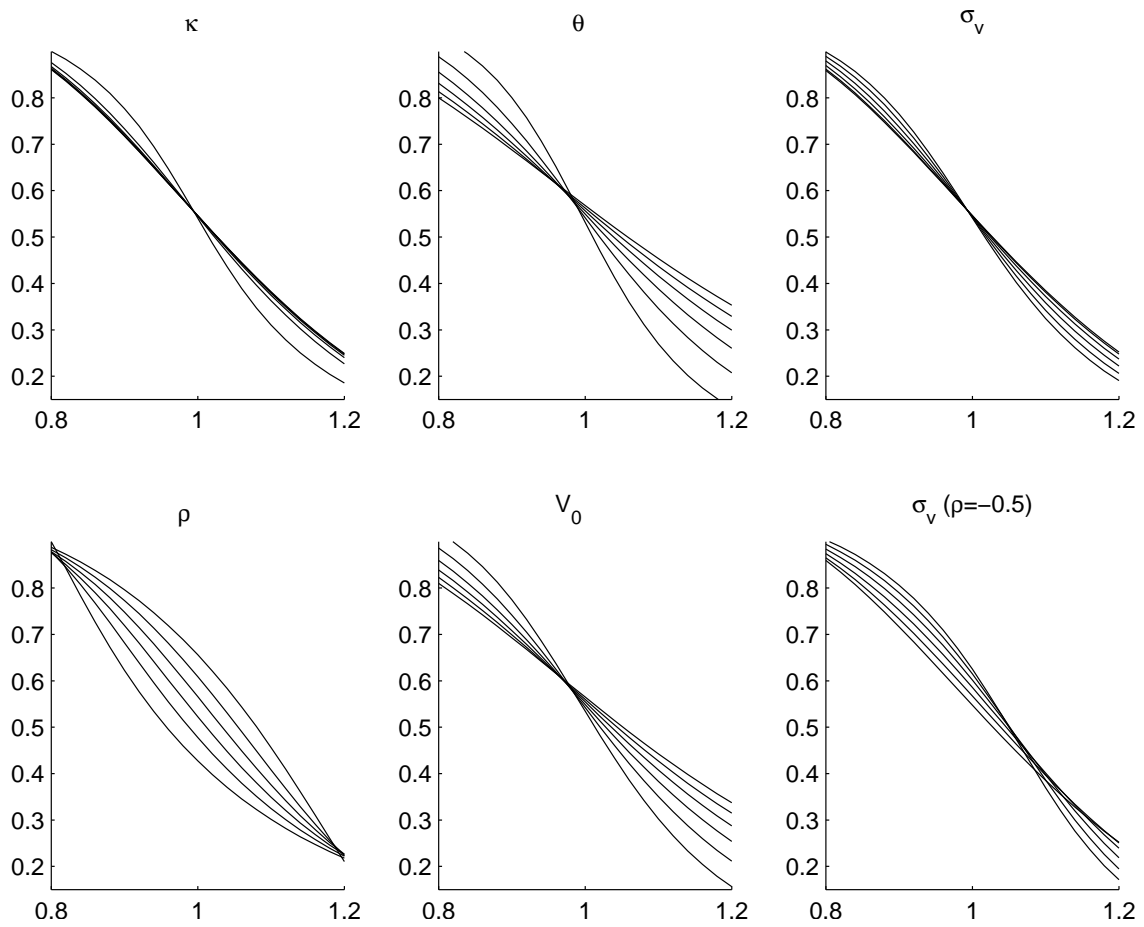


Figure 3. Sensitivity of Option Delta

The graphs show the sensitivities of the option delta in the Heston (1993) model. In each graph one parameter is varied within a certain range while all others are held constant. The base case and the parameter ranges were chosen as follows: $\kappa = 2.0$ [0.1; 10.0], $\theta = 0.06$ [0.01; 0.2], $\sigma_v = 0.5$ [0.01; 0.9], $\rho = 0.0$ [-1.0; 1.0], $V_0 = 0.06$ [0.01; 0.2]. The current stock price equals 100 and the interest rate is 0.0%.

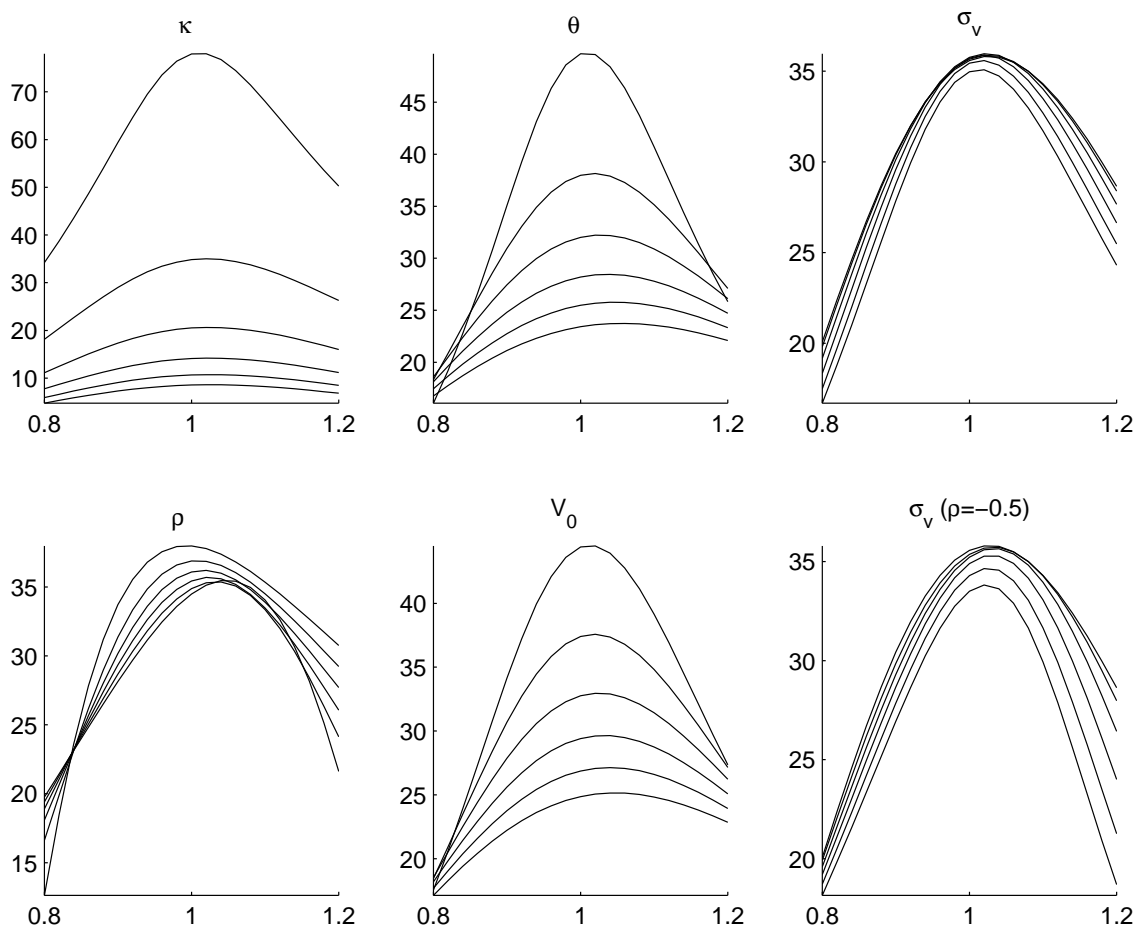


Figure 4. Sensitivity of Option Vega

The graphs show the sensitivities of the option vega in the Heston (1993) model. In each graph one parameter is varied within a certain range while all others are held constant. The base case and the parameter ranges were chosen as follows: $\kappa = 2.0$ [0.1; 10.0], $\theta = 0.06$ [0.01; 0.2], $\sigma_v = 0.5$ [0.01; 0.9], $\rho = 0.0$ [-1.0; 1.0], $V_0 = 0.06$ [0.01; 0.2]. The current stock price equals 100 and the interest rate is 0.0%.

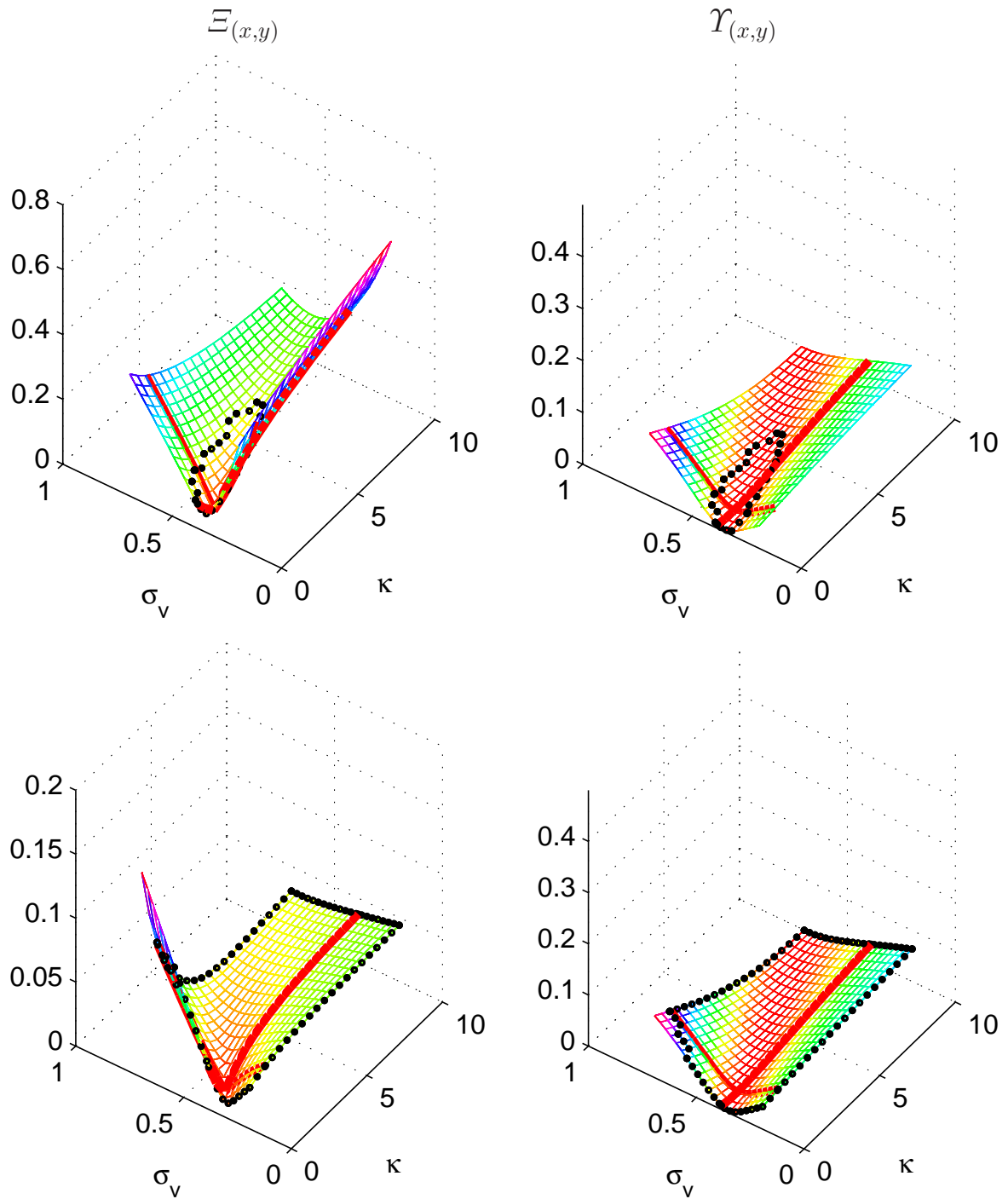


Figure 5. Objective Function and Standard Deviation of Hedging Errors for σ_v and κ

The graphs plot the objective function of calibration $\Xi_{(x,y)}$ (left) and the standard deviation of hedging errors (as percentage of the option price) $\Upsilon_{(x,y)}$ (right) as a function of the parameters σ_v and κ . In the upper graphs the calibration is done for 'all' options, in the lower graphs for 'atm' options only.

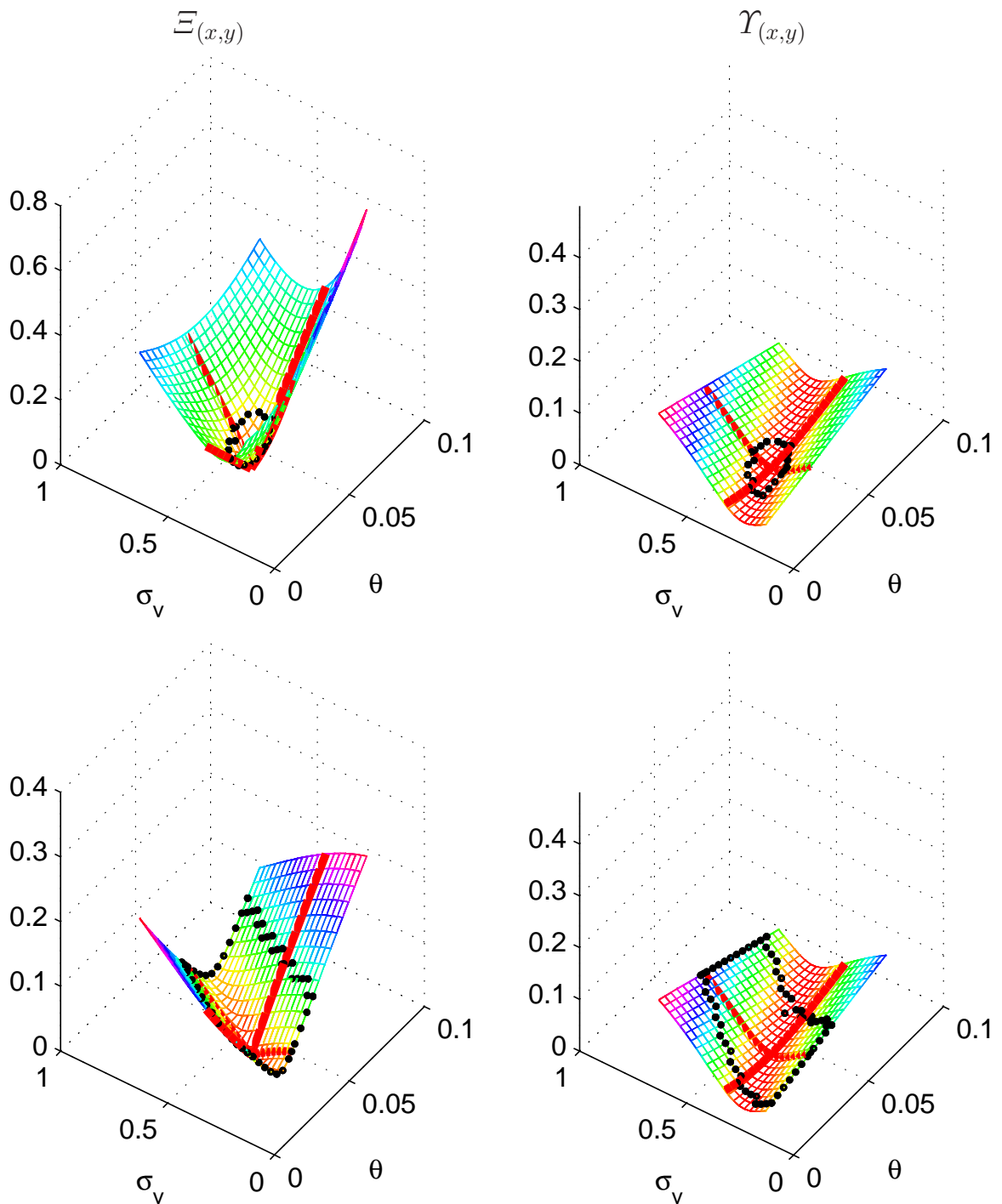


Figure 6. Objective Function and Standard Deviation of Hedging Errors for σ_v and θ

The graphs plot the objective function of calibration $\Xi(x,y)$ (left) and the standard deviation of hedging errors (as percentage of the option price) $\Upsilon(x,y)$ (right) as a function of the parameters σ_v and θ . In the upper graphs the calibration is done for 'all' options, in the lower graphs for 'atm' options only.

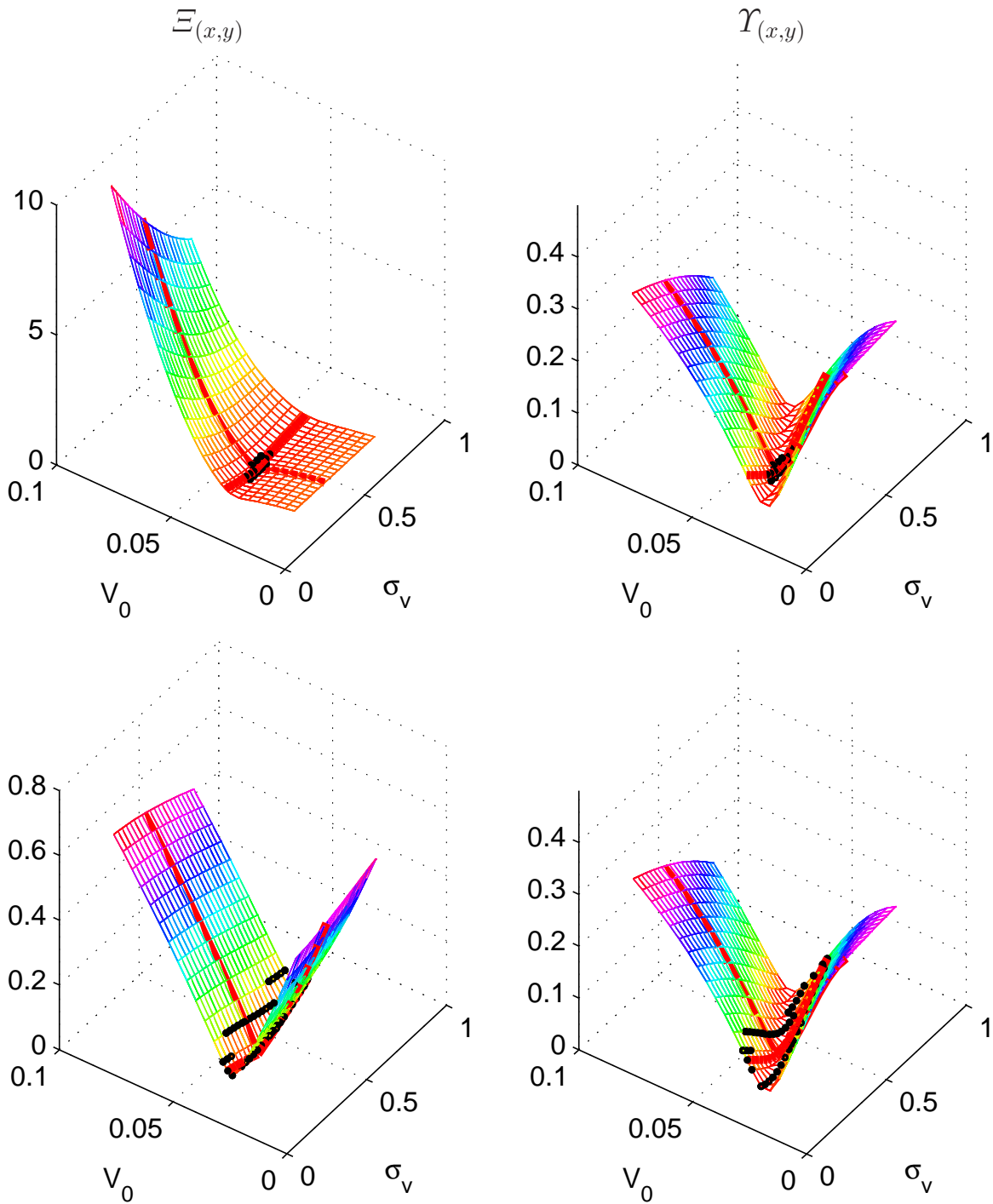


Figure 7. Objective Function and Standard Deviation of Hedging Errors for V_0 and σ_v

The graphs plot the objective function of calibration $\Xi_{(x,y)}$ (left) and the standard deviation of hedging errors (as percentage of the option price) $\Upsilon_{(x,y)}$ (right) as a function of the parameters σ_v and V_0 . In the upper graphs the calibration is done for 'all' options, in the lower graphs for 'atm' options only.

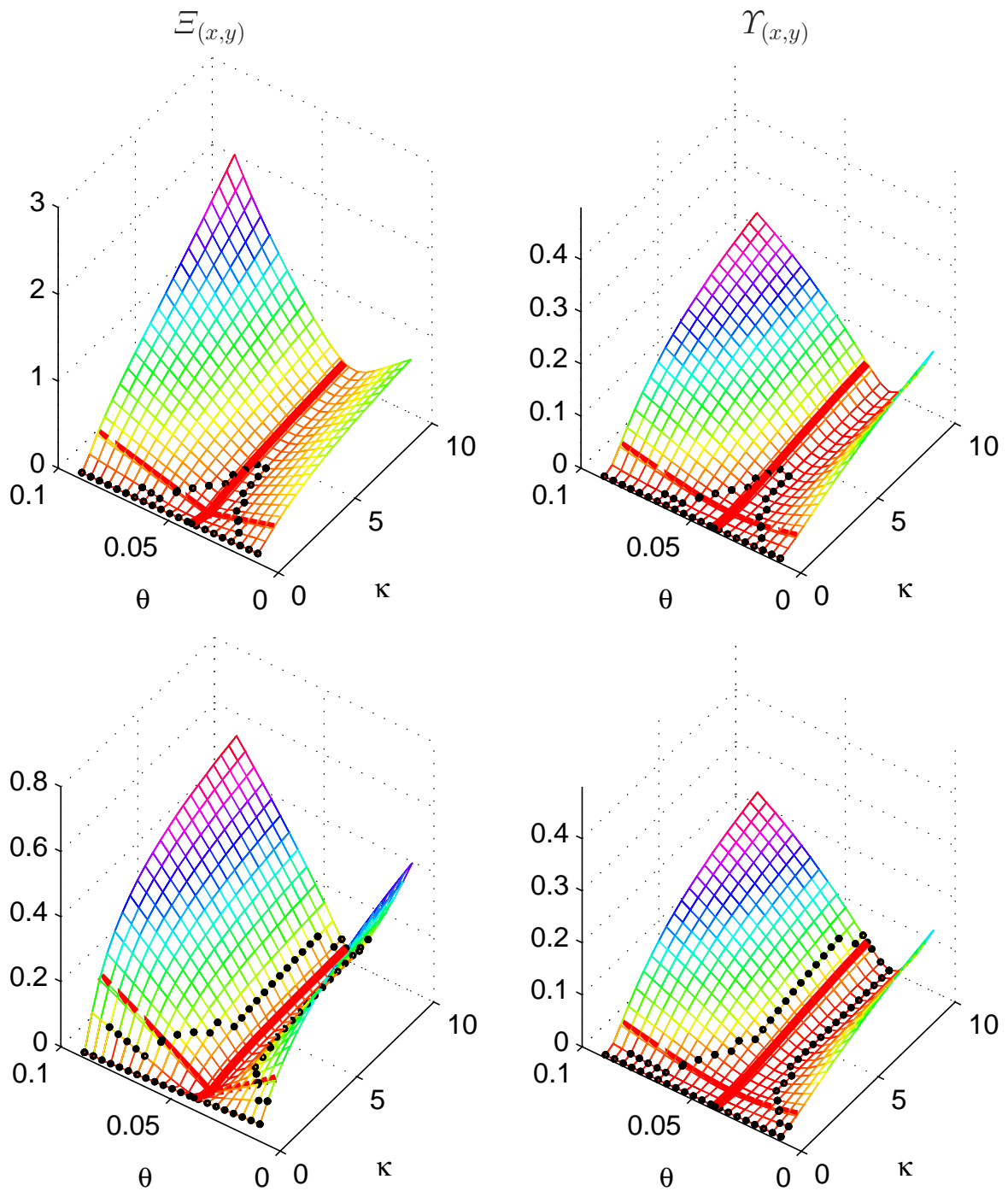


Figure 8. Objective Function and Standard Deviation of Hedging Errors for θ and κ

The graphs plot the objective function of calibration $\Xi_{(x,y)}$ (left) and the standard deviation of hedging errors (as percentage of the option price) $\Upsilon_{(x,y)}$ (right) as a function of the parameters σ_v and θ . In the upper graphs the calibration is done for 'all' options, in the lower graphs for 'atm' options only.

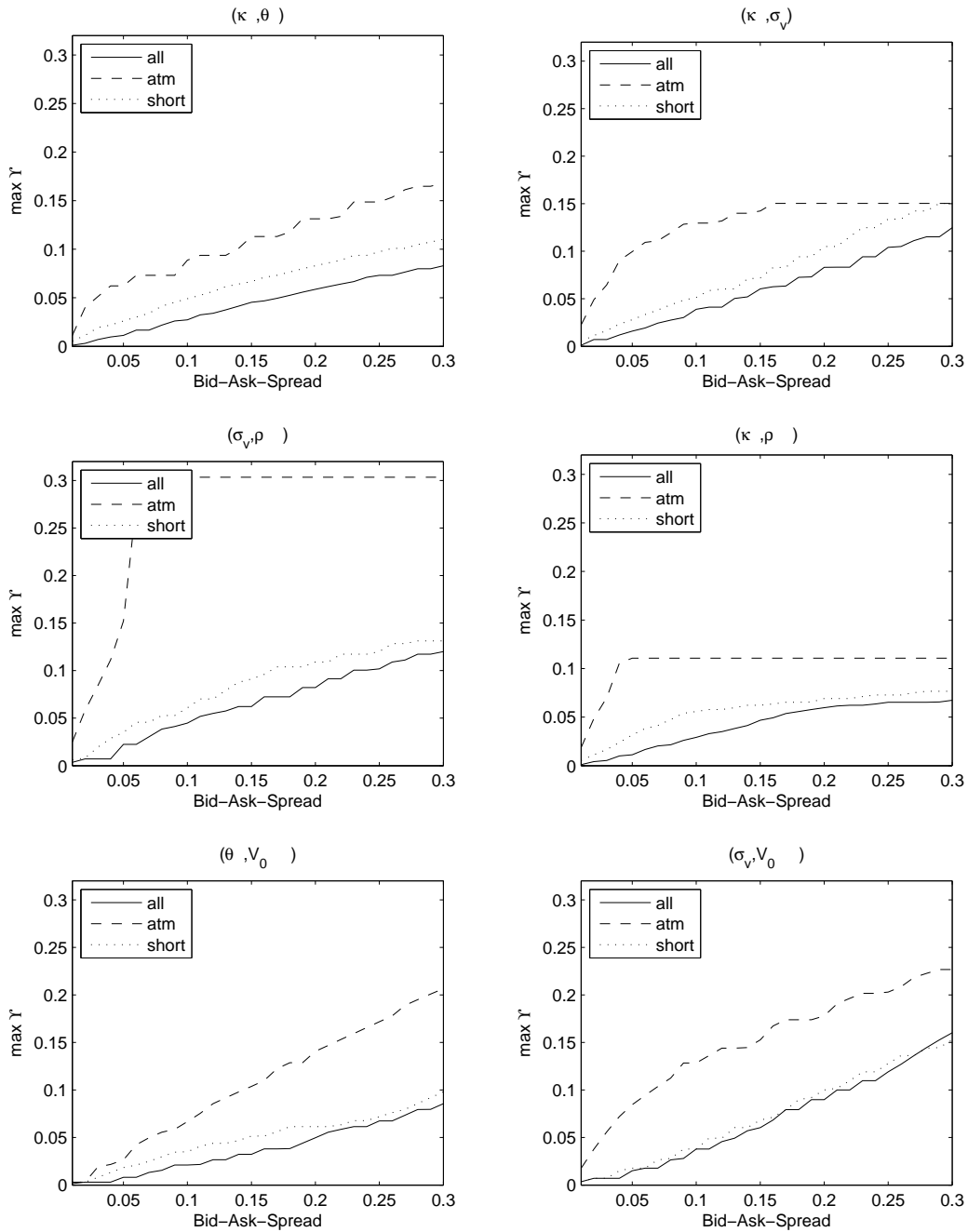


Figure 9. Bid-Ask Spread vs. Standard Deviation of Hedging Error

The graphs show the maximum of $\Upsilon_{(x,y)}$, i.e. the standard deviation of the hedging error, as a function of the mean bid-ask spread over all options used for calibration for different parameter combinations (x, y) . The solid lines represent the case where the model is calibrated to 'all' options, the dotted lines where it is calibrated to 'short' maturity options and the dashed lines where it is calibrated to 'atm' options only.

Appendix

Curriculum Vitae

EVA SCHNEIDER

Born September 12th, 1978 in Lich (Germany)

Neuhofstrasse 36

60318 Frankfurt am Main

Germany

+49-(0)69-13023829

schneider@finance.uni-frankfurt.de

EDUCATION

Johann Wolfgang Goethe-University, Frankfurt am Main since 10/2004

Ph.D. Student in Finance

Universite Paris-IX Dauphine 05/2004

Maîtrise d'économie appliquée, Double-Diploma-Program

Johann Wolfgang Goethe-University, Frankfurt am Main 10/1998 – 05/2004

Diploma in Economics (with distinction 1.1)

Universite Paris-IX Dauphine 02/2001 – 06/2002

Licence d'économie appliquée (among the best 5% of the year)

Liebigschule, Giessen 08/1995 – 06/1998

Abitur (1.3)

EMPLOYMENT EXPERIENCE

Landesbank Hessen-Thüringen, Frankfurt am Main since 10/2007
Specialist Financial Engineering

Johann Wolfgang Goethe-University, Frankfurt am Main 10/2004 – 10/2007
Research Assistant (Chair of Derivatives and Financial Engineering)

Johann Wolfgang Goethe-University, Frankfurt am Main 04/2006 – 07/2006
Lecturer (Interest Rate Derivatives)

Dresdner Kleinwort Wasserstein, Frankfurt am Main 05/2004 – 10/2004
Intern in Corporate Markets - Structured Trading

Deutsche Bundesbank, Frankfurt am Main 07/2002 – 10/2002
Intern in Statistics Department

Johann Wolfgang Goethe-University, Frankfurt am Main 12/2002 – 02/2004
Student Assistant (Chair of Industrial Organization)

Johann Wolfgang Goethe-University, Frankfurt am Main 10/1999 – 02/2004
Tutor in Mathematics, Statistics and Microeconomics

MSU Consulting, Bad Homburg 07/2000 – 02/2001
Intern in Telecommunications

PUBLICATIONS

”Optimal Portfolios When Volatility can Jump”
forthcoming Journal of Banking and Finance, coauthors: Nicole Branger, Christian Schlag

”Derivatives Trading in a General Equilibrium Model with Stochastic Volatility and Jumps”

Working Paper, coauthors: Nicole Branger, Christian Schlag

”Continuous-time Volatility Component Models: Option Pricing and Asset Allocation”

Working Paper

”Hedging in the Presence of Microstructural Noise”

Working Paper, coauthors: David Horn, Grigory Vilkov

”Systematic Risk and Option Prices”

Working Paper, coauthor: David Horn

”Using Hedging Errors to Identify Option Pricing Models”

Working Paper, coauthors: Nicole Branger, Christian Schlag, Norman Seeger

CONFERENCE PRESENTATIONS

”Optimal Portfolios When Volatility can Jump”

Swiss Society for Financial Market Research, Zurich (07.04.2006)

Gesellschaft für Klassifikation, Berlin (08.03.2006 - 10.03.2006)

Paris International Meeting on Finance, Paris (19.12.2005 - 20.12.2005)

Deutsche Gesellschaft für Finanzwirtschaft, Augsburg (07.10.2005 - 08.10.2005)

European Summer Symposium in Financial Markets, Gerzensee (23.07.2005-29.07.2005)

Brown Bag Seminar, Goethe University, Frankfurt am Main (01.06.2005)

”Derivatives Trading in a General Equilibrium Model with Stochastic Volatility and Jumps”

Paris International Meeting on Finance, Paris (18.12.2006 - 19.12.2006)

Verein für Socialpolitik, Bayreuth (26.09.2006 - 29.09.2006)

Western Finance Association, Keystone, Colorado (21.06.2006 - 24.06.2006)

Swiss Society for Financial Market Research, Zurich (07.04.2006)

16th Annual Derivative Securities and Risk Management Conference, Arlington, Virginia (07.04.2006 - 08.04.2006)

Brown Bag Seminar, Goethe University, Frankfurt am Main (07.12.2005)

”Continuous-time Volatility Component Models: Option Pricing and Asset Allocation”

Deutsche Gesellschaft für Finanzwirtschaft, Dresden (28.09.2007 - 29.09.2007)

Brown Bag Seminar, Goethe University, Frankfurt am Main (27.06.2007)

”Hedging in the Presence of Microstructural Noise”

Midwest Finance Association Annual Meeting, San Antonio, Texas (27.02.2008 - 01.03.2008)

Eastern Finance Association Annual Meeting, St. Pete Beach, Florida (09.04.2008 - 12.04.2008)

”Systematic Risk and Option Prices”

Midwest Finance Association Annual Meeting, San Antonio, Texas (27.02.2008 - 01.03.2008)

Swiss Society for Financial Market Research, Zurich (11.04.2008)

”Using Hedging Errors to Identify Option Pricing Models”

Workshop on Finance, Stochastics and Insurance, Bonn (25.02.2008 - 29.02.2008)

Swiss Society for Financial Market Research, Zurich (11.04.2008)

ADDITIONAL INFORMATION

Scholarships: German-French University (02/2001 – 06/2002)

Language Skills: German, English, French, Spanish

Computer Skills: C/C++, Mathematica, Matlab, MS Office, Latex, E-Views

Further Activities: Mountain Biking, Hiking, Piano

Ehrenwörtliche Erklärung

„Ich habe die vorgelegte Dissertation selbst verfasst und dabei nur die von mir angegebenen Quellen und Hilfsmittel benutzt. Alle Textstellen, die wörtlich oder sinngemäß aus veröffentlichten oder nicht veröffentlichten Schriften entnommen sind sowie alle Angaben, die auf mündlichen Auskünften beruhen, sind als solche kenntlich gemacht.“

Frankfurt am Main, 26. Oktober 2007